UNIWERSYTET IM. A. MICKIEWICZA W POZNANIU
WYDZIAŁ BIOLOGII
PRACOWNIA BIOLOGII EWOLUCYJNEJ

GENOMIKA DOBORU PŁCIOWEGO ROZKRUSZKA HIACYNTOWEGO, *RHIZOGLYPHUS ROBINI*

SEBASTIAN CHMIELEWSKI

ROZPRAWA DOKTORSKA

Promotor
prof. dr hab. Jacek Radwan
Promotor pomocniczy
dr Mateusz Konczal

POZNAŃ, 2024

ADAM MICKIEWICZ UNIVERSITY
FACULTY OF BIOLOGY
EVOLUTIONARY BIOLOGY GROUP

THE GENOMICS OF SEXUAL SELECTION IN THE BULB MITE, *RHIZOGLYPHUS ROBINI*

SEBASTIAN CHMIELEWSKI

DOCTORAL THESIS

Supervisor
prof. dr hab. Jacek Radwan
Auxiliary Supervisor
dr Mateusz Konczal

POZNAŃ, 2024

ACKNOWLEDGEMENTS

Niniejsza rozprawa doktorska nie mogłaby powstać bez cennego wsparcia moich promotorów: prof. dr. hab. Jacka Radwana i dr Mateusza Konczala. Bardzo dziękuję za niezmierzone pokłady cierpliwości, za ciągle otwarte drzwi i nakierowanie mnie w czasie, gdy moje badania trafiały w ślepą uliczkę. Dziękuję za pomoc w rozwikływaniu zagadek rozkruszkowego genomu i w interpretacji skomplikowanych wykresów, które przy Waszych biurkach stawały się zaskakująco zrozumiałe. Jackowi dziękuję również za otwarcie drzwi do genomiki oraz stworzenie świetnego zespołu, w którym nigdy nie zabrakło otwartości na dyskusję oraz wymianę myśli.

I thank Jonathan Parrett for being the best person I could imagine spending countless days of laborious work with mites. *Every time the sun came up* your sense of humor, good music, and excellent English tea made this work less of a struggle and more of a joy. The lyrics of *The Song* will stay with me through any hard days. Thank you for our shared mite projects (there were quite a few!), for your guidance in statistics, and for being a great leader during my work on your grant.

Podziękowania kieruję do członków Pracowni Biologii Ewolucyjnej- dziękuję za wsparcie, za litry wspólnej wypitej kawy i złotego trunku Za Kulisami. Za wspólnie spędzony czas na wyjazdach kajakowych i konferencyjnych. Szczególnie dziękuję Katarzynie Burdzie za wspólne doświadczanie wznosów i upadków w czasie doktoratowej wędrówki, Karolinie Przesmyckiej za wspólnie spędzony czas i Agnieszce Szubert-Kruszyńskiej za pomoc w nawigacji w labiryncie administracji uniwersyteckiej i codziennego kubka wyśmienitej herbaty o poranku.

Szczególnie wdzięczny jestem mojemu narzeczonemu Tomaszowi- bez Ciebie ukończenie tej pracy byłoby niemożliwe. Dziękuję, że zawsze byłeś blisko, za nieocenione wsparcie i wspólne realizowanie naszych pasji. I za nieprzychylne spojrzenie podczas kolejnego wieczora spędzonego przed laptopem, które przypominało mi o tym, że życie płynie także poza stronami publikacji i drzwiami laboratorium.

Szczególnie dziękuję za wierne (i cierpliwe!) kibicowanie w czasie doktoratu mojej najbliższej rodzinie- Rodzicom, Siostrom, Babci oraz Dziadkom, których pożegnałem w tym okresie. Dziękuję również przyjaciołom, którzy trzymają za mnie kciuki i byli wyrozumiali wobec mojego ciągłego "niedoczasu". Prof. Marlenie Lembicz dziękuję za liczne inspirujące rozmowy oraz porady, dzięki którym zyskiwałem świeże spojrzenie na codzienne sprawy.

WORKS INCLUDED IN THE DISSERTATION

The thesis consists of 3 chapters. First chapter has undergone a first round of review in *Genetics* and is available at bioRxiv (https://doi.org/10.1101/2024.04.15.589577). Two other chapters have not been published yet.

1. Chmielewski, S., Konczal, M., Parrett, J. M., Rombauts, S., Dudek, K., Radwan, J., & Babik, W. (2024). Sex-specific recombination landscape in a species with holocentric chromosomes. Under review in *Genetics*.
2. Chmielewski, S., Parrett, J.M., Konczal, M. & Radwan, J. (2024). The impact of sex ratio manipulation on genome-wide genetic diversity during experimental evolution. Unpublished manuscript.
3. Chmielewski, S., Konczal, M., Parrett, J.M. & Radwan, J. (2024). Supergene polymorphism and its role in male morph differentiation in the bulb mite, *Rhizoglyphus robini*. Unpublished manuscript.

OTHER WORKS PUBLISHED DURING DOCTORAL STUDIES

1. Parrett, J.M., Sobala, K., Chmielewski, S., Przesmycka, K. & Radwan, J. (2024). No evidence for negative-frequency dependent selection in maintaining alternative reproductive tactics in a bulb mite. Accepted in *Animal Behaviour*.
2. Plesnar-Bielak, A., Parrett, J. M., Chmielewski, S., Dudek, K., Łukasiewicz, A., Marszałek, M., Babik, W. & Konczal, M. (2024). Transcriptomics of differences in thermal plasticity associated with selection for an exaggerated male sexual trait. *Heredity*, 1-11.
3. Parrett, J. M., Łukasiewicz, A., Chmielewski, S., Szubert-Kruszyńska, A., Maurizio, P. L., Grieshop, K., & Radwan, J. (2023). A sexually selected male weapon characterized by strong additive genetic variance and no evidence for sexually antagonistic polyphenic maintenance. *Evolution*, *77*(6), 1289-1302.
4. Parrett, J., Wasilewska, J., Przesmycka, K., Chmielewski, S., Scholz, M., & Radwan, J. (2023). Cytoplasmic incompatibility associated with Wolbachia strains differing in the presence of cif genes. *Authorea Preprints*.
5. Parrett, J. M., Chmielewski, S., Aydogdu, E., Łukasiewicz, A., Rombauts, S., Szubert-Kruszyńska, A., ... & Radwan, J. (2022). Genomic evidence that a sexually selected trait captures genome-wide variation and facilitates the purging of genetic load. *Nature Ecology & Evolution*, *6*(9), 1330-1342.
6. Phillips, K. P., Cable, J., Mohammed, R. S., Chmielewski, S., Przesmycka, K. J., Van Oosterhout, C., & Radwan, J. (2021). Functional immunogenetic variation, rather than local adaptation, predicts ectoparasite infection intensity in a model fish species. *Molecular Ecology*, *30*(21), 5588-5604.
7. Konczal, M., Przesmycka, K. J., Mohammed, R. S., Phillips, K. P., Camara, F., Chmielewski, S., Hahn, M., Guigo, R., Cable, J. & Radwan, J. (2020). Gene duplications, divergence and recombination shape adaptive evolution of the fish ectoparasite *Gyrodactylus bullatarudis*. *Molecular ecology*, *29*(8), 1494-1507.

FUNDING

This research was supported by the following sources:

1. National Science Centre Opus grant 2017/27/B/NZ8/00077 awarded to Jacek Radwan.
2. Grant of the Dean of Faculty of Biology AMU GDWB-07/2020 awarded to Sebastian Chmielewski
3. 'Minigrant' financed from the project 'Passport to the future - Interdisciplinary doctoral studies at the Faculty of Biology, Adam Mickiewicz University.' POWR.03.02.00-00-I006/17 awarded to Sebastian Chmielewski

STRESZCZENIE

Dobór płciowy, działający na cechy związane z konkurencją rozrodczą, często prowadzi do ewolucji rozbudowanych trzeciorzędowych cech płciowych pełniących funkcję ornamentów zwiększających atrakcyjność ich właścicieli lub broni używanej w rywalizacji między osobnikami tej samej płci. Dobór płciowy kształtuje zmienność genetyczną, która jest głównym czynnikiem determinującym istotne procesy ewolucyjne, takie jak adaptację, specjację czy ekstynkcję. Ten rodzaj doboru może zwiększać dostosowanie populacji, jeśli silna konkurencja o partnerów do rozrodu premiuje osobniki o wysokiej jakości osobnika, które mogą przeznaczyć zasoby na kosztowne pod względem energetycznym zachowania reprodukcyjne lub silniejszą ekspresję trzeciorzędowych cech płciowych. Zatem dobór płciowy może wzmocnić selekcję alleli pozytywnych i eliminację szkodliwych. Aczkolwiek, poprzez silny dobór kierunkowy ograniczający dostęp do rozrodu jedynie do najbardziej konkurencyjnych osobników, dobór płciowy redukuje efektywną wielkość populacji (N_e), zmniejszając efektywność selekcji. Wpływ doboru płciowego na ilość zmienności genetycznej w populacjach naturalnych, przekładającej się na ich potencjał ewolucyjny jest więc trudny do przewidzenia. Z jednej strony, poprzez wzmożony dobór płciowy oraz zmniejszenie N_e, dobór ten powinien redukować zmienność genetyczną w populacji. Z drugiej strony, najnowsze modele genetyczne przewidują, że dobór płciowy zamiast zmniejszać, może przyczyniać się do utrzymywania zmienności genetycznej przez proces nazywany antagonizmem płciowym, w którym allel korzystny dla jednej płci zmniejsza przystosowanie płci przeciwnej, utrzymując polimorfizm w danym locus. Jednakże dowody na wpływ doboru płciowego na ilość i charakter zmienności genetycznej są bardzo ubogie. Badania opisane w niniejszej rozprawie wypełniają tę lukę poprzez zastosowanie narzędzi genomowych w celu zrozumienia jak dobór płciowy kształtuje zmienność genetyczną u rozkuszka hiacyntowego *Rhizoglyphus robini*- ważnego gatunku modelowego w badaniach nad doborem płciowym. Populacje tego gatunku podlegają silnemu doborowi płciowemu, obejmującemu zarówno walki o dostęp do samic, jak również intensywną konkurencję plemników o gamety samic. Pierwszy z tych czynników doprowadził do ewolucji alternatywnych taktyk rozrodczych, z agresywnymi samcami walczącymi posiadającymi oręż w formie zgrubiałej trzeciej pary odnóży oraz z samcami niewalczącymi, unikającymi bezpośredniego starcia z innymi samcami.

W rozdziale pierwszym skonstruowaliśmy mapę genetyczną rozkruszka hiacyntowego, która pozwoliła nam na złożenie genomu tego gatunku do skali chromosomalnej, pozwalając na lepsze poznanie architektury genetycznej morfu samca *R. robini,* jak również na przeprowadzenie skanów genomowych w poszukiwaniu regionów odpowiadających na selekcję, co opisano w rozdziale 2 i 3. Ponadto holocentryczne chromosomy tego gatunku pozwoliły nam na przetestowanie roli centromerów w kształtowaniu różnic między płciami w rozmieszczeniu rekombinacji mejotycznej. Pomimo zwiększonego ryzyka aneuploidii związanego z rekombinacją w pobliżu centromeru, u wielu taksonów obserwuje się zwiększone tempo crossing-over u samic, podczas gdy u samców jest ono zazwyczaj wyższe na końcach chromosomów. Według jednej z głównych hipotez tłumaczących ten paradoks, taki rozkład rekombinacji może być mechanizmem obronnym przed samolubnymi elementami genetycznymi wywołującymi odchylenie mejotyczne, które manipulują centromerami aby zwiększyć swoje szanse na segregację do oocytów, a nie do degenerujących ciałek kierunkowych. Zgodnie z tą hipotezą odkryliśmy, że u rozkruszka hiacyntowego rozkład rekombinacji jest podobny u samic i samców, a tempo rekombinacji wzrastało w kierunku końców chromosomów u obu płci. Dodatkowo stwierdziliśmy, że częstość rekombinacji samic była dwa razy wyższa niż u samców, a lokalne tempo rekombinacji było pozytywnie skorelowane z ilością sekwencji powtórzonych i negatywnie z gęstością genów.

W drugim rozdziale przeprowadziliśmy eksperyment typu 'ewoluuj i resekwencjonuj', w którym zmienialiśmy natężenie doboru płciowego przez manipulację stosunkiem płci przy jednoczesnym utrzymaniu równej proporcji samców walczących i niewalczących. Manipulacja ta nie wywołała wyraźnej różnicy w zmienności genetycznej pomiędzy liniami z przewagą samic i samców. Zaobserwowaliśmy zmniejszenie różnorodności genetycznej w obu procedurach, ale linie z przewagą samców wykazały mniejszą utratę zmienności nukleotydowej w miejscach synonimowych. Chociaż manipulacja proporcją płci spowodowała niską zmianę częstości alleli w wielu miejscach genomowych, zidentyfikowaliśmy duże haplotypy, które odpowiedziały na selekcję tylko w jednej z procedur. Nie znaleźliśmy jednak dowodów na to, że podwyższenie intensywności doboru płciowego poprzez zwiększenie proporcji samców w stosunku do samic wpływa na ilość niesynonimowej zmienności genetycznej segregującej w populacji.

Rozdział trzeci opisuje architekturę genetyczną leżącą u podstaw determinacji morfu samca u *R. robini.* Przeprowadziliśmy eksperyment typu Pool-GWAS, w którym porównaliśmy sekwencje genomowe pomiędzy pulami DNA samców walczących i niewalczących. Związek zidentyfikowanego rejonu genetycznego został dodatkowo potwierdzony analizą linii wsobnych, w których został utrwalony alternatywny morf samca. Obie metody wskazały na istotne powiązanie morfu z regionem o długości 3,5 Mb położonego na końcu chromosomu siódmego. Aby scharakteryzować ten region, wykorzystaliśmy sekwencje ogólnogenomowe roztoczy wykorzystanych do konstrukcji mapy genetycznej. Wykazaliśmy, że rejon ten wykazuje cechy typowe dla supergenów, takie jak zredukowane tempo rekombinacji między alternatywnymi allelami, istotną dywergencję między haplotypami specyficznymi dla morfu oraz znaczące wzbogacenie w transpozony. Te cechy są prawdopodobnie wynikiem zahamowanej rekombinacji, która utrzymuje adaptatywne zestawy alleli korzystne dla alternatywnych taktyk

rozrodcze. Ekspresja morfu była ponadto związana z setkami SNPów rozproszonymi w całym genomie, które były wzbogacone w allele o niskiej częstości u samców niewalczących, przypuszczalnie będących szkodliwymi mutacjami. Ostatni wynik jest zgodny uwarunkowaniem ekspresji trzeciorzędowych cech płciowych od kondycji, co czyni je wiarygodnymi wskaźnikami jakości genetycznej.

Podsumowując, niniejsza praca doktorska dostarcza istotnych informacji na temat genomowych podstaw doboru płciowego i determinacji morfu samców u *R. robini*. Odkrycia dotyczą roli doboru płciowego w kształtowaniu zmienności genetycznej, będącej jest kluczowym czynnikiem w zarządzaniu naturalnymi populacjami, zwłaszcza tymi zagrożonymi wyginięciem.

Słowa kluczowe: dobór płciowy, alternatywne taktyki rozrodcze, mapowanie genetyczne, GWAS, supergen

SUMMARY

Sexual selection promotes traits involved in reproductive competition and often leads to the evolution of elaborate secondary sexual traits, which function either as ornaments increasing the attractiveness of their bearers or as weapons used in competition between members of the same sex. Sexual selection shapes the genetic variance, which determines important evolutionary processes, such as adaptation, speciation or extinction. Sexual selection may improve population fitness if high reproductive competitiveness is associated with high organismal efficiency, which may allow for allocating resources to energetically demanding behaviours or developing more extreme sexually selected traits. In such a case, sexual selection can increase selection favoring beneficial alleles and purging detrimental ones. However, by imposing strong directional selection, limiting access to reproduction only to most competitive individuals may limit effective population size (N_e) and thus decrease the efficacy of selection. Also, the impact of sexual selection on the amount of genetic variance segregating in natural populations, and thus their evolutionary potential, is not easy to predict. On the one hand, by intensifying overall sexual selection, and by reducing N_e, sexual selection is expected to reduce genetic variance segregating in population. On the other hand, the latest genetic models predict that sexual selection, instead of decreasing, may contribute to the maintenance of genetic variation through a process called sexual antagonism, in which an allele beneficial to one sex decreases the fitness of the opposite sex, preserving polymorphism at a given locus. However, empirical evidence for the role of sexual selection on the amount and nature of genetic variance segregating in natural population is scarce. The research described in this thesis aims to fill this gap by applying genomic tools to understand how sexual selection shapes genetic variance in one of influential sexual selection models- the bulb mite, *Rhizoglyphus robini*. Populations of this species undergo strong sexual selection, consisting of struggles for the access to females as well as intense sperm competition for the access to female gametes. The former has led to the evolution alternative male reproductive phenotypes, with aggressive fighter males armed with a thickened third pair of legs and benign scrambler males.

In the first chapter, we constructed a genetic map of a bulb mite, which facilitated anchoring the reference genome of this species to a chromosome scale, allowing us to better understand the genetic architecture of the sexually selected weapon, as well as to scan a genome for regions responding to selection, as described in chapters 2 and 3. Additionally, holocentric chromosomes of bulb mites allowed us to study sex-specific recombination landscape without the influence of centromeres. Despite the increased risk of aneuploidy associated with crossovers near centromeres, across eukaryotes it is observed that females have higher recombination rates near centromeres, while in males crossover frequency increases toward chromosome ends. A major hypothesis suggests this paradox may be a result of a defense mechanism against selfish meiotic drivers, which manipulate centromeres to increase their chances of segregating into oocytes rather than inviable polar bodies. Consistent with this hypothesis, we found that in *R. robini* the crossover distribution is more similar between the sexes, and recombination rate increased toward chromosome ends in both males and females. Additionally, we found that female recombination rate was twice as high as that in males and sex-averaged recombination frequency was positively associated with repeat content and negatively with gene density.

In the second chapter, we conducted an *evolve-and-resequence* experiment in which we manipulated sexual selection intensity by skewing the sex ratio, but keeping the ratio of fighters to scramblers at constant 50:50 ratio. Our experimental procedure did not result in a clear genomic response. We observed a decrease in genetic variance in both male biased and female biased sex-ratio procedures, but male-biased lines exhibited slower loss of genetic variance, particularly at synonymous sites. Although the sex ratio manipulation triggered a weak polygenic response, we identified large haploblocks which responded uniquely to selection in each treatment. Overall, however, we have not found evidence that elevating sexual selection by increasing the ratio of males to females affects the amount of non-neutral genetic variance segregating in populations.

The third chapter characterises the genetic architecture underlying male morph determination in *R. robini*. Firstly, we conducted a Pool-GWAS comparing whole genome sequences of scrambler and fighter DNA pools. The association of this genomic region with morph determination was further confirmed by analysis of inbred lines which were fixed for alternative male morphs. Both methods identified significant morph association with a 3.5 Mb region near the end of chromosome seven. To characterize this region, we additionally used individually sequenced mites that were previously used for the genetic map construction. We found that the region exhibited characteristics typical of supergenes- genomic regions, such as reduced recombination between alternative alleles, high nucleotide divergence between scrambler- and fighter-specific haplotypes and significant enrichment in transposons. These signatures are likely to be the result of suppressed recombination, which maintains a co-adapted set of alleles beneficial for discontinuous traits, like alternative reproductive tactics. The morph expression was also associated with hundreds of SNPs scattered across the whole genome, which were enriched with low frequency alleles in scrambler samples, presumably representing deleterious mutations. This last result is consistent with the notion that condition-dependence of sexually selected traits makes them reliable indicators of genetic quality.

Overall, this thesis provides significant insights into the genomic basis of sexual selection and male morph determination in *R. robini*. The findings highlight the importance of sexual selection in shaping the distribution of genetic diversity, which is an important factor in managing wild populations, especially endangered ones.

Keywords: sexual selection, alternative reproductive tactics, genetic mapping, genome anchoring, GWAS, supergene

GENERAL INTRODUCTION

The evolution of elaborate and often bizarre sex-specific traits, which seem maladaptive in the context of survival, led Charles Darwin to formulate the theory of sexual selection (Darwin, 1872). In most animal species, males contribute less resources to offspring production than females, and their reproductive success increases with the number of mates. In contrast, female reproductive skew is relatively flat and is not associated with the number of mates (Bateman, 1948, but see Gowaty et al., 2012). This fundamental difference between the sexes leads to a reproductive competition, which is usually stronger between males, and to the evolution of secondary sexual characters, which serve either as ornaments that increase the attractiveness of their bearers (intersexual selection), or as armaments allowing them to outcompete rivals to obtain access to the opposite sex (intrasexual selection). Although sex role reversal is observed in some species, for the purpose of this summary, males are considered the competing sex (Andersson, 1994; Safari & Goymann, 2021).

Since sexually selected traits (SSTs) provide a reproductive advantage to their bearers, their expression is expected to be under strong directional selection, favouring males with the most elaborate ornaments or armaments. This intense selection should quickly fix male-advantageous alleles and erode heritable variation, leading to a loss of the benefits of mate choice (B. Charlesworth, 1987; Fisher & Bennett, 1999). On the other hand, sexual selection models based on the coevolution of SSTs and preferences for these traits assume genetic variance of these traits. This applies both to so-called Fisherian process, according to which preferences for the most elaborate SSTs evolve because sons of females exhibiting these preferences inherit the attractiveness of their fathers (Fisher, 1930), and to the 'good genes' mechanism, which explains the evolution of preferences through the relationship between the SST expression and genetic quality (Zahavi, 1975).

This apparent contradiction between the assumption of persistence of genetic variance in SSTs and the constant selection acting on them was termed the 'lek paradox' (Kirkpatrick & Ryan, 1991; Prokuda & Roff, 2014). The resolution of this paradox has been proposed in the genic capture hypothesis, which suggests that the expression of SSTs depends on an individual's condition (Andersson 1986, Rowe & Houle, 1996; Tomkins et al., 2004). This hypothesis assume that the condition is influenced not only by environmental factors, but also by genetic background, especially deleterious mutations, which constantly accumulate in genomes. Due to high variance in mutational load, only high-quality individuals can acquire enough resources

to develop. Indeed, SSTs often show higher condition dependence than non-SSTs (Bath et al., 2023; Bonduriansky, 2007; Bonduriansky & Rowe, 2005; Cotton et al., 2004; Delcourt & Rundle, 2011; Emlen et al., 2012), and are associated with a substantial somatic and developmental cost in order to ensure honesty of the signal (Iwasa et al., 1991; Zahavi, 1975). Therefore, despite strong selection on SSTs, the constant accumulation of deleterious load is expected to maintain a high variance in their expression, and only high-quality males can afford their development. Under the assumption of this mechanism, sexual selection should bring a range of benefits, including its potential to increase population fitness (Whitlock & Agrawal, 2009), rate of adaptation (Candolin & Heuschele, 2008; Iglesias-Carrasco et al., 2024), or preventing population extinction after a bottleneck (Jarzebowska & Radwan, 2009; Lumley et al., 2015). Also, due to its effect of removing deleterious load, sexual selection has also been proposed to compensate the costs associated with sexual reproduction (Agrawal, 2001; Siller, 2001).

On the other hand, the benefits of sexual selection might be offset by a decrease in male survival, particularly under stressful conditions, potentially leading to a population collapse and extinction (Kokko & Brooks, 2003). Moreover, higher variance in male reproductive success due to strong sexual selection may increase the impact of genetic drift, potentially reducing adaptive genetic variation and thus the evolutionary potential of the population. Furthermore, genetic diversity might be removed by strong directional selection on SSTs, as mentioned above. Sexual selection may also impose a negative influence on the population through sexual conflict. Firstly, many traits that increase male reproductive success, such as persistent courtship, can reduce the viability or fertility of females (Arnqvist & Rowe, 2005). Secondly, under strong sexual selection, the phenotypic optima of homologous traits in males and females diverge, resulting in selection of these traits in opposite directions. If the shared genome constraints the independent evolution of males and females, it may lead to a conflict within a genetic locus, where an allele beneficial to one sex decreases the fitness of the opposite sex (intralocus sexual conflict, Bonduriansky & Chenoweth, 2009). This process may reduce the benefits of sexual selection, because the sexes are constantly pushed away from their optimal trait expression (Pischedda & Chippindale, 2006, Arbuthnott & Rundle, 2012; Parrett et al., 2021). Intralocus sexual conflict results in a negative correlation between the fitness of a parent and offspring of the opposite sex (Calsbeek & Sinervo, 2004; Camperio-Ciani et al., 2004; Chippindale et al., 2001; Delph et al., 2004; Fedorka & Mousseau, 2004; Foerster et al., 2007). Although intralocus sexual conflict may be resolved by evolution of the sex-specific expression (Cox & Calsbeek, 2009; Mank, 2017a; Rice & Chippindale, 2001), its prevalence suggests that this resolution is not easily achieved.

However, according to recent theoretical models, intralocus sexual conflict may maintain genetic polymorphism under the mutation-selection balance for longer (Connallon & Clark, 2012; see also Rice & Chippindale, 2001a; Zajitschek & Connallon, 2018, Connalon & Clark 2014). The scope of balancing selection may be further increased if the expression of SSTs leads to pleiotropic effects, where a trade-off between SST expression and survival is present, or if the development of SST is associated with lower fitness in the opposite sex (Johnston et al.,

2013; Mérot et al., 2020; Plesnar Bielak et al., 2014; Radwan et al., 2016). Indeed, the footprint of balancing selection has been identified in sexually antagonistic loci in *Drosophila melanogaster* (Ruzicka et al., 2019), and in *Callosobruchus maculatus*, where sex-specifically expressed genes were assumed to be more sexually antagonistic (Sayadi et al., 2019). The evolve-and-resequence (E&R) approach offers a direct investigation of how sexual selection, and the associated sexual conflict shape the quality and quantity of genetic diversity. An E&R study on *D. melanogaster* did not show evidence for balancing selection associated with sexual conflict, but experimental lines selected for higher reproductive success exhibited more efficient purging of deleterious mutations (Dugand et al., 2019). However, this study used small populations, where the strong effect of genetic drift may have confounded the results. More robust evidence comes from an E&R study which controlled sexual selection intensity by performing mass selection on alternative mating phenotypes (ARPs) in the bulb mite, *Rhizoglyphus robini* (Parrett et al., 2022). The males of this species are dimorphic (Figure 1, Radwan, 2009; Radwan et al., 2000), and the existence of alternative reproductive tactics allows easy manipulation of the intensity of sexual selection and the associated sexual conflict. Fighter males are armed with a thickened third pair of legs, which they use to inflict fatal injuries during fights. In contrast, scrambler males, with unmodified legs, exhibit a typical 'sneaky' strategy, searching for unguarded females.

The expression of the weapon is costly (Łukasiewicz et al., 2020; Radwan, 1995) and can be suppressed by reducing diet quality, which indicates its dependence on physical condition (Łukasiewicz, 2020; Smallegange, 2011). Moreover, the expression of weaponry is suppressed by inbreeding, indicating its sensitivity to the effects of deleterious mutations that manifest with increased genomic homozygosity (Łukasiewicz et al., 2020a). Therefore, it can be predicted that the higher success of fighter males in reproductive competition (Radwan & Klimas, 2001) will lead to the purging of deleterious mutations from the genome. On the other hand, selection for this trait reduced reproductive success in females from the fighter-selected lines, suggesting the presence of intralocus sexual conflict (Łukasiewicz et al., 2020; Plesnar Bielak et al., 2014), which presumably results from the correlated expression of fighter-specific genes between sexes (Joag et al., 2016). This makes *R. robini* an excellent model for studying the impact of sexually-selected weapon evolution on the genetic variance maintained in populations. This species was used in the study I participated in (Parrett et al. 2022). The results revealed that fighter lines showed a greater decline in the number of non-synonymous segregating sites, which were enriched in rare, presumably deleterious variants, suggesting more effective purging of mutational load in this treatment, while scrambler lines accumulated deleterious load. Indeed, females from fighter lines exhibited lower inbreeding depression after one generation of full-sib mating. SNPs diverged between scrambler and fighter lines were scattered across the whole genome, but seven contigs showed particular enrichment in these SNPs. While this study provides compelling evidence of efficient purging of deleterious mutations occurring via sexual selection, it is possible that this effect was due to one or both of the following processes: sexual selection might have imposed strong direct selection on a male's condition, which is favoured during energetically demanding intrasexual fights, or alternatively, purging occurred via

condition-dependence in SST expression, as only high-quality males are able to develop the weapon (see above). Secondly, intrasexual fights may have intensified sexual selection and directly caused selection for high male condition, which gives an advantage in energetically demanding male combats. In the latter case, the 'genic capture' mechanism would not be directly associated with the weapon expression itself, but, for example, to metabolic traits affecting fighting efficiency, which were absent in lines selected towards scrambler males. This distinction is important from the point of view of testing the hypothesis about maintaining variability in SSTs. To understand which of the two factors prevails in purging deleterious mutations, additional experimental evidence and knowledge of the genetic architecture underlying this SST are necessary (Johnston et al., 2013). While selection on alternative male morphs in *R. robini* led to a divergence across many SNPs throughout the genome, seven contigs were significantly enriched in these diverged SNPs, suggesting their major role in morph determination (Parrett et al., 2022). Indeed, alternative male phenotypes have a significant heritable component, evidenced in quantitative genetic experiments (Parrett et al., 2023, Radwan 1995) suggesting a single-locus morph determination. Therefore, it cannot be ruled out that the aforementioned polygenic signal of divergence between fighter- and scrambler-selected lines does not result directly from selection for or against weaponry, but rather from the second mechanism, i.e., indirect selection of other traits, such as those related to metabolic efficiency, which give an advantage in fights. Additionally, due to the absence of a chromosome-scale assembly, we could not determine whether the seven contigs enriched in divergent SNPs originate from distinct genomic regions or reside in the close proximity, creating for example, a tightly-linked supergene.

AIMS OF THE THESIS

The aim of the research presented in this dissertation was (1) to assemble the bulb mite genome to a chromosome scale, (2) to examine whether components of sexual selection other than those related to the presence of weaponry effectively remove deleterious mutations from the population, and (3) to map genomic regions associated with the expression of weaponry in order to determine whether the male morph is determined by many polymorphisms scattered throughout the genome, in accordance with the genic capture hypothesis, or rather results from polymorphism in one or a small number of loci with large effects. These three objectives correspond to the three chapters described in the subsequent parts of the dissertation.

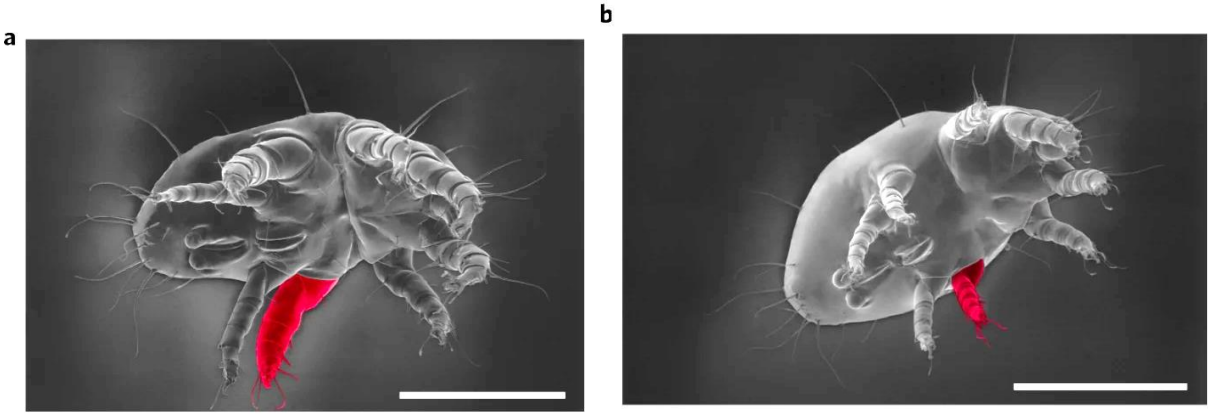

Alternative morphs of bulb mite males: fighter male possessing thickened third pair of legs (a) and scrambler male with unmodified legs (b). The scale bar is 300 μm. Source: Parrett et al. 2022, modified.

CHAPTER I

Sex-specific recombination landscape in a species with holocentric chromosomes

SEBASTIAN CHMIELEWSKI[1], MATEUSZ KONCZAL[1], JONATHAN M. PARRETT[1], STEPHANE ROMBAUTS[2,3], KATARZYNA DUDEK[4], JACEK RADWAN[1], WIESŁAW BABIK[4]

[1] Evolutionary Biology Group, Adam Mickiewicz University, ul. Uniwersytetu Poznańskiego 6, 61-614 Poznań, Poland
[2] Department of Plant Biotechnology and Bioinformatics, Ghent University, 9052 Ghent, Belgium
[3] Center for Plant Systems Biology, VIB, 9052 Ghent, Belgium
[4] Institute of Environmental Sciences, Faculty of Biology, Jagiellonian University, Gronostajowa 7, 30-387 Kraków, Poland

Abstract

The rate and chromosomal positioning of meiotic recombination significantly affects the distribution of the genetic diversity in eukaryotic genomes. Many studies have revealed sex-specific recombination patterns, with male recombination typically biased toward chromosome ends, while female recombination is more evenly distributed along chromosomes, or concentrated near the chromosome center. It has been proposed that such patterns in females may counteract meiotic drive caused by selfish genetic elements near centromeres and should not occur in species devoid of clearly defined centromeres, but evidence for the latter expectation is scarce. Here, we constructed a sex-specific genetic map of a species with holocentric chromosomes, the bulb mite (*Rhizoglyphus robini*), a sexual selection model with alternative male reproductive phenotypes. We found a similar recombination landscape in both males and females, with a consistent pattern of increased rates towards both chromosome ends, and a higher recombination rate in females than in males. A region on chromosome 7, carrying a high density of markers associated with the expression of alternative male reproductive phenotypes, was among several regions with a particularly low male recombination rate. We detected a positive correlation between the recombination rate and repeat density (highest at chromosome ends), and a negative correlation with gene density (peaking at chromosome centers). Our results are consistent with the meiotic drive hypothesis and suggest that recombination evolution is closely linked to chromosome features.

keywords: recombination landscape, heterochiasmy, holocentric chromosomes, linkage mapping, genome anchoring

1. Introduction

Intragenomic heterogeneity of recombination rate is a major determinant of genetic variance through its effect on the efficacy of both positive and purifying selection (Coop & Przeworski, 2007; Ellegren & Galtier, 2016; Webster & Hurst, 2012). Therefore, interpretation of studies aiming to understand processes shaping genetic variation, a key parameter determining the response to selection, is likely to be incomplete unless one takes the genome-wide recombination landscape into account. Local recombination rates are influenced by several factors. They correlate with genomic features including the densities of genes and repeat elements, the GC content, and the distance to the chromosome end (reviewed in Peñalba & Wolf, 2020; Ritz et al., 2017; Stapley et al., 2017). Chromosomal rearrangements, including inversions (Berdan et al., 2021; Wellenreuther & Bernatchez, 2018), or fusions and fissions (Näsvall et al., 2023), may also affect recombination rates. Moreover, large sex differences in recombination rates have been observed in many eukaryotic species (Lenormand & Dutheil, 2005; Stapley et al., 2017) with profound implications for the evolution of sex chromosomes (Charlesworth, 2017), the genetic architecture of complex sexually selected traits (Kasimatis et al., 2021), and the resolution of sexual conflict (Connallon & Clark, 2010).

Recent meta-analyses across a wide array of species have consistently highlighted sex differences in recombination rates, termed heterochiasmy, and in the distribution of crossover events along chromosomes, referred to as recombination landscape (Cooney et al., 2021; Lenormand & Dutheil, 2005; Sardell & Kirkpatrick, 2020). Female genetic maps are often longer than male maps, indicating a higher overall recombination rate in females. Heterochiasmy is hypothesized to be associated with various factors including differences in the intensity of sexual selection (Lenormand, 2003; Trivers, 1988), sexual antagonism (Sardell & Kirkpatrick, 2020), and the mechanistic differences during the progression of meiosis between males and females (Hunt & Hassold, 2002). The causes underlying sex-specific recombination landscapes are less well understood, though some mechanisms have been proposed (Cahoon et al., 2023; Sardell & Kirkpatrick, 2020). In females, crossovers are typically distributed evenly along the chromosomes or are somewhat biased towards chromosome centers. In contrast, males tend to exhibit recombination events near chromosome ends (Cooney et al., 2021; Peterson & Payseur, 2021; Sardell & Kirkpatrick, 2020).

The positioning of crossover events during meiosis is crucial from an evolutionary perspective because it regulates the amount of DNA exchanged between homologous chromosomes (Veller et al., 2019). If crossovers are strongly localized near chromosome ends in both sexes, the exchange of DNA occurs only at the chromosome tips, thereby largely preserving existing allelic combinations. Conversely, recombination near the centromere has been associated with a higher risk of chromosomal mis-segregation (Nambiar & Smith, 2016). This suggests that the pattern of crossovers in chromosome central regions has some benefits in female meiosis that outweigh this cost. One such benefit could be a defense against selfish elements causing meiotic drive. Unlike spermatogenesis, in which four gametes are produced, oogenesis results in a single viable

egg and three inviable polar bodies. The segregation of chromosomes into the egg or a polar body is influenced by the centromere's efficiency in kinetochore binding (Clark & Akera, 2021; Talbert et al., 2009). Selfish genetic elements can exploit this mechanism by enhancing the centromere's size or activity, thus favoring their transmission to the egg rather than to polar bodies (Haig, 2010). Brandvain & Coop (2012) hypothesized that recombination near chromosome centers in females could represent an adaptive response to meiotic drivers, effectively uncoupling drive alleles from the centromere.

Organisms with holocentric chromosomes, which lack a localized centromere, could help to evaluate the meiotic drive hypothesis and the centromere's influence on the evolution of sex-specific recombination landscapes. According to the meiotic drive hypothesis, holocentric organisms are expected to have similar recombination landscapes in both sexes (Brandvain & Coop, 2012). This is because, in the absence of a localized centromere, allowing crossovers to occur nearer to the chromosome center in females would not confer any evolutionary advantage. Currently, research on recombination in holocentric chromosomes remains sparse, primarily limited to studies on *Caenorhabditis elegans* and Lepidoptera (moths and butterflies). However, *C. elegans* is hermaphroditic (Meneely et al., 2002), and Lepidoptera are not well suited for testing the meiotic drive hypothesis because meiosis is achiasmatic in females.

Holocentric chromosomes, characterized by a diffuse centromere, have been found in approximately 350,000 animal and plant species (Král et al., 2019). Among these, acariform mites represent a group of particular interest due to their diverse roles in ecosystems and impacts on human activities. The acariform mites include species of economic importance such as agricultural pests (e.g., the spider mites *Tetranychus urticae* and bulb mites *Rhizoglyphus robini*) and allergenic species (e.g., dust mites *Dermatophagoides spp.*). However, genomic resources for mites remain scarce, and, to date, no sex-specific whole-genome linkage map has been published for any mite species. Considering the over 40 thousand described acariform species (Walter & Proctor, 2013), only five species currently have genomes assembled to chromosome-scale resolution. Next-generation sequencing technologies hold promise for the development of detailed genetic maps, which can be used for anchoring genomes to a chromosome scale (Fierst, 2015), and should yield reliable data concerning recombination patterns and possible sex differences (Peñalba & Wolf, 2020).

Here, we developed sex-specific linkage maps of the bulb mite (*Rhizoglyphus robini*), and characterized the genomic factors that correlate with local recombination rates. Furthermore, we used the linkage map to obtain a chromosome-scale genome assembly. Bulb mites are economically important pests (Díaz et al., 2002), but also a convenient laboratory model (Gerson et al., 1991) used in evolutionary and ecological studies (e.g. Plesnar-Bielak et al., 2013; Smallegange et al., 2017). In particular, it is valuable for studies of sexual selection, due to the presence of two distinct male morphs differing in expression of a sexually selected trait (Radwan, 2007). Fighter males possess an enlarged third pair of legs which they use as a weapon in intrasexual competition, while scrambler males, with unmodified legs, adopt a non-aggressive strategy to obtain access to females (Radwan, 2009). A recombination map anchored

to the genome assembly will facilitate identification of genomic regions affecting male morph determination, a trait which shows high additive genetic variance (Parrett et al., 2023). Pinpointing these regions has been problematic due to highly fragmented bulb mite genome assembly that has been published recently (Parrett et al., 2022). Finally, our linkage map allows us to examine the heterochiasmy and sex-specific recombination patterns in a species with holocentric chromosomes. This has implications for the meiotic drive hypothesis proposed by Brandvain & Coop (2012), which has not yet received empirical support.

2. Materials and methods

1.1. Experimental crosses

We used inbred lines established by 10 generations of sib-crossing before the experiment started (Łukasiewicz et al., 2020; Parrett et al., 2023). Four mapping families were created by crossing mites from different lines. Mites were housed at 23°C in glass vials (~1 cm diameter) with a plaster-of-Paris base soaked in water to maintain high humidity and fed with dry yeast ad libitum.

To select individuals for the crosses, we isolated juvenile mites from the inbred lines into separate glass vials, to ensure the females eclosed were virgins. Upon reaching maturity, we scored the mites for sex and male morph, then paired a single male and female in new vials to form the parental P-generation. After three days of mating, P individuals were transferred to low-DNA-binding tubes containing DNA isolation buffer (digestion solution from the MagJET gDNA Kit, Thermo Fisher Scientific) and stored at -20°C for subsequent DNA extraction. The eggs were left to hatch in the vials. The emerged F1 mites were separated into individual vials before reaching maturity, and subsequently sexed and mated with full-sibs. For each of the four families, we selected the F1 pair with the highest reproductive output for further breeding (Table 1). We separated F2 individuals as larvae, sexed them when mature, and then placed them in the DNA isolation buffer. In total, we used 199 bulb mites from the four families to construct the genetic map, comprising 8 P, 8 F1, and 183 F2 individuals, with the number of F2 individuals per family ranging from 32 to 60 (Table 1).

1.2. Repeat masking

We identified repeat sequences in the VIB_bulbmite_20200 genome assembly (Parrett et al., 2022) using the RepeatModeler pipeline, which integrates several software tools each designed to detect specific types of repeats (Flynn et al., 2020). This process produces a FASTA library of representative repeat elements, which was annotated to classify the types of repeats found. We then combined this file with the Repbase public reference data files, which contain known repeat elements from other organisms, to enhance the completeness of our library (Jurka et al., 2005). We used the merged FASTA library with RepeatMasker (http://www.repeatmasker.org, Tarailo-Graovac & Chen, 2009) to mask the genome before proceeding with mapping and annotation. The repeats were soft-masked (bases in masked regions were indicated by lowercase letters).

1.3. Whole-genome resequencing and calculating genotype likelihoods

We extracted genomic DNA from whole individuals using the MagJet Genomic DNA Isolation Kit (Thermo Fisher Scientific), following the kit's standard protocol. Next, we prepared genomic libraries with the NEBNext Ultra FS II kit (New England Biolabs) and resequenced the whole genomes at the SNP&SEQ Technology Platform in Uppsala, Sweden using Illumina NovaSeq6000 with the S4 flow cell, producing paired-end reads of 150 bp in length. We aimed for an expected coverage of 20X for parental and F1 samples, and 10X for the F2 samples.

To clean the data, adapter sequences and low-quality bases were removed using Trimmomatic (v. 0.39; Bolger et al., 2014). The reads were mapped to the VIB_bulbmite_20200 genome assembly (Parrett et al., 2022) using bwa-mem (v. 0.7.17; Li, 2013) with default settings. Samtools (v. 1.19; Li et al., 2009) was used to mark duplicates and retain only reads with mapping quality above 20.

To address genotyping errors arising from low sequencing coverage, instead of calling genotypes, we calculated genotype likelihoods for the initial set of SNPs using samtools mpileup and the mpileup2Likelihoods script (LepMap3, Rastas, 2017). We assessed the relatedness between individuals within each family using the Identity By Descent (IBD) module of Lep-Map3 (Rastas, 2017), using a subset of random 10% of the markers.

1.4. Linkage mapping

We constructed the bulb mite genetic map using Lep-Map3, following its standard pipeline. Initially, the ParentCall2 module was used to correct missing or erroneous parental genotypes, eliminate non-informative markers, and identify sex-linked markers. We filtered out markers showing significant segregation distortion (dataTol = 0.05), those with a minor allele frequency across families below 0.15, and those with a missing genotype rate within families exceeding 10%. Two F2 samples were discarded due to insufficient sequencing coverage (<0.1X), and one was excluded due to its high rate of missing data, as determined by PLINK (v. 1.9; see supplementary data). We retained only markers that were informative across all four families, except when a contig had fewer than five markers; in such cases, we included markers informative in three families. To assign markers to linkage groups, SeparateChromosomes2 was used with a LOD threshold optimized by testing values from 15 to 19. We chose the LOD threshold of 18, which distributed markers into eight linkage groups, the bulb mite haploid chromosome number (Parrett et al., 2022)

We generated a sex-averaged map using OrderMarkers2 with the Kosambi mapping function, relying on P-generation data to phase the F1 and F2 genotypes. The bulb mite has an XX/X0 sex-determining system. In contrast to the diploid autosomes, males carry only a single copy of the X chromosome. Therefore, only female-informative markers were used to establish the marker order on the sex chromosome. The ordering was repeated 60 times, selecting the iteration with the highest likelihood for our final map. Single markers that extended the ends of the chromosome map by more than 1 cM were excluded, as these are likely to indicate genotyping errors. LMPlots visualized with Lep-Map3 highlighted a single error on chromosome 4, which we corrected by removing three adjacent crossovers, following the

software author's recommendation (Pasi Rastas, personal communication; see supplementary data and Figure S6).

1.5. Genome anchoring

Lep-Anchor (Rastas, 2020) was used to anchor the bulb mite genome, based on the intervals of genetic marker positions determined by OrderMarkers2. The anchoring process was supported by Oxford Nanopore reads, which had also been used for assembling the original reference genome (Parrett et al., 2022), and were mapped to the reference genome with minimap2 (v. 2.24; Li, 2018).

To identify haplotigs—false apparently duplicated regions arising from high local heterozygosity—we used HaploMerger2 (S. Huang et al., 2017) with a custom score matrix and a chain file containing contig-contig alignments. Genetic markers from the haplotigs were transferred to the primary contigs using the LiftoverHaplotype module. Additionally, we identified a chimeric contig that erroneously spanned two chromosomes, which we split using CleanMap. PlaceAndOrientContigs was used to determine the order and orientation of contigs on chromosomes. This module organizes the contigs by iteratively maximizing the correlation between the physical and genetic distances of markers. Subsequently, the contigs were propagated using the long ONT reads and the chain file. Contig blocks without map support were removed. In the final step, we adjusted the chromosome labels to reflect their physical sizes.

1.6. Evaluation of the linkage map

We evaluated the genetic map based on the physical positions of markers after anchoring. The evaluation was conducted using the OrderMarkers2 module with the Kosambi mapping function, applying parameters: UsePhysical, ImproveOrder = 0, and EvaluateOrder = 1, using P-generation data to phase genotypes. To produce sex-specific maps, we generated a female map using markers informative in mothers or in both parents (infMask = 23), and a male map with markers informative in fathers or in both parents (infMask = 13). The evaluation of the sex chromosome was based only on the female-informative markers (infMask = 2). Diagnostics of the map using LMPlot identified a mis-join on chromosome 6, which we resolved by removing three adjacent crossovers, following guidance from Pasi Rastas (personal communication, see supplementary data and Figure S7). We analyzed the maps with custom R scripts and visualized them using the ggplot2 R package (Wickham, 2016).

1.7. Recombination landscape and heterochiasmy

We investigated the relationship between chromosome length and recombination rate or map length using linear models (LMs), incorporating sex as a categorical variable to allow for possible differences between males and females. To explore the sex-specific recombination landscape, we calculated recombination rates in 1Mb non-overlapping genomic windows by dividing the total genetic length of windows by their physical lengths. To standardize the comparison of the recombination landscape across all chromosomes, we scaled their lengths to unity by dividing the window positions by the total length of the relevant chromosomes. The recombination landscape was visualized separately for the male and female maps along each

chromosome using a LOESS smoothing line, with a span parameter of 0.75. Notably, we observed a sharp increase in recombination rate near chromosome ends. To quantify this effect, we calculated a periphery bias by dividing the recombination rate in the outer 10% of the physical length at each chromosome end (distal parts) by the average recombination rate across the entire chromosome, following Haenel et al. (2018).

To investigate whether sex differences in crossover positioning contribute to variation in the amount of DNA exchanged during meiosis, we calculated the probability that a random pair of positions (also referred to as a "locus") from the same chromosome will recombine due to a crossover event (termed intrachromosomal shuffling, or $\overline{r}_{intra}$ by Veller et al., 2019), using the following equation:

$$\overline{r}_{intra} = \sum_{k=1}^{n} 2p_k r_k L_k^2$$

In this equation p_k denotes the proportion of chromosome k carrying one parental haplotype, while r_k represents the proportion of the same chromosome inherited from the other parent. L is the proportion of the entire genome contributed by chromosome k. Due to minor gaps in phasing, as shown in Figure S9, the sum of, $p_k + p_l$ does not equal 1 (see Figure 5 in Veller et al., 2019). Next, we estimated the probability of recombination between two loci located on different chromosomes (interchromosomal shuffling, or $\overline{r}_{inter}$) using the following equation:

$$\overline{r}_{inter} = \frac{1}{2}\left(1 - \sum_{k=1}^{n} L_k^2\right)$$

1.8. Identification of genomic features affecting recombination rate

To assess which features within the bulb mite genome correlate with the recombination rate, we explored the relationship between crossover counts in 2 Mb windows and the following genomic features: gene and repeat element density, distance to chromosome ends, and GC content. We downloaded the bulb mite genome's predicted gene annotation from ORCAE (Parrett et al., 2022; Sterck et al., 2012, https://bioinformatics.psb.ugent.be/gdb/Rhizoglyphus_robini), which contains an unexpectedly high number of predicted genes (60,310 genes), suggesting the presence of pseudogenes or gene prediction errors. To refine the dataset, we excluded genes with expression levels below 1 FPKM, based on expression data from Plesnar-Bielak et al. (2022). This filtering retained 27,363 genes mapped to chromosomes. We determined the proportion of each window covered by genes (including introns), splitting genes at window boundaries when necessary. Repetitive sequences were quantified from the de novo dataset described above, and the distance to chromosome ends was calculated from each window's midpoint. The GC content of windows was determined using bedtools nuc (v2.27.1,Quinlan & Hall, 2010). Given the substantial collinearity among genomic features and the absence of crossovers in many windows, directly modeling associations with recombination counts proved challenging.

Instead, we calculated Pearson's correlation coefficients (ϱ) between crossover count and genomic features in 50 kb windows.

2. Results

2.1. Sequencing and linkage mapping

Whole-genome resequencing of the 196 samples in our families yielded a total of 6.26 $\times 10^9$ reads. After mapping and removal of reads with low mapping quality, we retained 4.43 $\times 10^9$ reads and 196 individuals (Table S1). The mean coverage was 21.3X in the P and F1 samples, and 9.25X in the F2 samples. Filtering based on minor allele frequency, family informativeness, and segregation distortion reduced the number of SNPs from 8,709,873 to 332,682. Subsequently, 300,355 markers (90.3% of the filtered SNPs) were assigned to 8 linkage groups, which were used to construct the linkage map.

2.2. Linkage map

The bulb mite autosomal map included 254,226 markers. The female autosomal map spanned 257.81 cM, being 2.08 times longer than the male autosomal map (123.98 cM; Figure 1A). The high density of markers allowed us to obtain high resolution, with a mean inter-marker distance of 881 bp in the female map and 921 bp in the male map. The sex chromosome, which is hemizygous in males, contained 45,500 markers across 51.6 cM and showed the highest recombination rate among all chromosomes in both sexes, at 1.74 cM/Mb. Our analysis revealed a negative association between chromosome size and the mean recombination rate (LM: recombination rate ~ physical length + sex, adjusted $R^2 = 0.68$, P for the physical length = 0.035, Figure 1B). However, this observed pattern was primarily influenced by a particularly long chromosome 1, as the association becomes insignificant once chromosome 1 is excluded from the analysis ($R^2 = 0.58$, $P = 0.39$). However, the association between the physical and map lengths of autosomes was not significant (LM, adjusted $R^2 = 0.63$, $P = 0.86$, Figure 1C), and genetic lengths of male and female maps were not significantly associated either (LM, adjusted R^2 = -0.19, $P = 0.82$, Figure 1D).

2.3. Heterochiasmy, recombination landscape and allelic shuffling

Consistent with the genetic map length, the genome-wide autosomal recombination rate was 2.08 times higher in females than in males, with females exhibiting a mean recombination rate of 1.11 cM/Mb and males only 0.56 cM/Mb (Table 2). The sex-averaged recombination rate in bulb mites was 0.86 cM/Mb. In total, 516 crossovers were identified in female, and 205 in male parents.

The degree of heterochiasmy differed between chromosomes (Figure 1A, Table 2). Among chromosomes with markedly low recombination rate in the male map was chromosome 7, (Figure 1A), which harbors a high density of SNPs associated with the male morph (Parrett et al., 2022, Chmielewski et al., unpublished data). A similarly low male recombination rate is observed on chromosome 1.

Analysis of the periphery bias and the recombination rates across all chromosomes revealed a similar recombination landscape in both males and females, with a consistent pattern of

increased rates towards both chromosome ends (Figure 2A). Notably, the value of periphery bias exceeded 1 for all chromosomes (Table 2), indicating that recombination rates at chromosome ends were consistently higher than in their central regions. Periphery bias did not show significant association with either sex or with chromosome length (LM: periphery bias ~ sex + chromosome length; adjusted $R^2 = 0.004$, $P = 0.39$).

The estimated sex-averaged value of $\overline{r}_{intra}$ in the bulb mite genome was 0.0043. However, we found that the value of $\overline{r}_{intra}$ was three times higher in females than in males ($\overline{r}_{intra\,females} = 0.0089$, $\overline{r}_{intra\,males} = 0.0028$, Figure 2B). This difference could be attributed to the variation in either crossover location, or the overall recombination rate, since a higher frequency of recombination in one sex could increase the value of $\overline{r}_{intra}$. Given the largely similar recombination landscape between sexes, underscored by the lack of significant sex-based differences in periphery bias, the observed difference in $\overline{r}_{intra}$ probably arises primarily from the increased recombination rate during female meiosis. $\overline{r}_{intra}$ values were not significantly associated with the chromosome lengths (LM: $\overline{r}_{intra}$ ~ sex + chromosome length; $P = 0.16$, adjusted $R^2 = 0.14$).

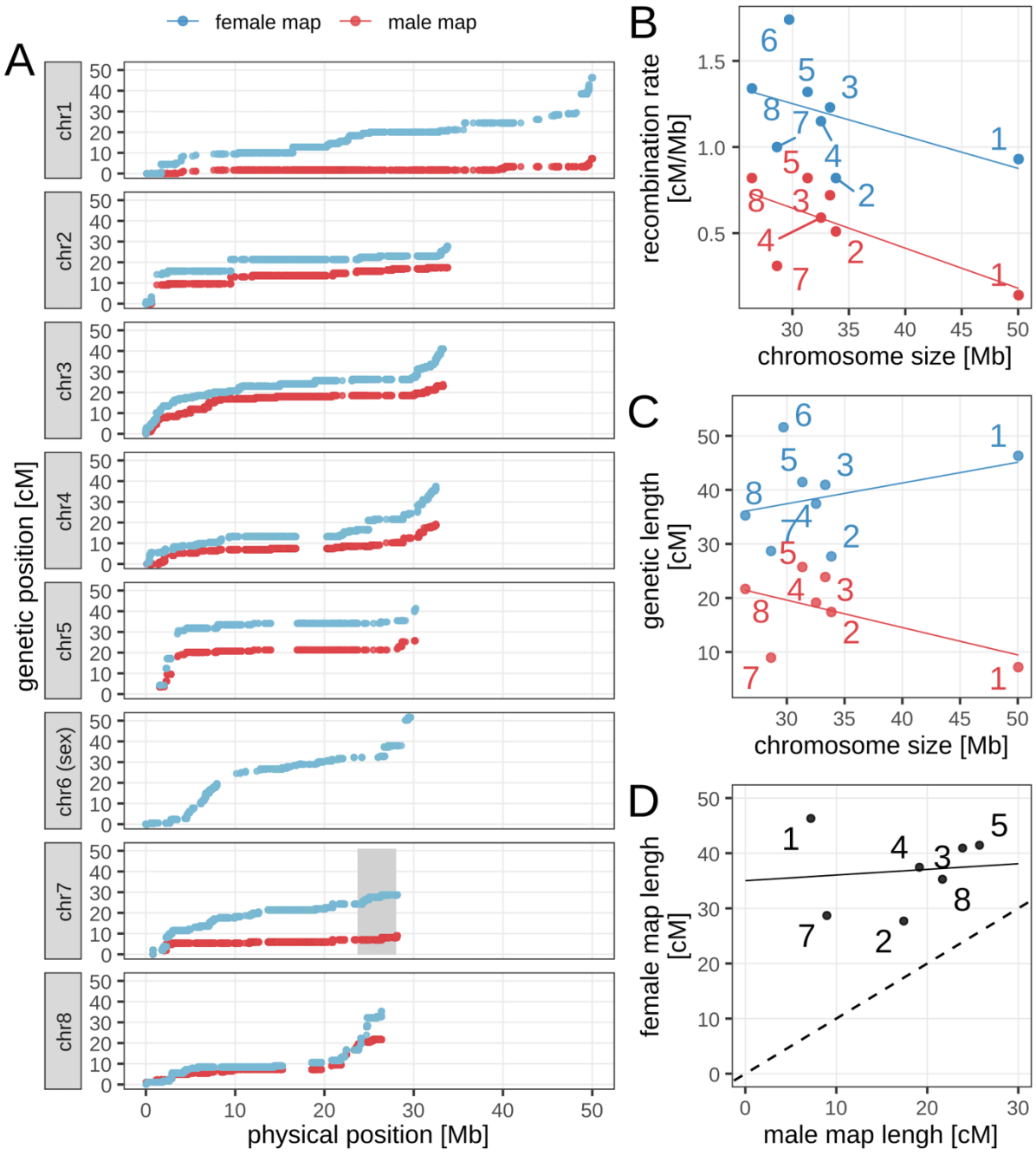

Figure 1: Sex-specific meiotic linkage maps and chromosome map length variation in the bulb mite. A: Marey maps displaying the genetic positions of markers in relation to their physical locations on the chromosomes. Regions with little change in genetic position, usually in chromosome centers, have low recombination rates, while steep slopes indicate high recombination rates. The locus responsible for determining male morph has been highlighted on chromosome 7. B: The relationship between recombination rate and chromosome size, showing higher recombination rates in shorter chromosomes ($P = 0.028$). C: The relationship between chromosomal map length and its physical size is not significant ($P = 0.86$). D: Comparison of map lengths for 7 autosomes, with female map lengths plotted against male

map lengths. The dashed line indicates expected relationship under equal map lengths for both sexes, and the solid line the observed regression slope ($P = 0.82$).

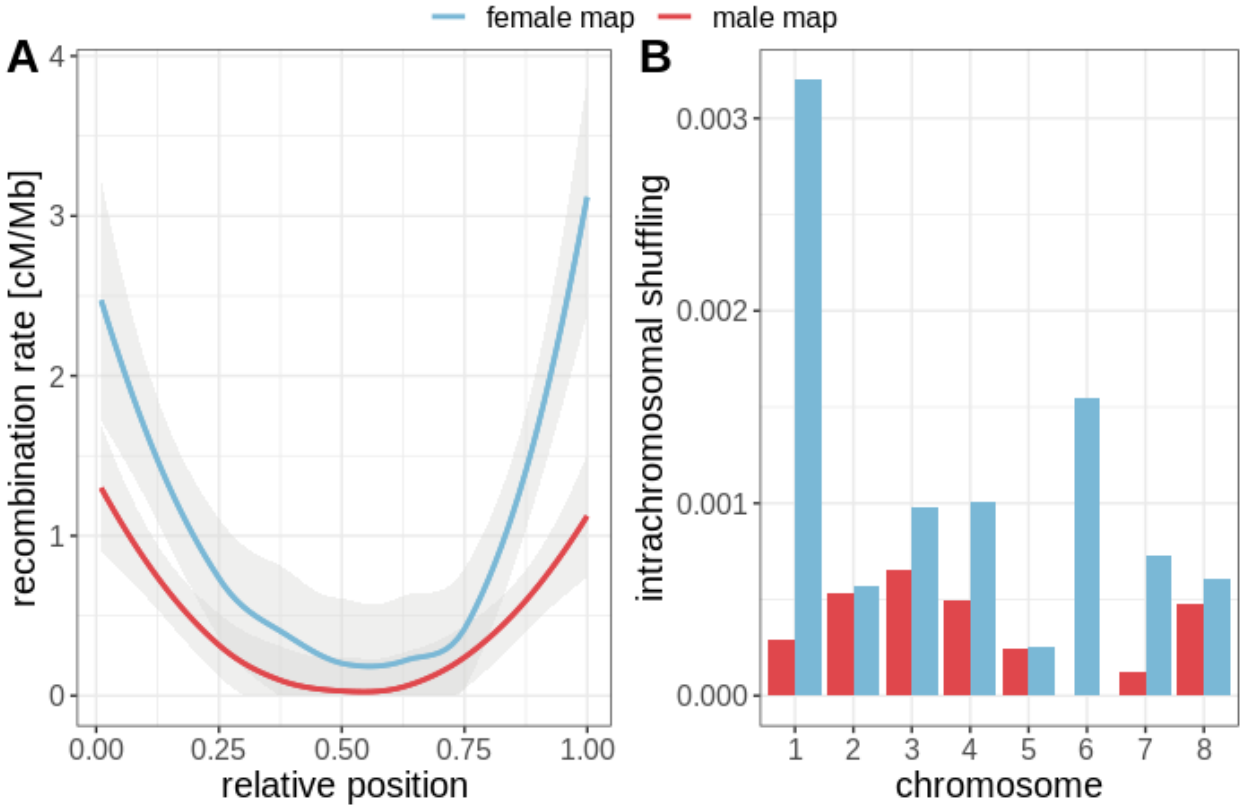

Figure 2: Sex-specific recombination patterns in the bulb mite genome. A: Smoothed loess line visualization of the recombination rates along the relative positions of all chromosomes, with the rates generally being lower in the central regions. The x-axis represents the relative position along the chromosomes, normalized from 0 to 1. B: Bar graph representing the average intrachromosomal shuffling value for each chromosome. Chromosome 6 is the sex chromosome.

2.4. Anchoring the bulb mite genome

The linkage map was used to anchor the contigs in order to obtain a chromosome-level genome assembly (Figure 1). A total of 397 contigs, accounting for 89.9% of the genome size, were successfully anchored onto 8 chromosomes. A total of 3.13 Mb, corresponding to 1.06% of the previous assembly length, was identified as redundant haplotigs and subsequently removed. Consequently, the overall genome size was reduced from the previous estimate of 307.49 Mb to 295.62 Mb, close to the 293 Mb predicted by flow cytometry (Parrett et al., 2022). The assembly's N50 value improved from 1.59 Mb for the previous bulb mite reference genome, to 32.53 Mb. The BUSCO score corroborates the high quality of the assembly, with 93.60% of the 2,934 core arachnid genes detected as complete (86% identified as full-length single-copy and 7.6% as duplicated), 1.6% classified as fragmented and only 4.8% missing. High N50 and BUSCO scores, along with the significant integration of the genome sequence into chromosomes, imply a comprehensive chromosome-level assembly, complete enough for

accurate genomic feature characterization and recombination landscape analysis in the bulb mite genome.

Aside from chromosome 1, the bulb mite chromosome sizes are quite uniform, ranging from 26-34 Mb. Overall, bulb mite chromosomes have gene-rich centers, with gene density tapering off towards the chromosome ends (Figure 3). The distribution of GC content mirrors that of gene density, while repeat density shows the inverse pattern, peaking near chromosome ends. Notably, the sex chromosome showed a greater abundance of repeat sequences (t-test = -2.65, $P = 0.008$) and lower gene density (t-test = - 25.17, $P < 0.001$) in 50 kb windows, compared to the autosomes.

Repeat sequences constitute 28.77% (85.06 Mb) of the bulb mite genome, with the most prevalent identified repeats being LTR retrotransposons and simple repeats, representing 2.07% and 1.98% of the genome length, respectively (Table 3). Notably, a significant proportion of repeats were unclassified. SINE transposons were absent in the assembly.

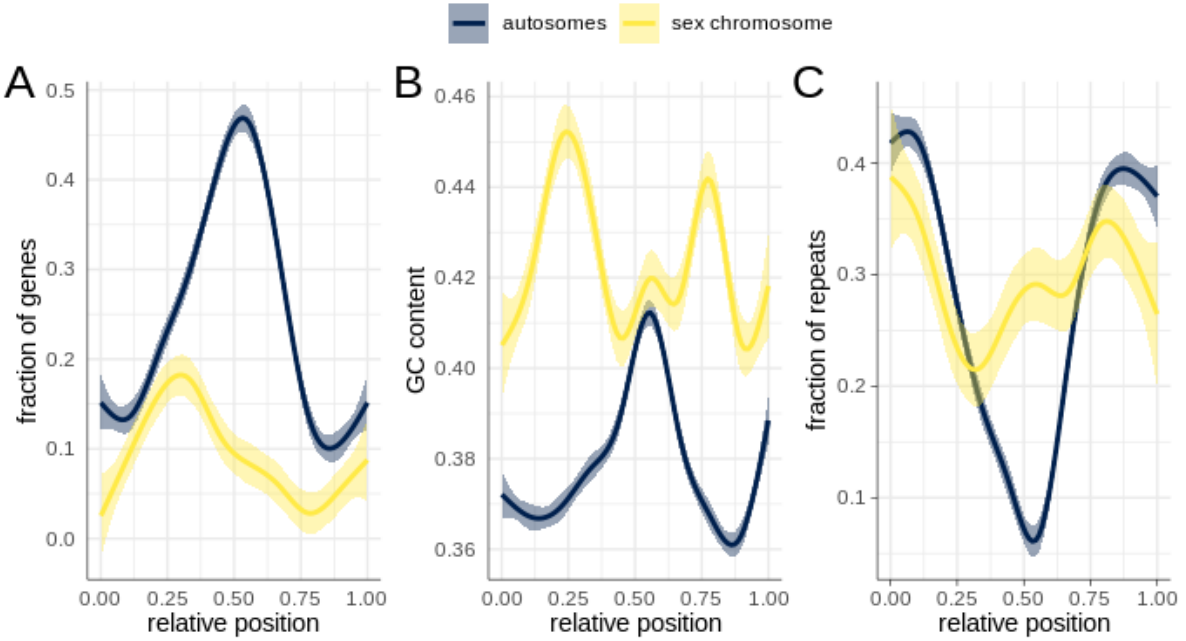

Figure 3: Distribution of genetic features across the autosomes and the sex chromosome in the bulb mite genome. Three measures are plotted in non-overlapping 50 kb windows, whose midpoints are normalized by the chromosome's total length, to show the results for relative chromosomal positions, and smoothed by a loess line with a 95% standard error. A: The proportion of window length covered by genes (including introns), B: GC nucleotides, C: repetitive elements.

2.5. Genomic features correlated with local recombination rate

To investigate the genomic features correlated with the recombination rate across the genome, we computed Pearson's correlation coefficients in 2 Mb windows. The crossover count is negatively correlated with both gene density (ρ = -0.27, $P = 0.0013$; Figure 4) and distance to

chromosome ends (ρ = -0.41, $P < 0.0001$). In contrast, it was positively correlated with repeat density (ρ = 0.3, $P = 0.0003$). No significant correlation was found between crossover count and GC content (ρ = -0.16, $P = 0.063$).

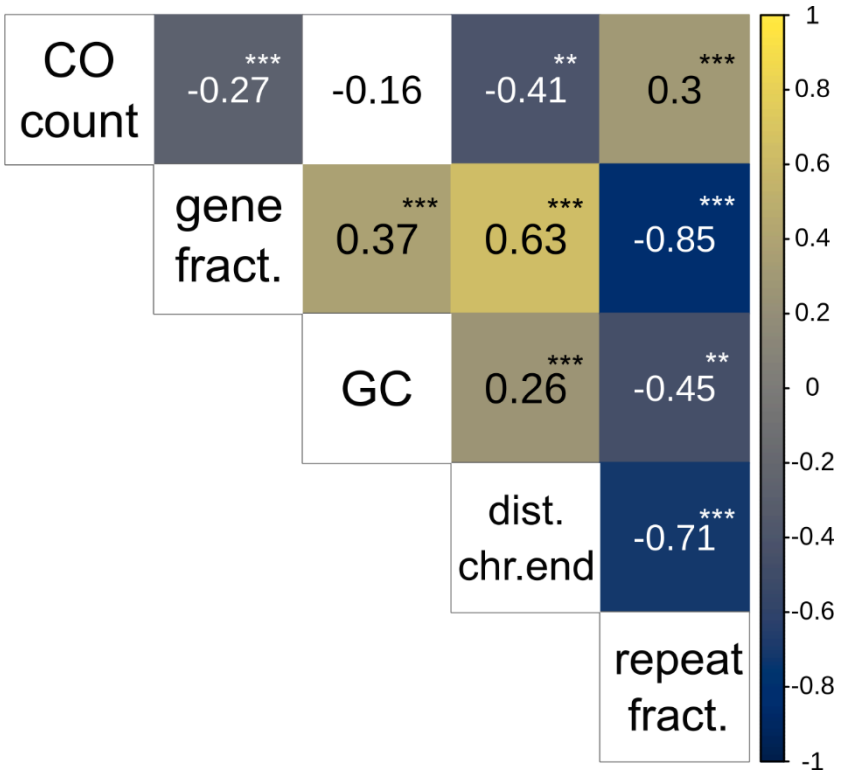

Figure 4: Correlation matrix showing Pearson's correlation coefficients. The matrix represents Pearson's correlation coefficients between various genomic features, with the intensity of the color indicating the strength and direction of the correlation (yellow for positive, blue for negative). Statistical significance levels are denoted by asterisks (*** *for* $P < 0.001$, ** for $P < 0.01$, and * for $P < 0.05$).

3. Discussion

To our knowledge, our genetic linkage map of *Rhizoglyphus robini* is the first sex-specific map for a gonochoristic organism with holocentric chromosomes. The absence of localized centromeres in chromosomes of this species enabled us to use our genetic map, constructed using whole genomes from nearly 200 individuals, to obtain a chromosome-level assembly of bulb mite, and then to evaluate the meiotic drive hypothesis for sex differences in the recombination landscape. Our results demonstrated that the recombination landscapes for females and males are similar, supporting the role of meiotic drive in evolution of sex specific recombination landscapes.

Our assembly of bulb mite chromosomes also allowed us to characterize the distribution of genomic features along them. We found a unimodal gene distribution with a central peak, the opposite of the distribution of repetitive elements. This pattern, with elevated recombination rates at chromosomal ends, mirrors the genomic architecture seen in *C. elegans*, another species with holocentric chromosomes (The *C. elegans* Sequencing Consortium, 1998). By contrasting

these observations with other species, we discuss the evolutionary importance of centromeres in the evolution of sex differences in recombination landscapes.

3.1. The bulb mite genome

The bulb mite genome, with a size of 295.62 Mb, is one of the largest acariform mite genomes. This group is characterized by notably compact genomes, with a median size of 129 Mb and a range from 32.5 to 487 Mb (Gregory & Young, 2020; Xiong et al., 2020). Our high-density linkage map enabled us to anchor 90% of the assembled genome length to chromosomes and to remove redundant haplotigs. Anchoring revealed that the chromosome sizes are fairly constant (Table 2), apart from chromosome 1 which is almost twice as long as other chromosomes. Conceivably, the increased size of this chromosome could be a result of chromosome fusion, which is further supported by its low recombination rate, characteristic of fused chromosomes (Näsvall et al., 2023), and bimodal distribution of gene, GC and repeat content of this chromosome (Figure S8).

Bulb mite chromosomes are characterized by gene-rich and GC-rich chromosome centers, as well as a high density of repetitive elements at the chromosome ends, similar to those observed in other holocentric animals (Cicconardi et al., 2021; The *C. elegans* Sequencing Consortium, 1998; Zhou et al., 2023). The sex chromosome exhibits a significantly lower gene density compared to autosomes, like in other holocentric organisms with X0 sex determination systems (N. Anderson et al., 2022; Y. Li et al., 2019; The *C. elegans* Sequencing Consortium, 1998). However, the pattern of reduced gene content on the sex chromosome is not universal and appears to depend on the age of the sex chromosome. Indeed, a similar gene density between autosomes and sex chromosomes has been reported in the dragonfly *Pantala flavescens* (Liu et al., 2022).

Repeated sequences constitute 28% of the bulb mite genome, nearly double the amount found in *Tyrophagus putrescentiae*, the only other acarid species with an available chromosome-scale reference genome assembly (Zhou et al., 2023). Importantly, most of these repeats have not been assigned to any known repeat category, indicating a potential area for future research. The observation that the sex chromosome is enriched in repeats compared to autosomes (Figure 3C), is probably because the sex chromosome spends one-third of its time in males in which it does not recombine; its overall recombination rate per generation is therefore lower than that of autosomes. The X chromosome also has a lower effective population size than the autosomes. At a 1:1 sex ratio, there are 4 autosomes per 3 X chromosomes, which might also contribute to the X chromosome having a higher expected repeat density, and lower gene density. These combined effects of reduced recombination rate and effective population size lead to higher Hill-Robertson interference, a genetic phenomenon where linked loci interfere with each other's ability to respond to natural selection. Consequently, TE insertions, which are generally harmful, are less effectively eliminated from the sex chromosome.

3.2. Genome-wide and chromosomal recombination rates

The sex-averaged recombination rate observed in the bulb mite is 0.86 cM/Mb, similar to the mean rate observed across insects (1.03 cM/Mb, Stapley et al., 2017; Wilfert et al., 2007). The

closest relative of the bulb mite that has been genetically mapped, the spider mite *Tetranychus urticae*, exhibits a significantly higher recombination rate of 7.63 cM/Mb (Sugimoto et al., 2020). In contrast, the recombination rate of more distantly related deer tick, *Ixodes scapularis* (Ullmann et al., 2003), has been estimated at 0.006 cM/Mb. However, the estimate for the *I. scapularis* was based on only 127 markers for the genome size of 2.1 Gb, compared to almost 300 thousand markers used in our study. Consequently, this may lead to an underestimation of recombination rate, for instance, if terminal markers were not consistently included and many crossover events occurred in terminal regions.

In our study, we observed that longer chromosomes had lower recombination rates (Figure 1B). This may reflect the requirement for at least one crossover per chromosome in eukaryotes (Brazier & Glémin, 2022; Hughes & Hawley, 2020; Otto & Payseur, 2019; Stapley et al., 2017), except in species in which meiosis in one sex is achiasmate (e.g., Lepidoptera females and *Drosophila* males), where alternative mechanisms have evolved to ensure proper chromosome segregation. Nevertheless, a chromosome's physical and map lengths were not associated (Figure 1C). This may be due to undetected recombination events, perhaps especially in male meiosis, as suggested by the relatively short genetic length of chromosomes (Table 2, Figure 1A). Given high density of marker distribution and accurate phasing based on the grandparental generation (Figure S9), it is unlikely that we missed crossovers perhaps except for close proximity to chromosome ends, where informative markers were absent. In monocentric chromosomes, such terminal chiasmata can lead to improper chromosome segregation due to insufficient tension between homologues, resulting in premature sister chromatid separation (Hassold et al., 2021; Hassold & Hunt, 2001; Koehler et al., 1996; Nagaoka et al., 2012; Nambiar et al., 2019; Ottolini et al., 2015). In contrast, in holocentric chromosomes, terminal chiasmata are common (de Bigliardo et al., 2011; Heckmann et al., 2014; John, 1990; Lukhtanov et al., 2018; Nokkala et al., 2004; White, 1973; Wrensch et al., 1994). Additionally, short genetic distances of our maps, which do not exceed 50 cM may stem from achiasmate meiosis in bulb mite, which could be more common in males. In more distantly related diplodiploid mite species the meiosis is achiasmate (Wrensch et al. 1994). This could be further studied with cytological observations of bulb mite chromosomes. Nonetheless, since terminal crossovers do not involve exchanges of genes, our characterization of the recombination landscape appears largely complete.

3.3. Heterochiasmy and sex-specific recombination landscape

The genetic map of the bulb mite reveals marked sex-based differences in recombination rates: females exhibit rates nearly double those of males. Bulb mites show fairly similar recombination landscapes in both sexes, with recombination rates increasing towards chromosome ends (Figure 2A). This finding diverges from those in the majority of taxa studied so far, where males generally show higher recombination rates at telomeres and females at chromosome centers, a difference often linked to meiotic driver defense mechanisms (Brandvain & Coop, 2012; Haig, 2010; Talbert et al., 2009). In contrast, the bulb mite's sex-specific genetic map demonstrates the absence of increased recombination in female chromosome centers. This finding supports the hypothesis that holocentricity mitigates centromere-biased meiotic drive.

However, to generalize our findings, additional sex-specific genetic maps from other holocentric taxa are necessary.

Despite similar recombination landscapes (Figure 2A), females exhibit intrachromosomal shuffling rates that are three times higher than in males. This disparity between sexes therefore appears to be largely due to a higher overall frequency of crossovers in females, rather than differences in recombination landscape. This is supported by the observation that periphery bias does not significantly differ between males and females. The difference in crossover location between sexes may stem from sex-specific crossover interference, which more strongly affects male crossovers, increasing physical distance between subsequent recombination at the same chromosome (Falque et al., 2007; Haenel et al., 2018; Otto & Payseur, 2019; Zhang et al., 2014), or from the sex difference in meiosis progression during synapsis (Cahoon et al., 2023; Cahoon & Libuda, 2019; Zickler & Kleckner, 2016). This pattern, with male recombination restricted to distal parts of chromosomes, aligns with observations in fish and amphibians (Bergero et al., 2019; Brekke et al., 2023; Brelsford et al., 2016; Jeffries et al., 2018; Kai et al., 2011; Sardell et al., 2018).

Heterochiasmy, the difference in recombination rates between sexes, is proposed to evolve in the sex that experiences more intense selection to maintain beneficial allele combinations (Sardell & Kirkpatrick, 2020; Trivers, 1988). In bulb mite males, intense sexual selection involves sperm competition and physical contests, initiated by fighter males and sometimes escalating to lethality (Radwan, 1997; Radwan, Czyz, et al., 2000). Being an effective fighter requires co-expression of the weapon with behavioral and physiological traits (e.g. aggression, motor patterns and energy mobilization), which could be facilitated if alleles making good fighters, but poor scramblers, are co-inherited. It is therefore suggestive that a large region on chromosome 7, where an important weapon-determining region has been located (Chmielewski et al., unpublished data; Parrett et al., 2022), coincides with a region with a markedly low male recombination rate, despite it being at the end of a chromosome (Figure 1A). On the other hand, it has been suggested that the sexual selection might promote increased recombination (Burt et al., 1991; Felsenstein, 1988; Maynard Smith, 1985), although empirical evidence does not support increased map length in the sex under stronger selection (Cooney et al., 2021; Mank, 2009). An alternative explanation for heterochiasmy involves sexual antagonism. Sardell & Kirkpatrick (2020) proposed a model where conflict arises over epistasis between alleles controlling the expression of a sexually antagonistic trait, with males benefitting from high linkage disequilibrium to maintain its high expression, while females gain from disrupting this allele association to mitigate fitness decrease associated with the pleiotropic effect of the male trait. This hypothesis has been supported in guppies (*Poecilia reticulata*), where strong heterochiasmy largely limits male recombination to a small, terminal pseudoautosomal region, whereas female recombination remains relatively uniform across the sex chromosome carrying sexually antagonistic color traits (Bergero et al., 2019; D. Charlesworth et al., 2020). Sexual antagonism may also shape heterochiasmy in bulb mites; the thick legs serving as a weapon are not expressed in females, but underlying genes appear

to be associated with negative pleiotropic effects on female fitness (Joag et al., 2016; Łukasiewicz et al., 2020; Plesnar Bielak et al., 2014).

3.4. Genomic features correlated with local recombination rate

Recombination occurs mainly in open chromatin, gene-rich regions, resulting in positive correlations with gene density, epigenetic modifications, and GC content (Arndt et al., 2005; Brazier & Glémin, 2022; Haenel et al., 2018; Kyriacou et al., 2023; Peñalba & Wolf, 2020; Stapley et al., 2017; Thuriaux, 1977), while within dense heterochromatin crossover rate is reduced, permitting transposable elements to accumulate, potentially disrupting gene expression and structure. Deciphering causative factors in this covariation network is complex. Contrary to expectations, we demonstrated that the recombination rate positively correlates with the repeat density, but negatively with the gene density and the distance to chromosome ends, suggesting that crossovers mostly occur in gene-poor, repeat-rich areas near chromosome ends (Figure 4). Similarly, in holocentric organisms like *C. elegans* or some lepidopterans, where gene density drops at chromosome ends, no discernible correlation between recombination rate and the density of coding sequence was reported (Bernstein & Rockman, 2016; Stapley et al., 2017; Talla et al., 2019; Torres et al., 2023). This highlights that recombination pattern may vary with chromosome types.

Surprisingly, we found no link between recombination rates and GC content in bulb mites, despite GC-biased gene conversion being a known driver of the correlation between recombination rates and GC content (Bolívar et al., 2019; Duret & Galtier, 2009; Mugal et al., 2015; Webster & Hurst, 2012). The absence of this association in bulb mites might be explained by the heterogeneous distribution of GC content across chromosomes, peaking in gene-dense central regions and similarly elevated in the highly recombining chromosome ends (Figure 3B). Yet, among holocentric organisms, the relationship between recombination rate and GC content shows variable patterns, ranging from negative association (Bernstein & Rockman, 2016; Kaur & Rockman, 2014; Torres et al., 2023) to positive ones (Stapley et al., 2017) suggesting a complex interplay between GC-biased gene conversion and opposing mutation bias toward AT nucleotides (Boman et al., 2021).

The positive correlation between recombination rate and the abundance of repetitive elements reflects the enrichment of repeats at the highly recombining chromosome ends (Figure 3C). Typically, regions with high recombination rate are thought to be more effective in purging transposable elements due to the effects mentioned above, and to decreased Hill-Robertson interference which enhances the effectiveness of purifying selection (Kent et al., 2017; Stapley et al., 2017). The prevalence of TEs in areas of high recombination may be attributed to their role in repairing double-strand breaks associated with recombination process (Onozawa et al., 2014), along with a propensity for certain TEs to integrate into distal parts of chromosomes (Kejnovsky et al., 2006; Pardue & DeBaryshe, 2011; Zou et al., 1996). For example, certain transposon types show a positive correlation with recombination rates in organisms such as *C. elegans* (Duret et al., 2000) and Lepidoptera (Cicconardi et al., 2021; Stapley et al., 2017; Torres et al., 2023), as well as birds (Kawakami et al., 2014; Singhal et al., 2015).

In conclusion, our study presents the first sex-specific genetic linkage map for a gonochoristic organism with holocentric chromosomes, the bulb mite (*Rhizoglyphus robini*). Our comprehensive analysis shows that this species' recombination landscape is similar in males and females across most of the genome, supporting the hypothesis that the female recombination rate is shaped to counteract centromere-associated meiotic drive in species with monocentric chromosomes. Lower recombination rate in males may facilitate the maintenance of male-beneficial allele combinations by reducing the exchange of DNA between homologous chromosomes. This may be particularly pronounced in areas harboring genes under sexual selection, such as those located on chromosome 7 of the bulb mite. The bulb mite genome's structure and recombination patterns, including a high density of repeat elements at the chromosome ends and a concentration of genes in the central regions, illustrate the complex interplay between genomic architecture and recombination landscapes, and opens avenues for further research on the implications of holocentric chromosome structure for genome evolution.

4. Data availability statement

Raw sequence data have been deposited in NCBI Sequence Read Archive (BioProject PRJNA1088092). Code needed to repeat analyses has been deposited in GitHub (https://github.com/sebchm/genetic-map-of-the-bulb-mite) and datafiles are publicly available at Zenodo (DOI: 10.5281/zenodo.10959789). Additionally, GFF files with annotation of genes and repeat elements have been uploaded to ORCAE (https://bioinformatics.psb.ugent.be/orcae/overview/Rhrob).

5. Acknowlegements

We thank Aleksandra Łukasiewicz and Agnieszka Szubert-Kruszyńska for performing the crosses, Pasi Rastas for his generous advice on map construction and Deborah Charlesworth for her comments on the earlier version of the manuscript. Computations were partly performed at the Poznan Supercomputing and Networking Centre. This work was supported by National Science Centre grant no. 2017/27/B/NZ8/00077 awarded to J.R.

References

The references for this chapter are located after the Conclusions section of the thesis.

Table 1. Overview of the experimental crosses and their reproductive output.

Family	dam line	sire line	F1 male morph	number of F2 individuals
A	scrambler-selected IN1	fighter-selected IW9	scrambler	32
B	scrambler-selected IN5	fighter-selected IW22	scrambler	32
C	fighter-selected IW15	scrambler-selected IN7	scrambler	60
D	scrambler-selected IN3	fighter-selected IW17	scrambler	59

Table 2. Summary of the linkage map for each chromosome and sex.

chromosome	physical length [Mb]	Genetic length [cM]		number of markers		F:M length ratio	recombination rate [cM/Mb]		periphery bias	
		female map	male map	female map	male map		female map	male map	female map	male map
1	50	46.3	7.2	9,616	9,616	6.43	0.93	0.14	2.95	3.46
2	33.8	27.7	17.4	32,822	32,821	1.59	0.82	0.51	3.69	2.92
3	33.3	40.9	23.9	57,804	57,804	1.71	1.23	0.72	3.64	2.91
4	32.5	37.4	19.1	66,884	66,884	1.96	1.15	0.59	2.92	3.11
5	31.3	41.4	25.7	1,988	1,986	1.61	1.32	0.82	2.99	2.22
6 (sex)	29.7	51.6	-	45,551	-	-	1.74	-	1.6	-
7	28.6	28.7	8.96	59,844	59,845	3.2	1	0.31	2.02	3.76
8	26.4	35.3	21.7	25,268	25,267	1.63	1.34	0.82	2.95	1.22
sum	265.84	309.4	123.98	299,777	254,223					

Table 3. Summary of repetitive elements annotated to the major repeat classes.

Repeat class	Type	Number of elements	Length occupied [bp]	Fraction of the genome
Interspersed elements	Unclassified	129,314	60,378,963	20.42%
	LTR elements	11,990	6,123,192	2.07%
	LINEs	6,672	4,141,649	1.40%
	DNA transposons	10,350	4,315,236	1.46%
	SINEs	0	0	0.00%
Simple repeats		106,850	5,864,289	1.98%
Satellites		4,634	1,279,523	0.43%
Small RNA		1,000	386,370	0.13%
Low complexity		16,073	798,431	0.27%

Supplementary data: Sex-specific recombination landscape in a species with holocentric chromosomes

1. *Genetic map diagnostics*

1.1. *IBD module*

Before linkage mapping, IBD module (Rastas, 2017b) was used to verify the relatedness between all individuals within families. In order to reduce computational needs, a subset of 10% of genetic markers was used. Heatmaps with IBD value plotted against each individual revealed that all samples were related, except from grandparents, which originated from different inbred lines (left bottom part of the plot).

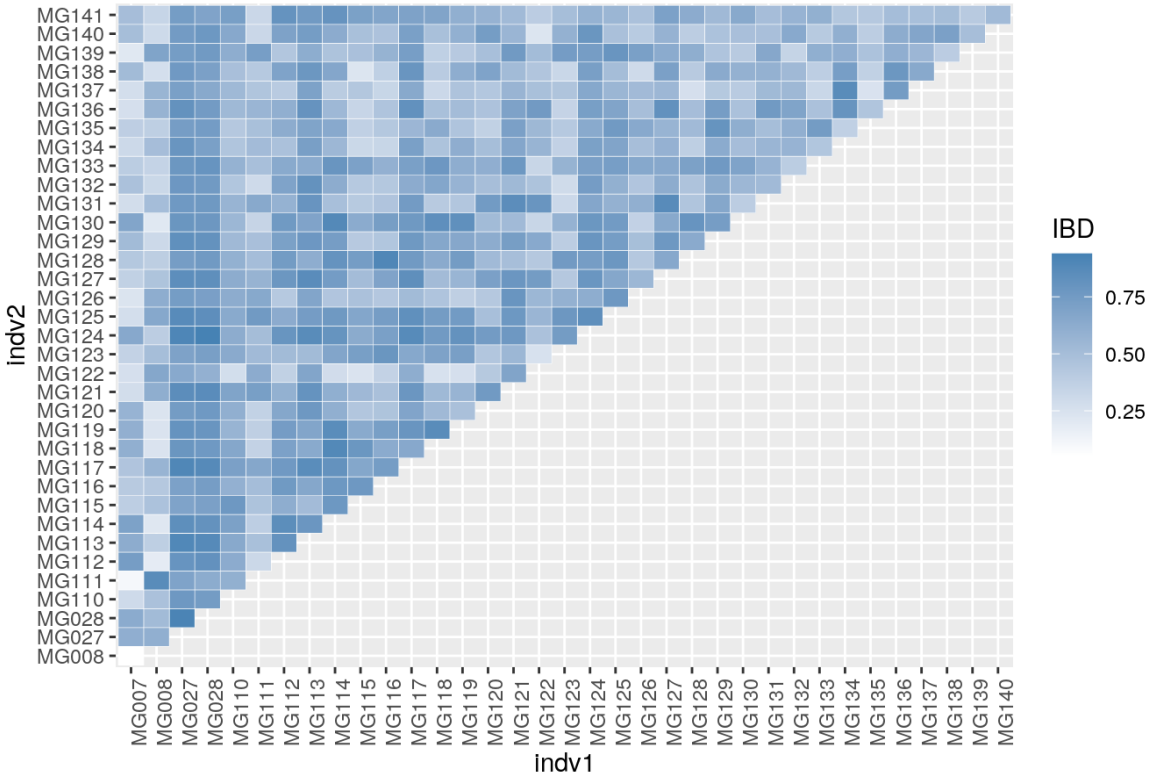

Figure S1. IBD calculated between individuals from family A.

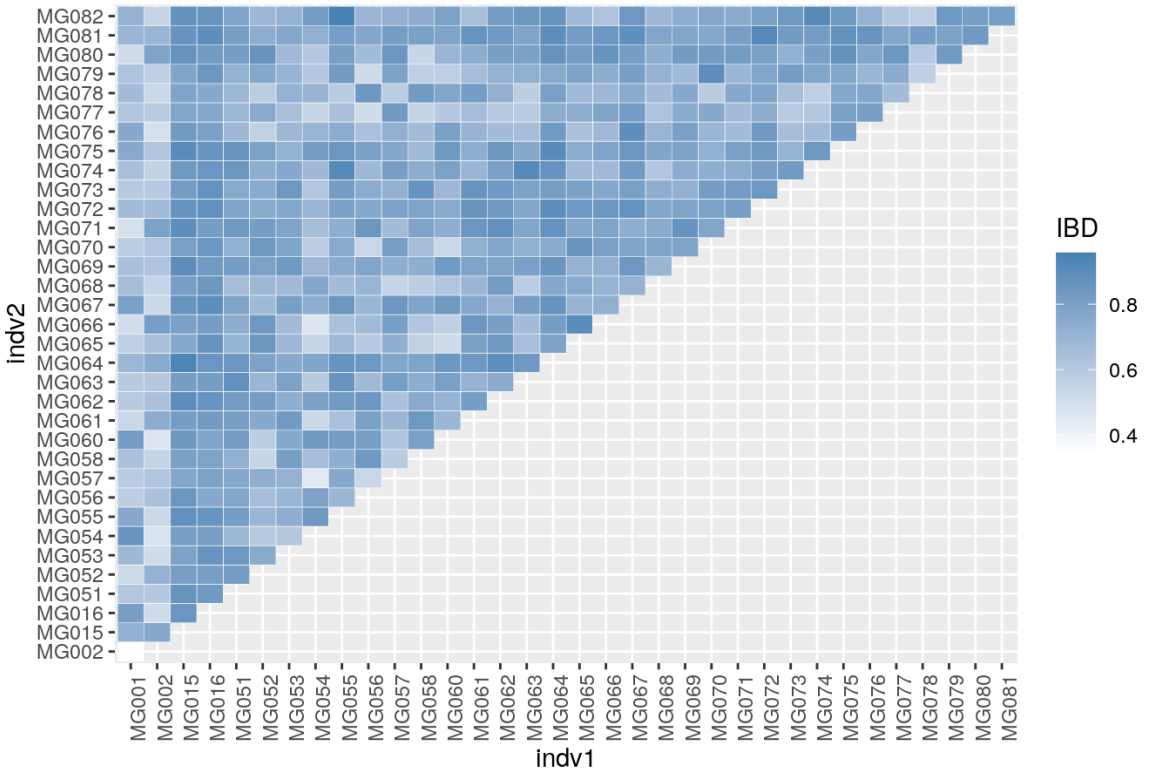

Figure S2. IBD calculated between individuals from family B.

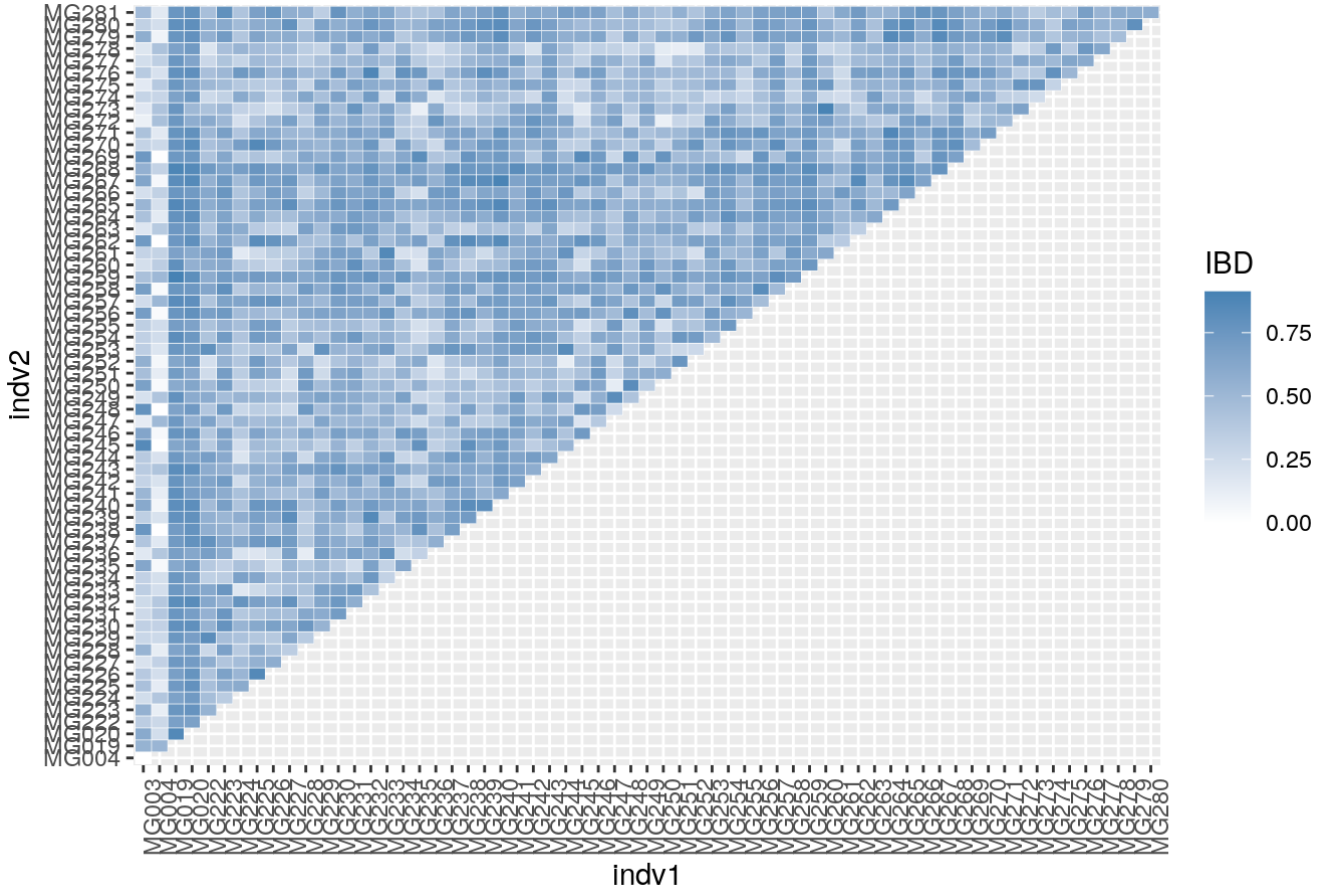

Figure S3. IBD calculated between individuals from family C.

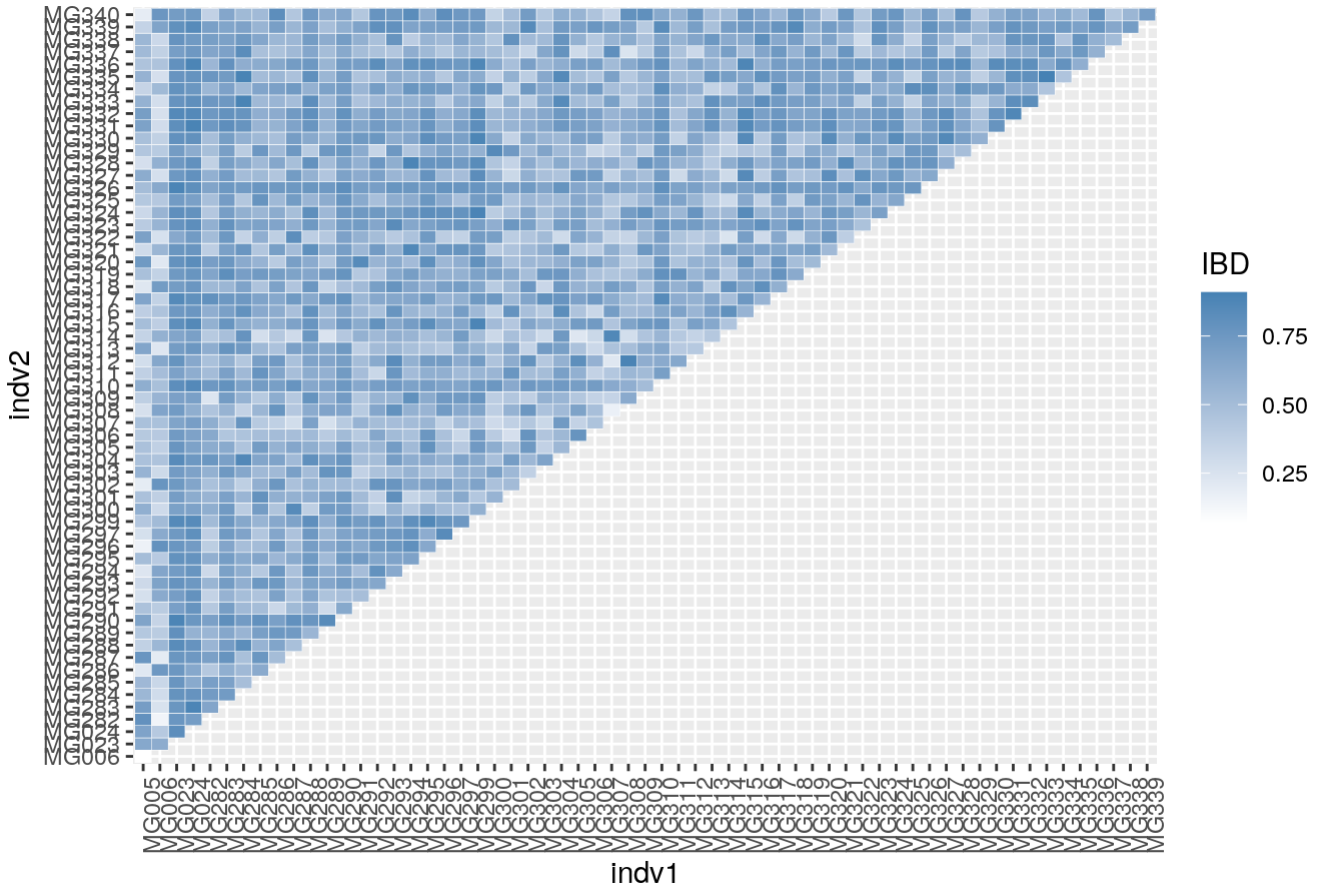

Figure S4. IBD calculated between individuals from family D.

1.2. Checking genotype missingness

To inspect the genotype missingness per sample, we called genotypes from 10 contigs, including 8 longest contigs from reference genome, and 2 sex-linked contigs using ANGSD (v. 0.937, Korneliussen et al., 2014) with parameters: -doPlink 2 -doGeno -4 -doPost 1 -doMajorMinor 1 -GL 1 -doCounts 1 -doMaf 2 -postCutoff 0.95 -SNP_pval 1e-6 -geno_minDepth 2. Next, the genotype file was used to check fraction of missing genotypes with plink (v. 1.9, Purcell et al., 2007) with –missing flag. The analysis revealed one outlier sample with 47% of missing genotypes, which was excluded from the subsequent analysis.

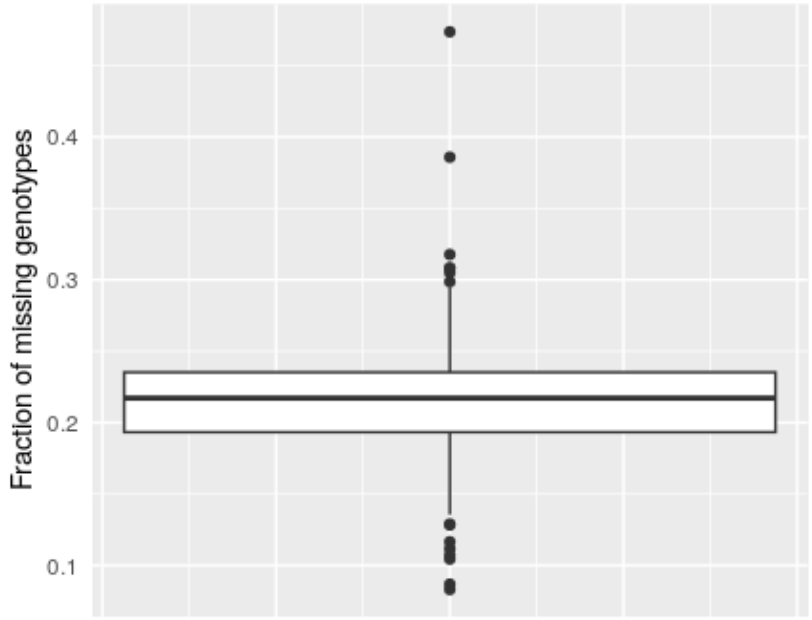

Figure S5. Boxplot displaying fraction of missing genotypes calculated for each sample. Central line is a median; box represent 25th and 75th quartiles; whiskers denote interquartile range.

1.3. Genetic map diagnostics with LMPlots

Map diagnostics was performed using LMPlot module. In LMPlots nodes represent distinct genetic positions with their size proportional to number of comprised genetic markers. Each line between nodes indicates one individual recombining between genetic positions.

LMPlots of sex-averaged maps used for genome anchoring were examined, and a single misjoin at chromosome 4 was observed (Supplementary Figure 6). According to the software author's reccomendation (Pasi Rastas, personal communication), these problematic recombinations were removed manually by equalizing the value of genetic distance between nodes with the misjoin (the changes in genetic distance within the misjoin were removed). Following this correction, the map was evaluated with OrderMarkers2 module with following parameters: improveOrder=0 and evaluateOrder.

After anchoring the genome and genetic map evaluation, the maps were inspected again with LMPlots, and single misjoin was detected at chromosome 6 (Supplementary figure Y). The error was corrected again by manually equalizing the genetic distance value within the misjoin.

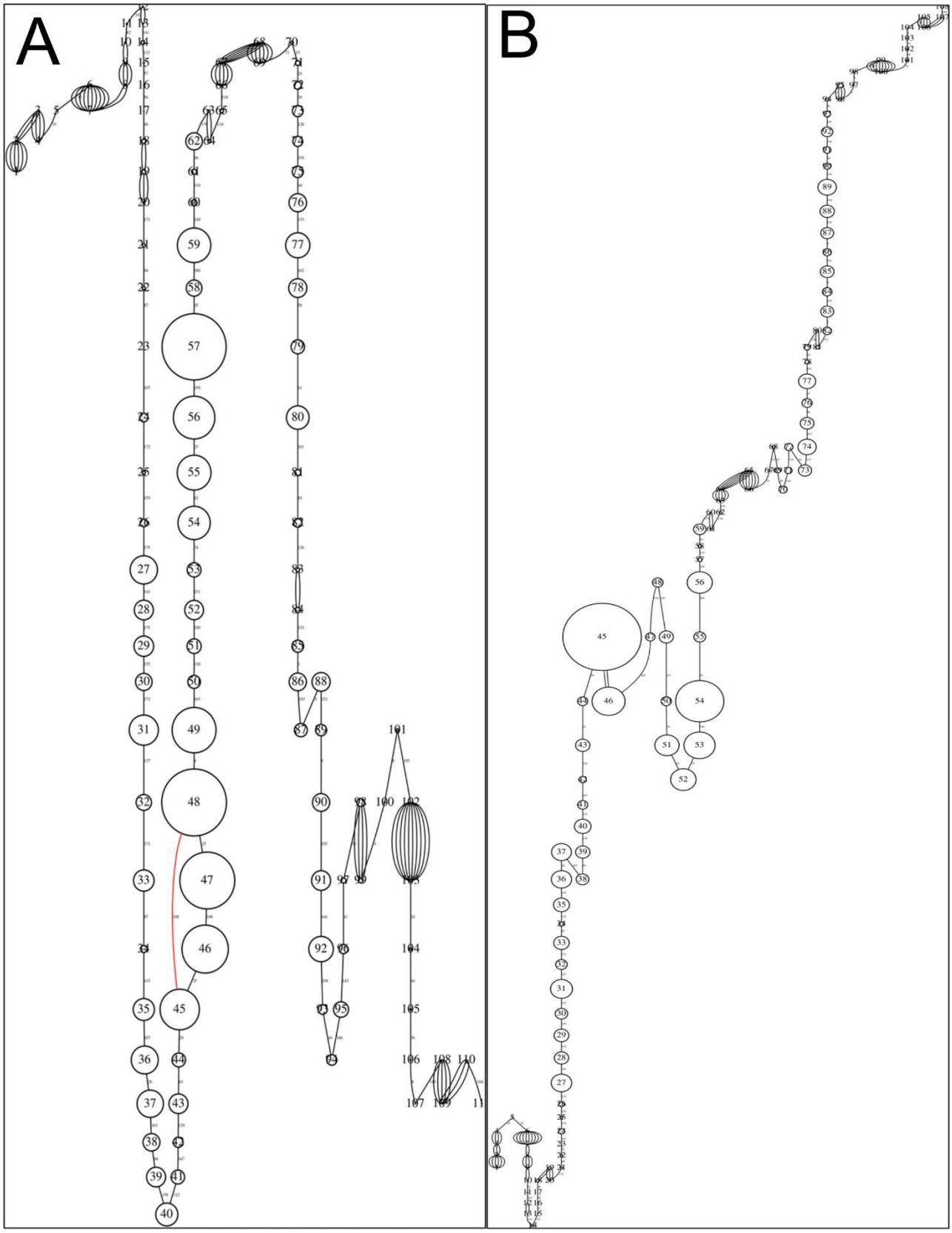

Figure S6. LMPlot of chromosome four before (A) and after (B) removing spurious recombinations (highlighted in red).

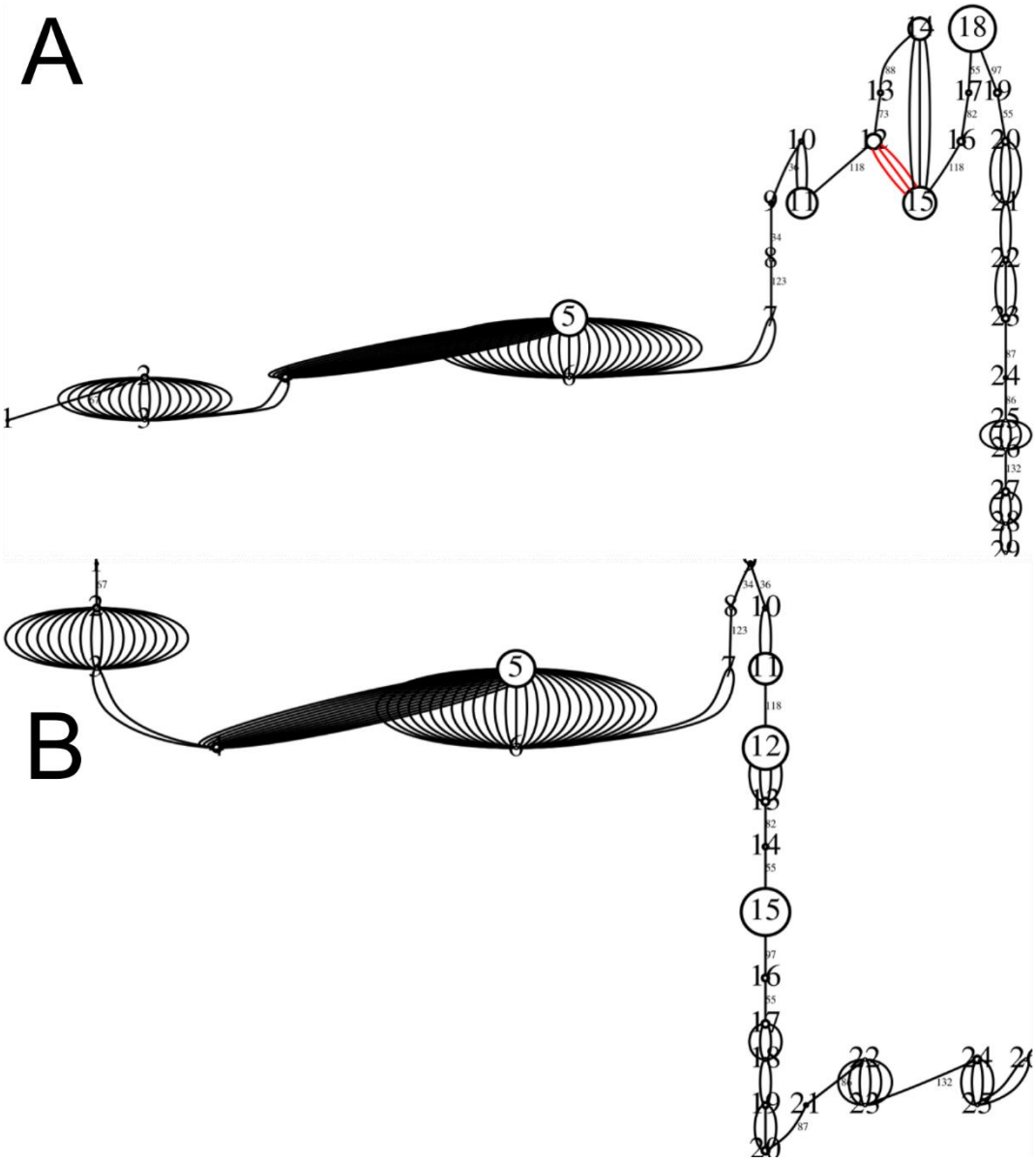

Figure S7. LMPlot of chromosome five before (A) and after (B) removing spurious recombinations (highlighted in red).

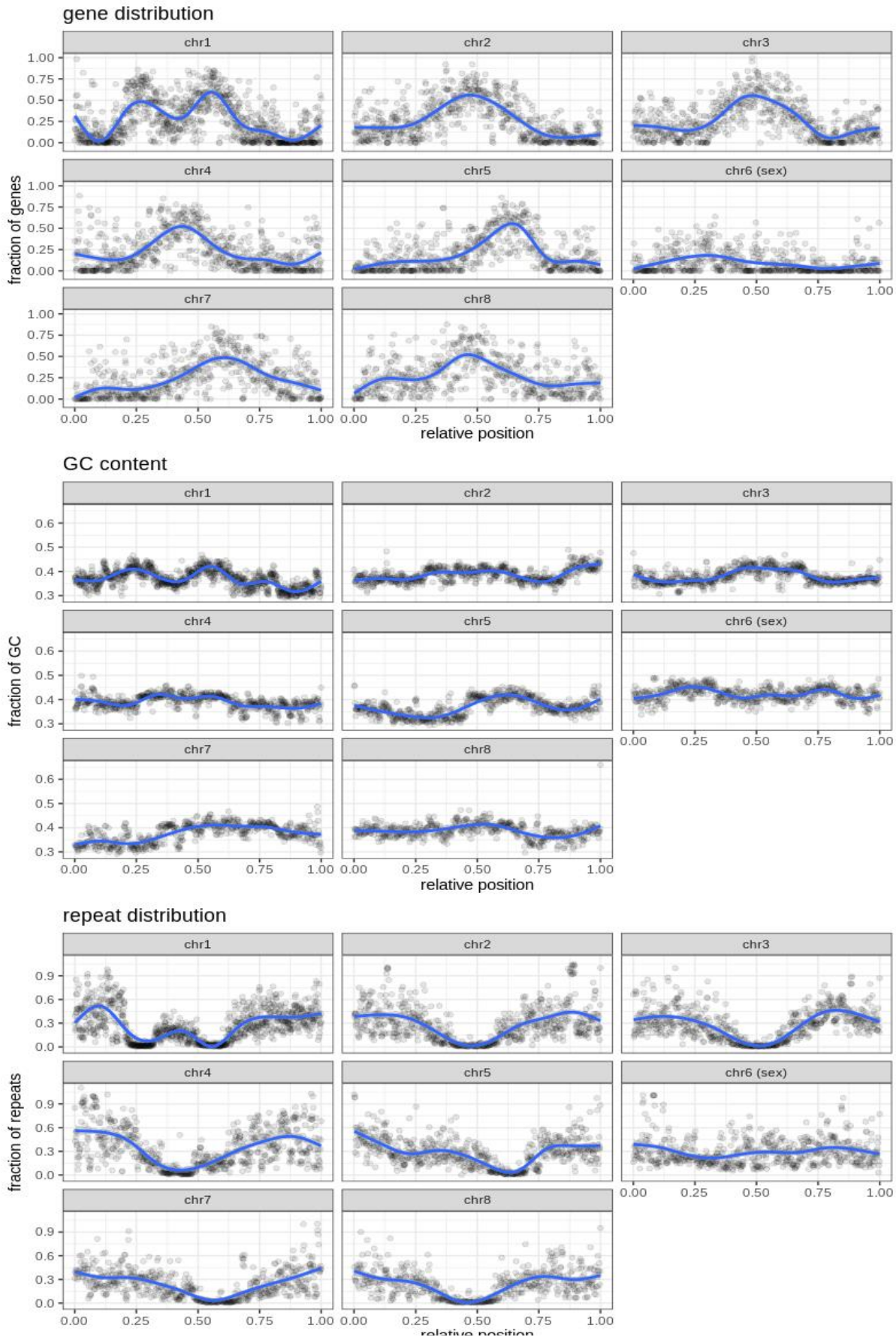

Figure S8. distribution of genomic features along bulb mite chromosomes measured in 50 kb windows

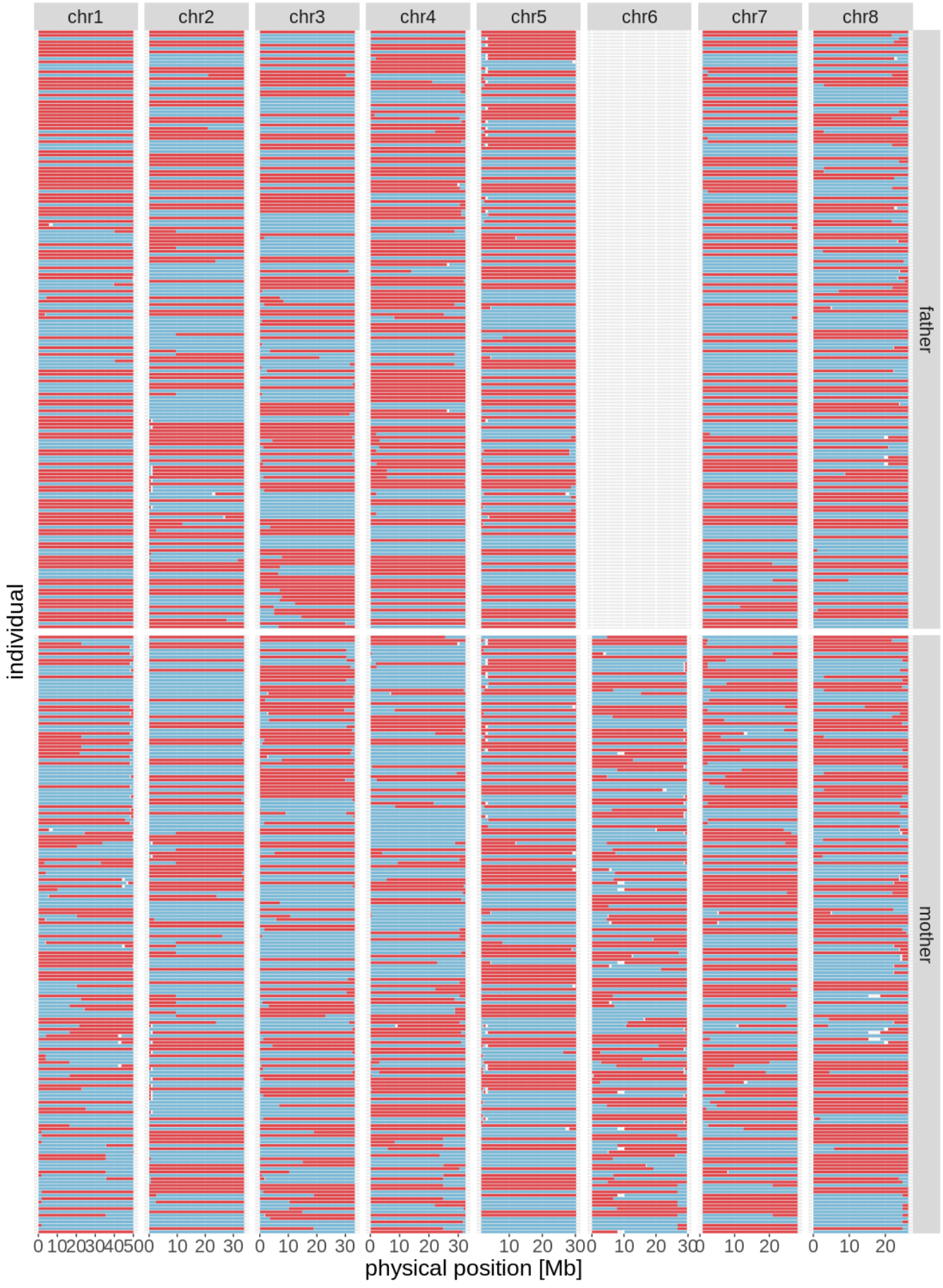
chr1
chr2
chr3
chr4
chr5
chr6
chr7
chr8
father
mother
individual
0 10 20 30 40 50
0 10 20 30
0 10 20 30
0 10 20 30
10 20 30
0 10 20 30
0 10 20
0 10 20
physical position [Mb]

Figure S9 (continued). Chromosome phasing indicates the location of crossovers during paternal (top panel) and maternal (bottom panel) meiosis. Each row is one individual and X axis is chromosomal position in Mb. Small gaps in phasing are visualized by white horizontal bars.

Table S1. Summary of sample sequencing metrics for each sample. The table presents the number of reads after filtering out ambiguously mapping reads, the percentage of duplicated reads, the mean coverage achieved using the final reads, and the mean mapping quality of these reads.

sample name	number of reads after filtering (ambigously mapping reads removed)	% duplicates	mean coverage (from final reads)	mean mapping quality (from final reads)
MG001	49,320,631	29.12	21.3161X	42.4375
MG002	55,567,064	24.91	24.7967X	38.9561
MG003	40,096,260	22.55	17.5411X	39.3295
MG004	48,392,452	23.39	21.6343X	39.1752
MG005	46,246,310	22.34	20.7511X	38.2294
MG006	45,302,948	22.47	20.2823X	40.2796
MG007	46,460,325	23.26	20.3642X	39.255
MG008	38,266,494	24.61	15.9367X	40.3143
MG015	48,689,847	23.02	21.5538X	39.6847
MG016	53,727,025	24.14	23.61X	39.5299
MG019	53,041,189	22.6	23.9896X	39.9245
MG020	52,615,689	22.55	23.8428X	40.2312
MG023	51,556,763	23.03	23.3572X	40.5441
MG024	54,643,659	23.99	24.8449X	39.478
MG027	40,293,454	22.51	17.1832X	39.3128
MG028	45,199,475	22.74	19.8663X	39.7938
MG051	18,334,933	17.03	8.2251X	38.1529
MG052	14,932,165	15.41	6.7509X	37.6548

MG053	18,616,735	16.84	8.4065X	37.9414
MG054	17,220,126	16.73	7.7605X	38.1677
MG055	42,051,741	21.83	19.065X	39.1247
MG056	15,562,165	16.73	6.9441X	38.0231
MG057	21,112,095	17.29	9.5632X	38.2136
MG058	23,345,990	17.85	10.469X	38.4413
MG059	2,216,963	45.38	0.2062X	29.632
MG060	14,829,915	15.62	6.6936X	37.8986
MG061	16,930,035	16	7.68X	38.0797
MG062	21,317,737	17.68	9.5385X	38.2892
MG063	17,896,624	17.32	8.0337X	38.4846
MG064	31,816,643	19.43	14.2242X	38.5967
MG065	22,099,079	17.6	9.7973X	38.4711
MG066	25,138,783	18.34	11.2122X	38.6429
MG067	20,689,554	16.15	9.3412X	38.0417
MG068	19,994,986	17.51	9.0091X	37.8816
MG069	20,636,019	16.61	9.3186X	38.1271
MG070	16,829,108	15.03	7.6485X	37.4943
MG071	13,873,469	15.48	6.207X	37.6577
MG072	19,868,916	16.95	8.999X	37.957
MG073	31,265,953	18.7	14.0787X	38.2511
MG074	23,835,640	17.31	10.6526X	38.3364
MG075	18,460,118	16.11	8.1758X	38.2748
MG076	15,090,832	15.06	6.8454X	37.5065
MG077	21,432,527	18.38	9.6918X	37.9319
MG078	16,183,225	15.75	7.2909X	37.7639
MG079	15,117,100	14.64	6.8764X	37.7236

MG080	19,600,337	16.33	8.904X	38.2072
MG081	19,294,422	17.08	8.56X	38.2075
MG082	25,996,065	17.39	11.805X	38.423
MG110	17,111,953	14.91	7.7461X	37.0857
MG111	19,087,137	16.51	8.6554X	37.5813
MG112	12,170,862	14.63	5.5135X	37.4544
MG113	18,633,938	16.72	8.4669X	37.9393
MG114	18,296,783	15.97	8.3291X	37.654
MG115	14,438,646	14.95	6.5243X	36.6746
MG116	14,465,456	15.25	6.5258X	36.9579
MG117	32,199,900	18.73	14.6019X	38.5957
MG118	23,045,163	16.99	10.4347X	37.7408
MG119	22,511,971	17	10.2149X	37.8256
MG120	22,122,376	17.02	9.9696X	38.2099
MG121	18,581,723	15.48	8.4771X	37.6006
MG122	19,370,532	16.4	8.7742X	37.9047
MG123	15,898,102	16.14	7.1814X	36.639
MG124	36,165,467	19.75	16.3863X	38.3637
MG125	32,153,492	19.08	14.5288X	38.6666
MG126	39,878,120	19.94	18.1941X	38.555
MG127	39,897,930	20.48	18.1054X	38.4447
MG128	22,658,254	16.92	10.2445X	37.8557
MG129	13,382,735	14.68	6.0779X	37.5066
MG130	22,403,844	17.17	10.1071X	37.8017
MG131	15,757,968	14.82	7.1652X	37.3244
MG132	19,534,014	16.28	8.8736X	37.4949
MG133	33,360,004	20.11	15.1998X	37.9913

MG134	28,222,386	18.5	12.7946X	38.0349
MG135	21,797,599	17.44	9.8916X	37.6387
MG136	22,767,637	18.7	10.1281X	38.2788
MG137	21,834,321	17.49	9.8402X	37.2239
MG138	17,600,918	16.6	7.9005X	37.5852
MG139	16,535,177	15.52	7.5243X	37.5647
MG140	21,444,678	16.85	9.7292X	37.061
MG141	38,557,165	20.99	17.482X	38.7201
MG222	16,500,701	25.07	7.4997X	38.5594
MG223	19,259,366	28.43	8.8372X	37.6083
MG224	21,366,262	26.18	9.796X	38.1067
MG225	20,089,691	29.15	9.1935X	37.2349
MG226	18,829,003	25.92	8.5882X	38.0667
MG227	17,120,881	26.8	7.8732X	37.8734
MG228	24,364,483	28.77	11.0247X	38.6517
MG229	18,338,858	27.72	8.2895X	38.3568
MG230	18,728,256	25.7	8.5986X	38.6598
MG231	7,835,501	26.68	3.575X	37.576
MG232	21,107,617	26.21	9.7038X	38.2681
MG233	22,840,264	26.68	10.4987X	37.9508
MG234	13,289,249	23.78	6.0895X	37.7502
MG235	23,529,168	27.14	10.7358X	38.0168
MG236	22,858,557	26.9	10.4672X	37.8738
MG237	18,578,164	27.6	8.5055X	37.1519
MG238	22,339,835	26	10.1769X	37.5072
MG239	21,980,444	27.14	10.0784X	37.9149
MG240	18,769,538	24.24	8.574X	38.0064

MG241	17,984,095	25.88	8.217X	37.0709
MG242	24,564,411	25.55	11.2643X	37.5546
MG243	17,273,514	25.86	7.8851X	37.8931
MG244	25,871,342	27.38	11.8303X	37.8105
MG245	23,631,170	28.84	10.8005X	37.4313
MG246	18,631,301	24.77	8.4895X	37.7506
MG247	16,679,503	26.15	7.6179X	36.8621
MG248	18,048,436	24.73	8.2644X	37.3168
MG249	19,837,011	26.34	9.0992X	37.5108
MG250	15,492,585	23.5	7.1219X	37.0357
MG251	15,340,727	24.86	7.0199X	37.145
MG252	19,444,447	24.77	8.8845X	37.0833
MG253	17,888,041	25.91	8.1685X	37.3585
MG254	25,047,178	28.62	11.4804X	37.5572
MG255	21,576,037	30.14	9.9045X	37.3825
MG256	23,239,098	25.33	10.6657X	37.9888
MG257	16,960,379	25.5	7.7714X	37.5926
MG258	20,533,188	24.68	9.4256X	37.7126
MG259	16,919,701	25.35	7.7689X	37.9151
MG260	22,019,667	26.2	10.0582X	37.3529
MG261	17,462,365	27.13	7.993X	38.1842
MG262	21,764,849	25.47	9.9281X	37.2485
MG263	20,490,142	26.74	9.4008X	38.1054
MG264	22,482,947	25.02	10.3125X	37.6197
MG265	19,539,794	26.34	8.9401X	38.2892
MG266	15,993,647	24.64	7.3174X	37.4855
MG267	23,567,219	27.34	10.7983X	38.1774

MG268	18,795,823	25.12	8.5702X	37.5997
MG269	21,579,136	27.38	9.8925X	38.0905
MG270	19,381,542	25.05	8.9092X	37.761
MG271	18,365,798	26.71	8.3946X	37.6058
MG272	22,513,818	27.47	10.2868X	37.4515
MG273	24,730,530	29.28	11.3415X	37.4465
MG274	22,781,414	25.83	10.4242X	38.1988
MG275	22,841,983	28.11	10.3932X	37.4362
MG276	19,601,267	24.82	8.9345X	37.9931
MG277	17,727,467	26.72	8.0177X	37.1071
MG278	20,125,884	25.26	9.2412X	38.1365
MG279	23,510,073	27.48	10.7921X	38.2759
MG280	20,065,675	24.8	9.1674X	37.6683
MG281	19,303,401	26.37	8.8299X	38.0778
MG282	15,871,397	24.93	7.2098X	37.0626
MG283	17,019,598	26.89	7.7306X	36.4887
MG284	15,467,431	25.24	7.0073X	37.1007
MG285	20,105,657	27.65	9.1309X	37.2484
MG286	17,623,510	25.38	8.0052X	37.7782
MG287	22,540,311	27.83	10.2204X	37.5099
MG288	18,110,165	24.97	8.2408X	37.1668
MG289	18,072,898	26.39	8.2148X	37.7054
MG290	19,016,559	25.29	8.6377X	37.5066
MG291	19,744,377	26.94	8.9769X	36.1304
MG292	17,770,665	26.23	8.0555X	37.2259
MG293	19,220,177	27.68	8.7753X	37.5818
MG294	17,135,412	25.44	7.7939X	36.8922

MG295	10,130,248	26.33	4.4125X	37.2905
MG296	18,243,557	25.05	8.3056X	37.3675
MG297	20,039,462	27.4	9.1191X	37.4632
MG298	911,587	19.87	0.4135X	32.8506
MG299	22,785,820	27.43	10.3217X	37.4906
MG300	16,393,155	25.34	7.3889X	37.2626
MG301	21,487,627	27.28	9.7592X	37.904
MG302	17,614,466	24.88	8.025X	37.812
MG303	22,244,186	27.45	10.0847X	37.2691
MG304	15,623,064	24.86	7.1287X	36.8496
MG305	20,920,623	28.05	9.4953X	37.2621
MG306	19,275,481	25.39	8.776X	36.8638
MG307	31,063,773	29.26	14.172X	37.1388
MG308	17,911,420	24.42	8.1491X	37.4942
MG309	22,024,494	26.4	10.0472X	36.7212
MG310	17,513,903	24.32	7.9774X	37.2959
MG311	21,392,329	27.19	9.733X	37.5963
MG312	18,609,030	27.69	8.4562X	37.909
MG313	23,485,784	30.52	10.6678X	37.2929
MG314	16,971,460	25.57	7.7693X	36.4991
MG315	22,740,534	27.74	10.3537X	36.6965
MG316	21,422,174	27.13	9.7632X	37.466
MG317	21,422,452	28.34	9.7379X	37.8756
MG318	23,273,238	26.93	10.6395X	37.4611
MG319	22,430,552	28.44	10.1987X	37.5885
MG320	19,909,379	26.21	9.0535X	36.2457
MG321	19,854,600	26.97	9.0707X	36.7025

MG322	19,500,059	26.37	8.8302X	35.9214
MG323	19,883,401	27.42	9.0682X	36.6883
MG324	20,796,156	25.74	9.4934X	36.6975
MG325	20,273,784	27	9.2403X	36.5866
MG326	16,992,110	24.52	7.7492X	37.2067
MG327	20,129,046	27.32	9.1461X	36.3472
MG328	18,463,253	26.05	8.409X	36.2795
MG329	20,494,707	27.75	9.3447X	36.9537
MG330	15,145,110	24.17	6.896X	36.0838
MG331	17,209,963	26.12	7.8331X	36.7727
MG332	19,196,243	28.27	8.7087X	37.0894
MG333	26,485,738	30.94	12.032X	36.93
MG334	18,534,843	24.7	8.4343X	37.1385
MG335	19,357,224	26.23	8.8194X	36.8368
MG336	17,939,555	25.42	8.158X	36.8976
MG337	18,051,009	27.92	8.1841X	37.0874
MG338	12,011,243	23.14	5.483X	36.3989
MG339	19,085,960	25.78	8.7371X	37.0395
MG340	17,633,560	24.58	8.0239X	36.7252

CHAPTER II

The impact of sex ratio manipulation on genome-wide genetic diversity during experimental evolution.

SEBASTIAN CHMIELEWSKI, JONATHAN PARRETT, MATEUSZ KONCZAL, JACEK RADWAN

Evolutionary Biology Group, Adam Mickiewicz University

(unpublished)

Abstract

Sexual selection is a potent evolutionary force that can drive significant changes in genetic variation within populations. It may facilitate the purging of deleterious genetic load by favouring individuals in the best condition, while also potentially maintaining polymorphism at loci where an allele is beneficial to one sex but detrimental to the other. In this study, we investigated the genomic consequences of manipulating sex ratio to enhance or reduce sexual selection intensity in the bulb mite, *Rhizoglyphus robini*. Through experimental evolution and whole-genome resequencing, we studied changes in genetic diversity over 28 generations in populations subjected to male-biased and female-biased sex ratios. Our results revealed that the male-biased lines lose nucleotide diversity at a slower rate compared to the female-biased lines, particularly at synonymous positions. However, we did not observe signatures of purifying or balancing selection as a consequence of sex ratio manipulation. Additionally, we observed no significant changes in effective population sizes between the treatments. Although we detected allele frequency changes in opposite directions between female- or male-biased lines at only six SNPs, we identified large genomic regions that responded to selection uniquely within treatments. The treatment-specific haplotypes were enriched for genes associated with transcription regulation in male-biased lines and processes associated with cell membrane in female-biased lines. Our findings suggest that sex ratio manipulation triggers weak selection with a polygenic response.

Keywords: sexual selection, sex bias, sexual conflict, *6Pgdh,* experimental evolution

1. Introduction

Sexual selection, a process arising from reproductive competition, leads to a number of spectacular adaptations such as weapons used in fight over mates, or ornaments that attract mates, but also act on many other traits such as body size, metabolic efficiency, locomotion or sensory systems (Andersson, 1994; Whitlock & Agrawal, 2009). Because sexual selection can enhance or oppose other modes of selection, it has a potential to shape genetic variance in

populations, with consequences for key evolutionary processes such as adaptation, speciation and extinction. For example, provided that success in reproductive competition depends on the competitor's general health and vigour (often referred to as condition), sexual selection has a potential to enhance removal of deleterious alleles from populations (Andersson, 1986; Whitlock & Agrawal, 2009). In consequence, sexual selection can improve population fitness, compensating lower potential growth rate of sexual population vs. asexual ones (Agrawal, 2001; Siller, 2001) or counteracting extinction during population bottlenecks (Jarzebowska & Radwan, 2009; Lumley et al., 2015). However, sexual selection often acts unevenly on sexes (typically more strongly on males), and alleles beneficial to males can be detrimental when expressed in females, breaking down alignment between natural and sexual selection. Rather than enhancing the rate of elimination of deleterious variants (and fixation of beneficial ones), such sexual antagonism may slow down depletion of genetic variance from population or even instigate balancing selection, potentially enhancing long-term evolutionary potential of populations (Connallon & Clark, 2012, 2014; Mank, 2017a; Rusuwa et al., 2022). However, sexual selection can also reduce genetic variation due to increased variance in male reproductive success negatively affecting effective population size (Parrett et al., 2021). The net effect of sexual selection on the amount and nature of genetic variance segregating in populations will depend on the relative contributions of the above mechanisms. With the increasing availability of genomic data, evolutionary biologists are now in position do directly address this complexity. There is some support for both purifying and balancing selection associated with sexual selection in *Drosophila melanogaster*. On the one hand, artificial selection on high male mating success led to increased purging of low frequency, presumably deleterious variants in this species (Dugand et al., 2019). On the other hand, sexually antagonistic SNPs have been associated with signatures of balancing selection (Ruzicka et al., 2019). Focal traits analysed in this latter study were male and female lifetime reproductive success, which in case of males is determined by their success in reproductive competition (Davies et al., 2023), indirectly implying the role of sexual selection in instigating balancing selection reported by Ruzicka et al. (2019). Balancing selection has also been implicated in the study of seed beetles *Callosobruchus maculatus* (Sayadi et al., 2019). Another line of evidence comes from studies selecting for male weapons, which, along with extreme ornaments, have been hypothesised to enhance sexual antagonism (Radwan et al., 2016). Indeed, negative genetic correlations between male armaments and female fecundity have been reported in broadhorned flour beetle *Gnatocerus cornutus* (Harano et al. 2010) and bulb mites *Rhizoglyphus robini* (Plesnar Bielak et al., 2014). However, for the latter species, evolve and re-sequence (E&R) study of Parrett et al. (2022) has found only weak genomic signature of balancing selection associated with selection for male weapon. Instead, high prevalence of male weapon in populations was associated with stronger genome-wide purifying selection, and with lower effective population size, both processes leading to depletion of genetic variation. However, sexual selection associated with male fights is just one aspect of reproductive competition, which also includes such components as mate searching, mate choice and sperm competition. These different aspects of reproductive competition may vary in their effects on genome-wide variation. For example, Sayadi et al. (2019) showed that genes which show male-biased expression, possibly

associated with their role in sexual selection, are subject to mostly purifying selection, whereas those with moderate sex-bias are more likely to be under balancing selection. Based on reasoning that sexual conflict is resolved for genes with sex-limited expression, this last result was interpreted by the authors as a support for the role of sexual antagonism as a driver of balancing selection. If so, their results would suggest that the effect of sexual selection on the amount and nature genetic variance segregating in population will vary for sexually selected traits depending on degree of resolution of sexual antagonism associated with them. It is therefore important to understand how various facets of sexual selection shape genetic variation within populations.

In this study, we used experimental evolution combined with genome re-sequencing to study the effect of the intensity of sexual selection on genetic variation segregating in populations. Experimental evolution is a powerful tool to test evolutionary hypotheses because effects of experimental treatment accumulate over many generations. At the same time, experimental evolution can better control for confounding variables than comparative studies across natural populations or species (Kawecki et al., 2012). However, experimental evolution has its own limitations, mostly resulting from limited population size which accentuates drift, and possibly also inbreeding, potentially the confounding the evolutionary response to experimental treatment (Snook et al., 2009) Here, however, we overcome these limitations by using replicate lines each consisting of a census size of 1000 individuals.

To manipulate sexual selection intensity, we used a commonly used method of altering sex ratio (e.g. Aronsen et al., 2013; Sharda et al., 2024). Male-biased sex ratio is expected to increase competition among males for females, accentuating sexual selection, whereas the reverse should be true for female-biased sex ratio. In a bulb mite, increased competition for mates should affect several levels of sexual selection known to be operating in this species, including selection for mate-searching, the frequency of fights over females (Radwan, Czyż, et al., 2000) and probability of female re-mating which mediates sperm competition intensity (Radwan & Siva-Jothy, 1996). Previous work has demonstrated that 15 generations of experimental evolution under male-biased sex ratio (70% males) increased the frequency of *6Pgdh* locus variant associated with higher male sperm competitiveness, but also with increased harm caused by males to females (Skwierzyńska & Plesnar-Bielak, 2018), compared to evolution under even or female-biased sex ratio (Plesnar-Bielak et al., 2020). However, within the range of sex ratios we used (3:1 and 1:3) access to males should not limit female reproductive success given that one mating every couple of days allows females to achieve maximum reproductive output (Kołodziejczyk & Radwan, 2003). These considerations led us to the following predictions. If the overall effect of increased inter-male competition is to enhance selection against unconditionally deleterious variants, we expected genetic variance to be lower after 28 generations of experimental evolution in male-biased lines compared to female-biased lines. Because deleterious mutations are expected to segregate at low frequencies, the difference should be particularly pronounced in Watterson's estimator (hereafter ϑ, Watterson, 1975), a measure of diversity based on the number of segregating sites and thus sensitive to the loss of rare variants. If, on the other hand, sexual selection is associated with

widespread sexual conflict maintaining sexually antagonistic variants at intermediate frequencies, the effect of manipulation of sexual selection should mostly affect nucleotide diversity π, and to do so in a less predictable way. This is because π has the maximum at even proportions of alleles, so how π will change will depend on initial equilibrium frequency and in which direction the equilibrium would move following experimental evolution. However, the role of balancing selection could be inferred if manipulation of sexual selection caused change in frequency in the loci bearing signatures of balancing selection, such as elevated Tajima's D. In addition to testing the effect of sex ration manipulation on genetic diversity, we characterised nucleotide polymorphism and genomic regions that responded to the manipulation, with particular focus on the sexual conflict gene *6Pgdh*.

2. Methods

2.1. Experimental evolution

To enhance the genetic diversity of the basal population, three outbred populations (Mosina, Kwiejce, and Kraków) were mixed in equal proportions approximately 16 months (approximately 32 generations) before the start of the experiment. The experimental design comprised eight lines of 1000 individuals: four female-biased lines with a 3:1 female-to-male ratio and four male-biased lines with a 1:3 female-to-male ratio. The experimental procedures were similar as described in Parrett et al. (2022).

Briefly, the mite colonies were reared in tightly sealed plastic boxes with dimensions 9 x 7 x 4.5 cm (length x width x height). To allow for airflow, the lid had small holes that prevented mites from escaping. High humidity was ensured by soaking a plaster-of-Paris base (˜1 cm) with water, and the mites were fed with dry yeast provided *ad libitum*.

At each generation, upon reaching maturity, the desired number of males and females were manually selected and transferred to new dishes. To control the morph ratio, we selected an equal proportion of fighter and scrambler males—125 and 375 of each morph in female-biased and male-biased lines, respectively. After selection, the mites were allowed to interact for six days.

After the interaction period, eggs were separated from the adults and removed by rinsing the colony on a fine mesh that allowed the eggs to pass through while retaining the adult mites. The 'cleaned' adults were then transferred to new dishes to lay eggs for one additional day. These eggs were used a source of next generation, and adults were discarded. Frequent mating (few copulations a day, Radwan & Siva-Jothy, 1996) coupled with last sperm precedence observed in bulb mites (Radwan, 1997) implies that the eggs used to start next generation were fertilized mostly with the sperm of the selected males available during the interaction period. Because there were three times as many ovipositing females in female-biased treatment, we mechanically removed approximately two-thirds of the dish surface area in the female-biased lines after the oviposition period to maintain similar mite density across treatments. The eggs were left to develop for 14 days. This procedure was repeated up to generation 28.

2.2. DNA isolation and sequencing

DNA samples were collected from mites at generations 1 and 28 for sequencing. To prevent contamination from food, the mites were transferred to dishes with a 5% agarose base and starved for three days. In total, 32 pooled samples were selected for sequencing (2 generations x 4 lines x 2 treatments x 2 sexes), containing either 100 males or 100 females from each line. The sampled mites were stored at -20°C in ATL buffer until DNA extraction.

DNA was extracted using the MagJet Genomic Kit for generation 1 and the DNeasy Blood & Tissue Kit for generation 28, following the manufacturer's protocols. The quality and quantity of the extracted DNA were assessed using Nanodrop and Qubit, respectively. Genomic library preparation was conducted using the Nextera NebNext Ultra FS II kit. Sequencing was performed at the SNP&SEQ Sequencing Facility in Uppsala on a NovaSeq 6000 system, using S4 flow cell to produce 2 x 150 bp paired-end reads.

2.3. Bioinformatic analyses

Reads were trimmed with Trimmomatic (v. 0.39, Bolger et al., 2014) using default settings and mapped to a reference chromosome-scale genome assembly (Chmielewski et al., 2024) using BWA-MEM (v. 0.7.17, Li, 2013). Duplicate reads and those with a mapping quality score below 20 were removed with Samtools (v. 1.9, Li et al., 2009). Quality control of the sequencing reads was conducted using FastQC (v. 0.12.1) and MultiQC (v. 1.14; Ewels et al., 2016). Quality control of mapped reads was performed with qualimap (v. 2.2.1, García-Alcalde et al., 2012) and MultiQC.

Mpileup files were generated based on each of the 32 bam files using Samtools mpileup, including only positions with a base quality score greater than 30. Due to decreased accuracy of SNP detection in regions flanking indels, which is caused by incorrect realignment (DePristo et al., 2011; H. Li & Homer, 2010), we removed 5 base pairs flanking indels using the filter-pileup-by-gtf.pl script. Indels were detected using the PoPoolation (v. 1.2.2, Kofler et al., 2011) script identify-genomic-indel-regions.pl with a minimum indel count of 5 and removed along with repeated elements using filter-pileup-by-gtf.pl. The resulting mpileup file was then converted into a sync format using mpileup2sync.jar.

Allele counts of female and male samples from the same replicate lines and time points were merged. To mitigate errors in SNP calling from regions of both high and low coverage, often caused by e.g. paralogs or collapsed copy number variants, we performed coverage-based filtering as in Parrett et al. (2022). Using randomly selected 100,000 autosomal and 10,000 sex chromosome positions, we drew the distribution of the mean coverage across all samples to determine the value of the target coverage, which we define as the peak of the highest coverage density. The target coverage (101X for autosomes and 75X for the sex chromosome) was used as a reference point for filtering genomic positions. We retained only loci with mean coverage across all samples within the range of 50-200% of the target coverage (Supplementary Figure

1). The difference in coverage between sex chromosome and autosomes is consistent with the expectation for a pool containing an equal ratio of sexes, as males carry a single copy of the sex chromosome, while females carry two copies of the sex chromosome (Parrett et al 2022).

2.4. Estimates of the autosomal genetic diversity

The sync file, filtered for mean coverage across all lines, was split into 16 individual sex-merged lines. Because genetic diversity measures are sensitive to variation in the coverage, each line was subsampled to a coverage of 53X using the subsample-pileup.pl script from the PoPoolation pipeline, ignoring loci with coverage above 215X. Only autosomes were used to estimate the genetic diversity, so sex chromosome positions were removed. Next, only positions having required coverage in all samples (84,222,639 positions) were retained. These data were used to estimate autosomal diversity patterns and effective population sizes.

Genetic diversity measures, including nucleotide diversity (π) and Watterson's estimator (θ) were calculated at both synonymous and non-synonymous sites using the Syn-nonsyn-at-position.pl script with a minimum allele count of 3 (approximately 5% of the subsampled coverage). Due to the presence of unexpectedly high number of gene models in the bulb mite gene annotation (60,309 gene models), we analysed only genes showing significant expression in adult bulb mites (13,389 genes, Plesnar-Bielak et al., 2024) to avoid taking into account false positives. Additionally, we retained only genes which exons had at least 60% of SNPs with coverage of 53X (12,334 genes) in all 16 samples.

π and θ were computed across exons using the Variance-at-position.pl script from PoPoolation software. To assess genome-wide diversity beyond genes, π and θ were estimated across the entire genome in 10 kb non-overlapping windows using the script Variance-sliding.pl. We used analysis of variance using *aov* function in R to compare the genetic diversity mean values across different experimental lines, with treatment, generation, and their interaction included as explanatory variables.

To separate the effects of selection from drift, we tested whether changes in π or ϑ between generations at non-synonymous sites differed from changes at synonymous sites, where the former is primarily affected by selection, and the latter reflects drift. Changes in non-synonymous diversity were calculated by dividing the value of π (θ) at each gene at F28 by the value at F1. For synonymous genetic variation, the genome-wide average of π (θ) at F28 was divided by the same measure at F1. To reduce data skewness and the influence of outliers, the natural logarithm of these values was calculated after adding one. The formula used was:

$\Delta_{\pi(\theta)} = \log\left(\frac{non\text{-}syn_{\pi(\theta)F28}}{non\text{-}syn_{\pi(\theta)F1}} + 1\right) - \log\left(\frac{syn_{\pi(\theta)F28\,G-W}}{syn_{\pi(\theta)F1\,G-W}} + 1\right)$, where non-syn and syn are the mean values of π or θ at non-synonymous and synonymous positions for each gene, respectively, and G-W represents the genome-wide autosomal average of π or θ. All computations were conducted using R (v. 4.1, R Core Team, 2024).

2.5. Effective population size estimates

Effective population size (N_e) estimates were based on allele frequency shifts between basal and evolved samples, analysed separately for autosomal and sex-linked loci. The N_e estimates were obtained using the function estimateNe from the poolseq R package (Taus et al., 2017), with the following parameters: method = P.planII, poolSize = 200 diploid individuals, and excluding SNPs with allele frequencies below 0.01 or above 0.99.

2.6. Divergence between basal and evolved lines

To detect SNPs that significantly changed their frequency during experimental evolution, we performed the ACER test (Spitzer et al., 2020). This test is a modification of the classical Cochran-Mantel-Haenszel test, specifically designed to account for genetic drift, pool sequencing, and consistent changes between replicates. We used the sync file before coverage subsampling as an input for the ACER test, after applying additional filters.

Firstly, loci with a minor allele frequency below 5% across lines in F1 or F28 were removed, as true polymorphism in such positions is indistinguishable from sequencing errors (Anderson et al., 2014; Futschik & Schlötterer, 2010). Secondly, we filtered loci to ensure coverage in each line ranged between 53-215X for autosomes and 36-147X for the sex chromosome. The test was applied using the ACER R package (Spitzer et al., 2020) with the adapted.cmh.test function and resulting P values were transformed to q values using the qvalue R package (Storey JD, Bass AJ, Dabney A, 2024) to correct for multiple comparisons. SNPs with q values below 0.05 were grouped into three categories: diverged in both treatments, diverged only in the female-biased lines and diverged only in the male-biased lines. The first category is expected to contain both loci underlying adaptation to experimental conditions and loci responding divergently to sex ratio manipulation. For the former, SNPs are expected to concordantly change their frequencies in the same direction in male- and female-biased lines, while the latter are expected to change in opposite directions between treatments or be selected in one treatment and not in the other. To distinguish these, we calculated allele frequencies using the af() function from the poolSeq R package and averaged the values within generations and treatments. Allele frequency change was calculated by subtracting the frequency at the starting generation from the frequency at the evolved generation.

In E&R studies, it is commonly observed that the number of selection targets identified is much higher than expected (Kofler & Schlötterer, 2014). This is primarily due to the tight linkage between selection targets and the genetic background, which increase their frequency along with the selection target (genetic hitchhiking; Franssen et al., 2015; Long et al., 2015; Nuzhdin & Turner, 2013; Tobler et al., 2014). To increase the power of identifying true selection targets and reduce the number of candidates to a few selected regions, we performed haplotype identification based on allele frequency changes. Assuming that the true selection targets are among the most differentiated SNPs within each haplotype, we selected top 10% of significant SNPs with the lowest q values from each haplotype (Otte & Schlötterer, 2021). Haplotype

identification was carried out with the haploValidate R library (Otte & Schlötterer, 2021) using mncs = 0.015 and default settings.

To make our results directly comparable to those of Parrett et al. (2022), we also performed Generalized Linear Models (GLMs) with quasi-binomial distribution to identify SNPs that consistently diverged between male- and female-biased lines during experimental evolution. The input for the GLMs was the same as that used for the ACER test but included allele counts only from F28 samples. For each genomic locus, allele frequencies were compared between the treatments using the formula: *glm(cbind(major allele count, minor allele count) ~ treatment)*. If any line had an allele count of 0, we added 1 to the allele counts of all lines (Wiberg et al., 2017). To control for the false discovery rate due to multiple testing, the P values obtained from the GLM were converted to q values as described above.

We additionally carried out an analysis focused on the *6Pgdh* gene, which previous work has shown to be a sexually antagonistic loci in bulb mites (see introduction). We selected SNPs from the *6Pgdh* gene which significantly changed their frequency in either treatment, based on ACER test. To test if selection on these SNPs differ between treatments, we used GLMs with minor and a vector of major allele counts as a response variable and generation, treatment and interaction between them as explanatory variables. We used quasibinomial error distribution to account for overdispersion detected in the data.

2.7. Gene Ontology Term Enrichment

To determine whether selection targets share functional characteristics, we performed gene ontology (GO) term enrichment analysis separately for the SNPs that diverged in the male- and female-biased lines. The low number of SNPs that diverged in both treatments but in opposite directions (5 SNPs) precluded GO enrichment analysis for this set.

The set of background genes comprised only genes with significant expression in adults, a high proportion of informative coverage (>60% length within 53-215X), and an assigned GO category. GO enrichment was performed using the clusterProfiler R package (Yu et al., 2012), with Benjamini-Hochberg correction to adjust for multiple comparisons.

3. Results

3.1. Reads & mapping statistics

The sequencing of pooled samples resulted in 6.1 G reads, yielding a total of 601 G bases (Supplementary Table 1). On average, we obtained 191 M reads per sample (range: 128 – 257 M reads), with the average of 118 M reads per sample (62%, range: 50-167 M reads) mapped to a reference genome with a mapping quality above 20.

The sync file, after removing indels and repeated sequences, contained over 194 M positions for which allele counts were aggregated between male and female samples. After removing sites with very low and very high mean coverage across samples (<53 and >215X, see methods), 113.6 M autosomal and 13.6 M sex chromosome loci were retained in the sync file. For

estimating genetic diversity measures and Ne, we used 84.2 M autosomal positions, with the same coverage across all samples (min 53X).

3.2. Estimates of the autosomal genetic diversity

We found a significant decline between generation 1 and 28 in π and θ in all analysed classes of SNPs- in exons, both in synonymous and non-synonymous sites, and in 10 kb windows- when comparing evolved to basal populations (Figure 1 and Table 1). Male-biased lines showed significantly lower decline in π compared to female-biased lines (Figure 1), as indicated by a significant treatment by generation interaction (Table 1), but the interaction was not significant for 10kb windows (Table 1). Within exons, there was a significant interaction between treatment and generation for synonymous, but not non-synonymous sites. Treatment did not significantly affect the change in θ over generations (Table 1).

Table 1. Results of analysis of variance of genetic diversity measures.

measure	class	term	$F_{(1,12)}$	*P*
π	exon	treatment	4.785	0.0492
		generation	102.747	<0.0001
		treatment:generation	4.989	0.045
	syn	treatment	4.527	0.055
		generation	212.515	<0.0001
		treatment:generation	5.442	0.038
	nonSyn	treatment	2.643	0.129977
		generation	28.127	<0.0001
		treatment:generation	2.340	0.152
	10 kb windows	treatment	2.127	0.170
		generation	35.759	<0.0001
		treatment:generation	0.563	0.467
θ	exon	treatment	0.584	0.459
		generation	161.616	<0.0001
		treatment:generation	3.302	0.094
	syn	treatment	0.475	0.504
		generation	223.709	<0.0001
		treatment:generation	3.952	0.07
	nonSyn	treatment	0.705	0.42
		generation	98.386	<0.0001
		treatment:generation	2.393	0.148
	10 kb windows	treatment	0.534	0.479
		generation	95.323	<0.0001
		treatment:generation	1.931	0.19

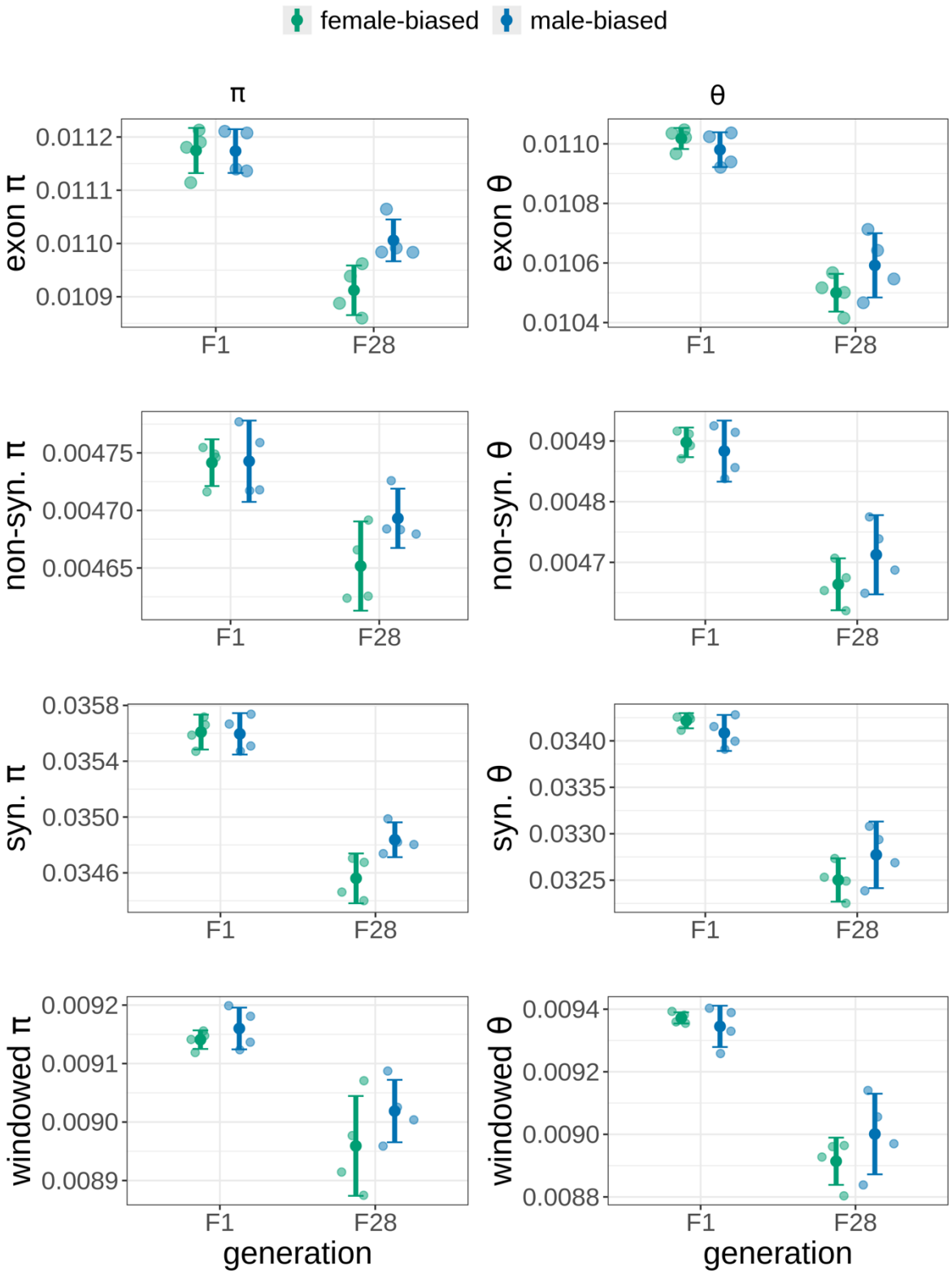

Figure 1. Changes in autosomal diversity patterns. Left-side panels show changes in nucleotide diversity (π), and changes in number of segregating sites (θ) are shown on the right-side panels. For each generation, mean across all lines are indicated by filled points, with +/- 1 standard deviation indicated by whiskers, and faded points indicating genome-wide line averages.

The decline in π and θ could be driven by purifying selection, or by genetic drift. To distinguish between these effects, we compared the rate of change in non-synonymous diversity relative to synonymous diversity by calculating Δπ and Δθ. The 95% confidence intervals of the line-averaged values for Δπ overlapped with zero, suggesting that changes in nucleotide diversity did not differ between synonymous and non-synonymous (Figure 2, 95% CI female-biased: -0.005 to 0.003l; 95% CI male-biased: -0.003 to 0.005). Values of Δπ did not show significant differences between male- and female-biased lines (t-test, t = -1.06, d.f. = 6, P = 0.33). In contrast, significantly negative values of Δθ suggested that the number of segregating sites is being lost at a greater rate than expected solely from drift (95% CI female-biased: -0.014 to -0.005, 95% CI male-biased: -0.009 to -0.001). The values of Δθ, however, did not differ significantly between the treatments (t-test, t = -1.86, d.f. = 6, P = 0.11).

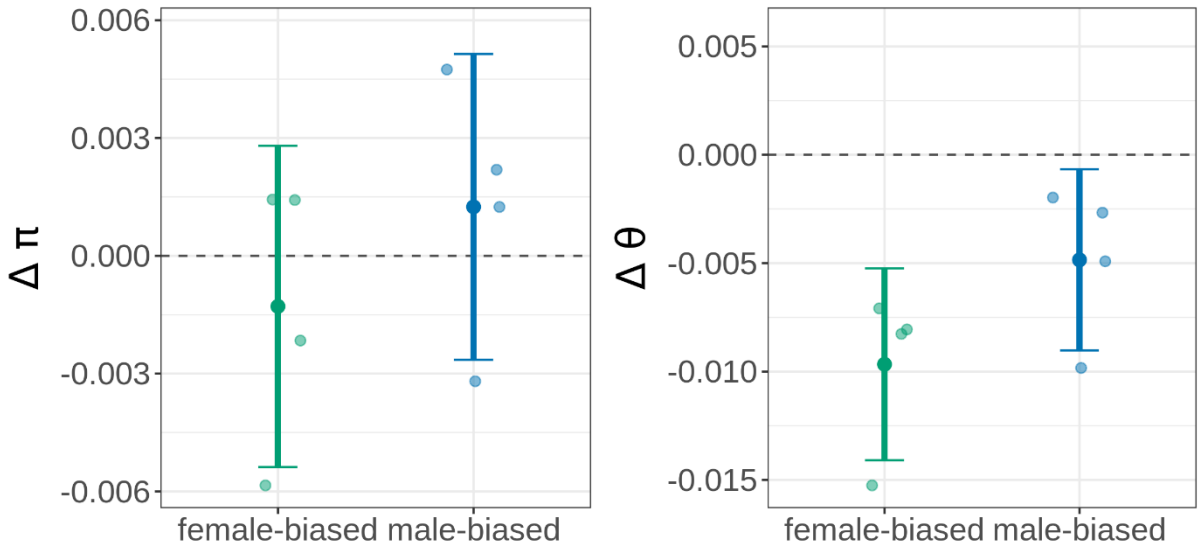

Figure 2. Changes in non-synonymous sites relative to synonymous sites are indicate by Δπ (A) and Δθ (B). Faded points indicate line-averaged value, and whiskers show 95% confidence intervals. Dashed horizontal lines show 0.

3.3. Estimates of effective population sizes

Estimates of effective population sizes did not differ significantly between the selection regimes (Figure 3, t = 0.394, d.f. = 6, P = 0.71; mean of male-biased lines = 397, range: 356 - 478; mean of female-biased lines = 409, range: 395 - 441). Estimates of effective population sizes for all lines are provided in Supplementary Table 2.

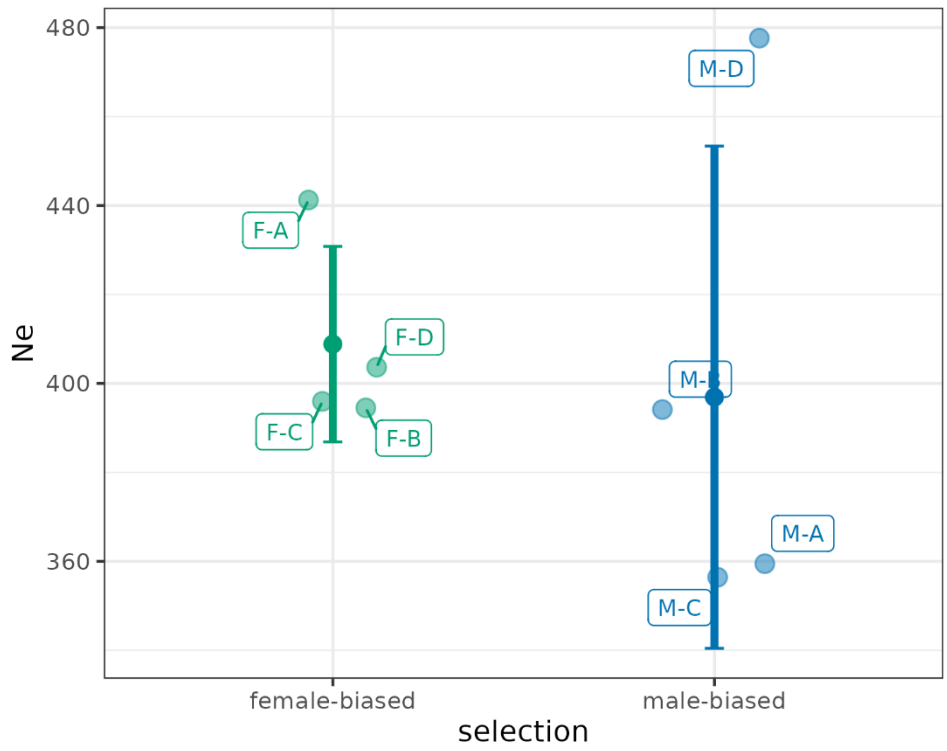

Figure 3. Estimates of effective population sizes based on allele frequency change between basal and evolved lines.

3.4. Divergence between basal and evolved lines

From 6.1 M loci tested, 17,918 SNPs significantly changed frequency in both selection regimes. The allele frequency changes of these SNPs were highly positively correlated between male- and female-biased lines, suggesting that most of these SNPs underlie adaptation to the experimental conditions (Figure 4, Pearson's correlation r = 0.96, $P < 0.0001$). Only five of these SNPs responded to selection in opposite directions in male- and female-biased lines (Supplementary Table 3). Notably, only a single SNP (chr8: 6,268,648) was located within a protein-coding gene, which is a homologue of a nuclear hormone receptor HR96. Another three SNPs were located up to 673 bp upstream to the nearest genes: two of them were located near the gene encoding tripartite motif-containing protein and another close to a gene with unknown function. The last SNP was located 719 bp upstream to a heat shock protein gene.

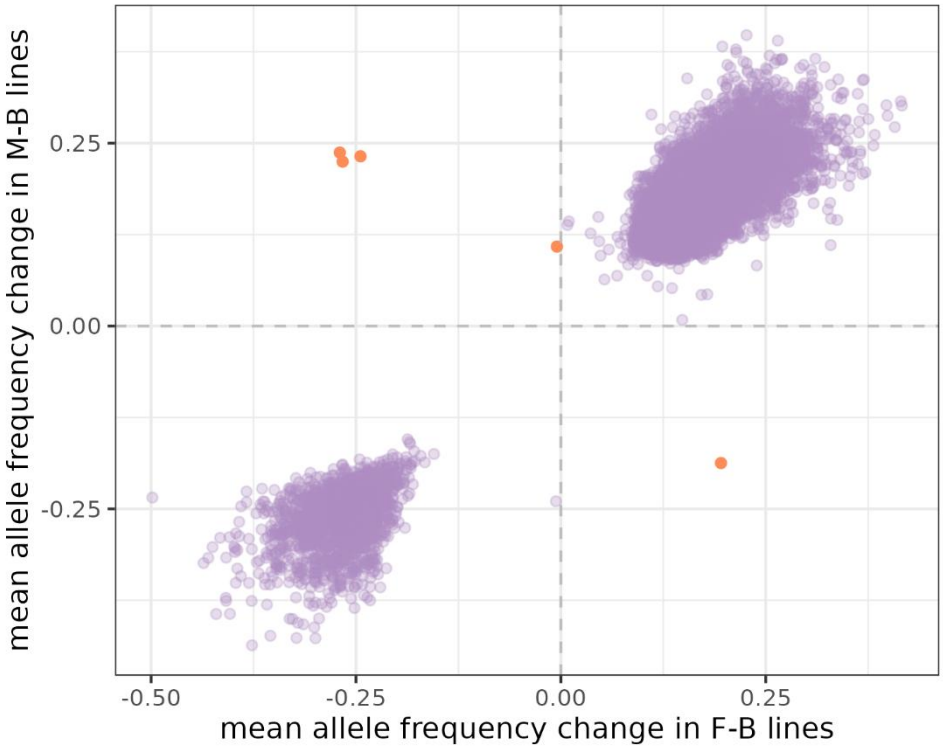

Figure 4. Correlation of allele frequency change between female- and male-biased lines. Only SNPs that significantly changed their frequency between basal and evolved populations in both treatments, as indicated by the ACER test, are shown. Violet points indicate concordant allele frequency changes between treatments, while orange points indicate SNPs that changed their frequency in opposite directions in male- and female-biased lines.

Additionally, we found 49,228 SNPs that changed their frequency exclusively in female-biased lines and 79,390 SNPs in male-biased lines. These SNPs formed 46 independent haplotype blocks in female-biased lines and 58 in male-biased lines (Figure 5). Distribution of haplotype length was similar between treatments (Wilcoxon rank-sum test: W = 1391, $P = 0.47$), and ranged from 2.2 kb to 33 Mb.

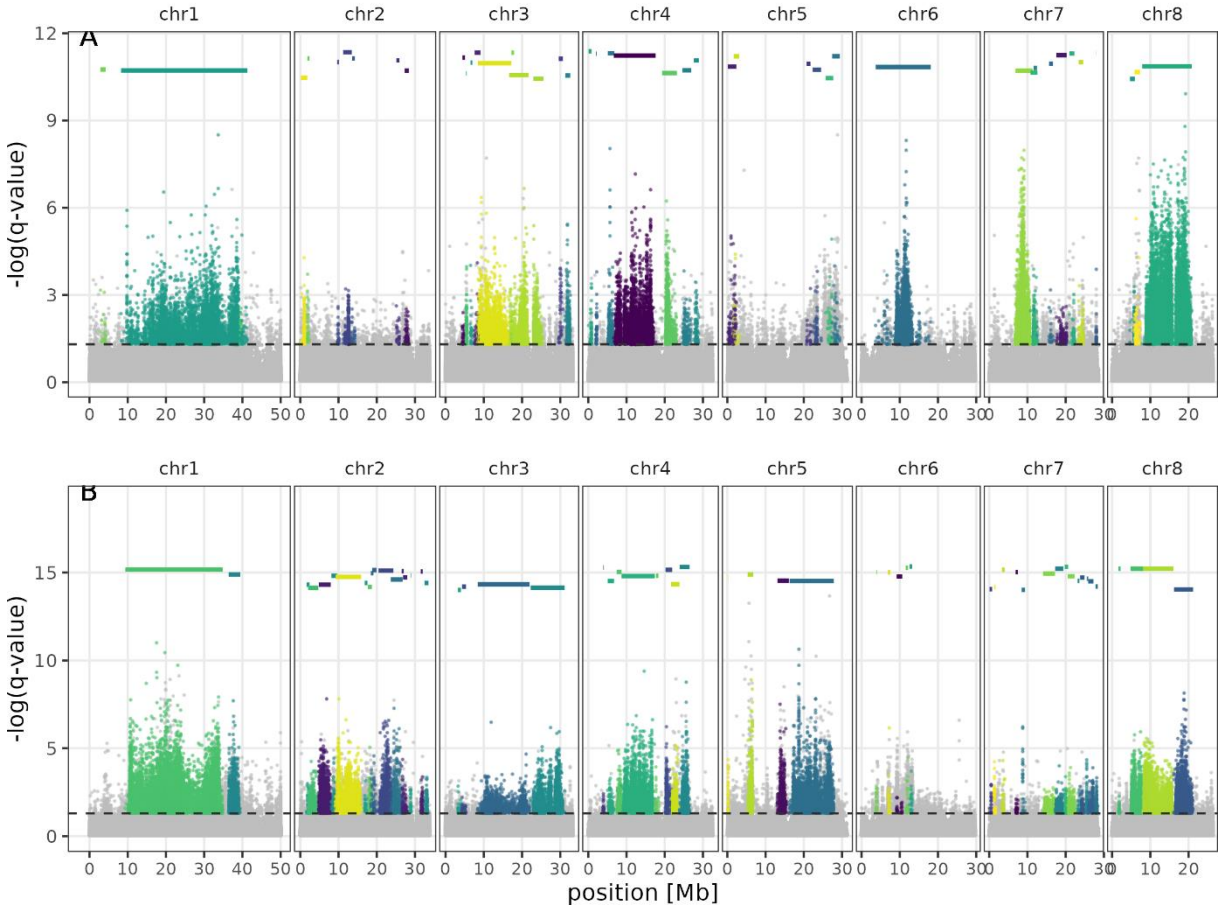

Figure 5. Haplotype identification based on SNPs that diverged specifically in the female-biased lines (A) and male-biased lines (B). Haplotypes are color-coded, with additional horizontal lines at the top of each panel. The X-axis presents the genomic position, and the Y-axis shows the negative log-transformed q values from the ACER test. Dashed line presents q value of 0.05.

In male-biased lines, genes containing selection targets- defined as the top 10% most differentiated SNPs from each haplotype- showed significant enrichment in genes functionally associated with transcription coregulation (GO:0003712) and gene regulation via histone acetylation (GO:0004402). Selection targets in female-biased lines were enriched in genes associated with the cell membrane (GO:0016020).

Using GLMs, we identified only one SNP that significantly diverged between treatments in the evolved populations (Supplementary Figure 4). This SNP was located at position 4,172,390 on chromosome 1 and was not situated near any protein-coding gene. The mean allele frequency of this SNP was 0.63 in female-biased lines and 0.84 in male-biased lines. Although this SNP was diverged between treatments in the evolved populations, it did not change it frequency compared to the basal populations (female-biased lines: $q = 0.32$; male-biased lines: $q = 0.63$).

Table 2. GO term enrichment of SNPs which significantly diverged during experimental evolution

treatment	GO term	GO description	adjusted P	gene ratio
female-biased	0016020	membrane	0.011	0.1
male-biased	0003712	transcription coregulator activity	< 0.0001	0.02
male-biased	0004402	histone acetyltransferase activity	0.002	0.02

Focusing on *6Pgdh* gene, we observed significant allele frequency change in 2 our of 21 SNPs identified in this gene, located at chromosome two at positions 15,186,738 (T>A) and 15,186,797 (T>A, both changes are synonymous). While these two SNPs changed frequency in male-biased lines (Figure 7, ACER test, SNP 15,186,738: $q = 0.0045$; SNP 15,186,797: $q = 0.0053$), their frequency did not change in female-biased lines (ACER test, SNP 15,186,738: $q = 0.7866$; SNP 15,186,797: $q = 0.8782$). The interaction between generation and treatment was significant for both SNPs (GLM, SNP 15,186,738: $P = 0.0032$; SNP 15186797: $P = 0.0039$).

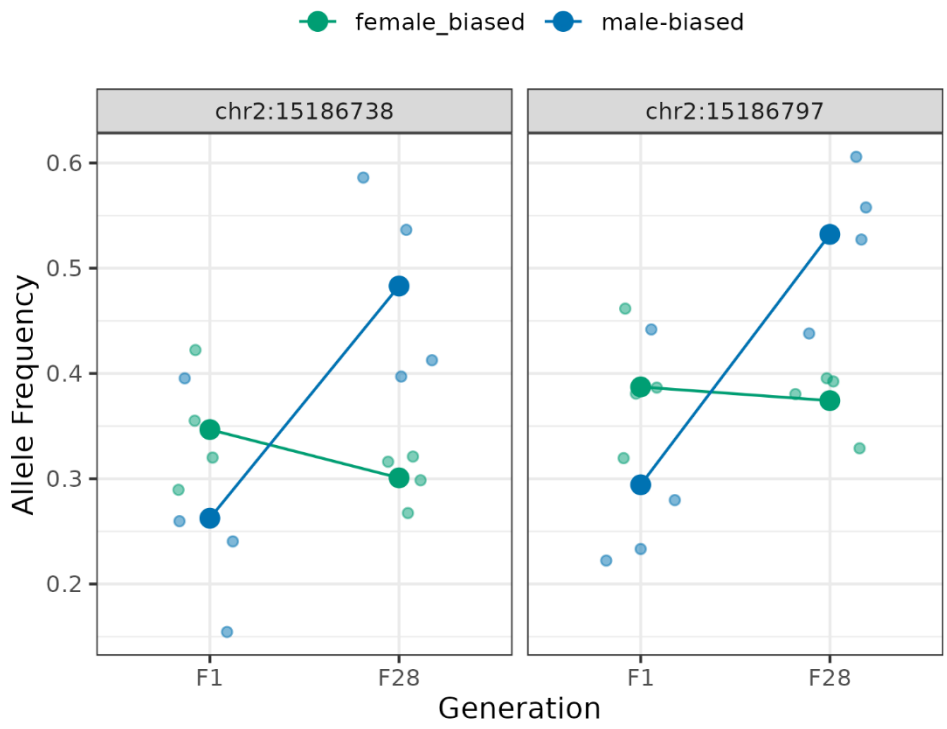

Figure 7. Allele frequency changes across generations for significant SNPs in the *6Pgdh* gene identified by the ACER test. Larger points connected by lines represent averaged allele frequencies across treatments, while smaller points depict line-specific allele frequencies. SNPs

are presented in separate panels, illustrating significant interaction between treatment and generation at both SNPs.

4. ***Discussion***

In the present study, we manipulated intrasexual reproductive competition by varying sex ratio over 28 generations and traced genomic consequences of this manipulation. In particular, we aimed to infer whether enhanced sexual selection leads to depletion of genetic variance due to enhanced purifying selection and/or genetic drift, or on the contrary, maintains it by fostering balancing selection associated with widespread sexual antagonism. We found no evidence for enhanced purifying selection in male-biased lines. However, the sex ratio significantly affected nucleotide diversity in exons, as we reported relatively lower decline of π in exons in male-biased lines. Additionally, we identified and characterised large genomic regions which responded to sex-biased selection exclusively in male-biased or female-biased lines.

Previous work in the same system that artificially mass-selected for male morph found that populations enriched for a morph expressing the sexually selected weapon (fighter lines) lose genome-wide genetic variance faster compared to lines nearly fixed for an alternative male morph not expressing the weapon (scrambler lines). The latter treatment was particularly enriched for putatively deleterious variants that initially segregated at low frequency. Apparently weaker purifying selection in scrambler lines could be a direct effect of selection against a fighter genotype. Expression of fighter phenotype, while strongly impacted by additive genetic effects, is also condition dependent (Radwan, 1995; Smallegange, 2011) and sensitive to inbreeding (Parrett et al., 2023), so males expressing fighter morph are likely to be less burdened with deleterious mutations. Furthermore, there is evidence that large portion of these mutations is unconditionally deleterious, as inbred lines derived from scramblers show higher inbreeding depression for female fecundity compared to inbred lines derived from fighters (Łukasiewicz et al., 2020). Additionally, overall sexual selection could have been stronger in fighter lines than in scrambler lines due to elimination of male fights in the latter.

In present study, we did not directly select on morph, and furthermore, we counteracted morph ratio evolution by keeping equal proportions of morphs in both sex-ratio treatments. However, male fights could occur in both treatments, contributing to overall sexual selection that would also include mate searching and sperm competition. Surprisingly, we found no significant effect of sex ratio treatment on the amount of genetic variance segregating in populations except for nucleotide diversity (π) within exons, particularly at synonymous positions. However, non-synonymous positions, as well as 10-kb window showed a similar trend toward lower loss of nucleotide diversity in male-biased lines. As we mentioned in the introduction, the change in the value of π as a result of selection is hard to predict because it would depend on initial allele frequencies and the direction of a change. It seems that allele frequencies in female-biased lines

have become more biased in effect of experimental evolution, and this was probably not due to stronger drift as the treatments did not differ significantly in effective population size.

Finally, the treatments did not differ how the π or θ changed over 28 generations at non-synonymous substitutions relative to synonymous ones. Thus, in contrast to Parrett et al. (2022) morph selection experiment, our results do not reveal enhanced purifying selection associated with increased reproductive competition induced by male-biased sex ratio. The lack of significant effect of treatments on genetic diversity could either reflect much weaker selection imposed by our sex ratio treatment compared to direct selection on male morph in Parrett et al. (2022), or stronger balancing selection counteracting the loss of genetic diversity. However, the latter possibility seems unlikely given that the differences in the strength of balancing selection between the treatments should affect alleles segregating at intermediate frequencies and thus affect π, while stronger the difference in purifying selection should still be reflected as a difference in θ.

We intended to investigate the role of balancing selection by testing for enrichment of its signature (elevated Tajima's D) among SNPs that significantly diverged between our selection treatments. However, in contrast to (Parrett et al., 2022), our GLMs have revealed only a single diverged SNP, and the number of SNPs identified by ACER was too small to allow for a meaningful analysis. This paucity of significantly diverged SNPs suggests that the selection in the current study was weaker compared to a direct selection on male weapon in Parrett et al. (2022). In addition to the strength of selection, the two studies could also differ in selection target, which could be larger in the present study due to the highly polygenic nature of the response associated with multiple aspects of phenotypes being under selection as mentioned above. Highly polygenic adaptation may lead to only small allele frequency changes, and to little overlap between replicate populations, making them difficult to detect (Barghi et al., 2020; Jain & Stephan, 2017; Otte et al., 2021; Sella & Barton, 2019). Nevertheless, using an alternative statistical approach (ACER test) we did identify a large number of SNPs that were significantly selected for in our experimental evolution lines. A significant proportion of these SNPs (12%) were selected consistently in all lines, probably reflecting adaptation to experimental conditions, which differed from those in stock, for example in more constrained development time, lower colony density, or higher food abundance. However, most SNPs were selected in treatment-specific manner. While number of SNPs overestimates the number of selection target, we identified 46 and 58 haplotypes in female- and male-biased lines, respectively, supporting polygenic response to sex ratio treatments.

We found that the SNPs that exhibited the most significant response to selection in female-biased lines were enriched for genes interacting with a cell membrane, whereas male-biased lines were enriched with genes controlling gene transcription and histone acetylation. Histone acetylation controls gene expression by adding acetyl groups to lysine residues on histone tails, leading to a relaxed chromatin structure (euchromatin) that allows transcription factors and other proteins to access DNA and initiate transcription (Sterner & Berger, 2000; Turner, 1991).

Similarly, the only SNP located within a protein-coding sequence that diverged between treatments is located in the homologue of the nuclear hormone receptor HR96, which regulates polymerase II transcription in e.g. *D. melanogaster* (Fisk & Thummel, 1995), and plays a significant role in xenobiotic response in *Teteranychus urticae* (Ji et al., 2023) or *Tribolium castaneum* (Kim et al., 2022).

The longest haplotype on chromosome one, as well as a few other long haplotypes overlapped between male-biased and female-biased lines (Figure 5). This indicates incomplete linkage within these haplotypes, with some SNPs within them selected only within female biased lines, while other selected only in male-biased lines. Their length likely reflects low recombination. In particular, chromosome one has been shown to have the lowest recombination rate among all chromosomes (Chmielewski et al., 2024). Alternatively, these long haplotypes could contribute to lab adaptation, but random assortments of some SNPs within them could lead to their detection only in male-biased or only in female biased lines. Notwithstanding the reason for the overlap, many haplotypes, including some long ones, did not overlap within treatments, suggesting sex-ratio-specific adaptation.

Notably, two SNPs from the *6Pgdh* gene, with a well-documented genetic polymorphism underlying inter-locus sexual conflict in bulb mites, significantly changed their frequency. Previous work showed that males carrying the S allele of this gene had higher reproductive success as a result of longer copulations and increased sperm production, but copulation with such males decreased female fecundity (Konior et al., 2006; Skwierzyńska & Plesnar-Bielak, 2018). Sex bias manipulation in bulb mites was already shown to cause an increase in the frequency of the S-form in male-biased lines compared to female-biased lines, although similarly to our study, the allele was not selected against in female-biased lines (Plesnar-Bielak et al., 2020).

Polymorphism in 6Pgdh allozymes in previous work was associated with one specific non-synonymous SNP (chromosome 2: 15,189,091; Agata Plesnar-Bielak, personal communication; Skwierzyńska & Plesnar-Bielak, 2018; Unnikrishnan et al., 2024).However, we observed no amino acid polymorphism at that site, with arginine, associated with S allele, fixed in all our lines. It is likely that S variant fixed in our populations before our experimental evolution commenced, as it is strongly favoured under lab conditions (Skwierzyńska & Plesnar-Bielak, 2018). Instead, our study detected significant frequency changes at different SNPs within the 6Pgdh gene, approximately 2.3 kbp away from the previously reported amino-acid polymorphism. Because synonymous SNPs we detected are a part of a larger 6.7 Mbp haploblock, it is possible that they were not under direct selection but instead in linkage disequilibrium with functional polymorphisms elsewhere in the haploblock. Given our result, however, the causal role of *6Pgdh* in underlying sexual conflict in the bulb mite requires further study, as previous results could also be explained by *6Pgdh* polymorphism being in LD with other gene under sexual selection.

Concluding, our study provides evidence that manipulating sex ratio over multiple generations can lead to significant changes throughout the genome. In contrast to Parrett el al. (2022), we

found no enhanced purifying selection, but the genetic diversity was maintained at a higher level in male-biased lines, at least at synonymous positions within exons. This suggests that components of sexual selection may differ in their effect on genome-wide diversity, and consequently the outcome of experimental evolution studies may vary depending on the way sexual selection is manipulated. Additionally, our findings underscore the importance of gene expression regulation in response to sex-specific selection pressures. These insights highlight the complexity of sexual selection dynamics and the multifaceted genomic responses that can arise from altering reproductive competition.

5. Code availability statement

Code used in this study is available at the GitHub repository under the link: https://github.com/sebchm/sex_ratio_expEvol

References

The references for this chapter are located after the Conclusions section of the thesis.

Supplementary Table 1. Summary of sequencing yield per sample. Counts of reads and bases are provided in millions and rounded to 0 decimal places. M-B and F-B mean male-biased and female-biased lines, respectively. MapQ- mapping quality.

Sample Name	Line	Content	Generation	Total Reads (Million)	Mapped Reads (Million)	Filtered Reads (Mapq >20, Million)	Sequenced Bases (Million)	Duplication Rate
SR01	F-B A	100 ♀	F1	194	154	130	20822	40.9%
SR03	F-B A	100 ♂	F1	190	96	80	12837	35.14%
SR05	F-B B	100 ♀	F1	160	132	111	17797	38.1%
SR07	F-B B	100 ♂	F1	213	110	91	14416	36.19%
SR10	F-B C	100 ♀	F1	192	157	132	21120	40.94%
SR11	F-B C	100 ♂	F1	204	99	82	13104	34.63%
SR14	F-B D	100 ♀	F1	195	139	117	18651	38.88%
SR15	F-B D	100 ♂	F1	257	61	51	7875	33.02%
SR17	M-B A	100 ♀	F1	172	129	108	17195	38.12%
SR20	M-B A	100 ♂	F1	201	86	71	11335	34.52%
SR21	M-B B	100 ♀	F1	164	110	93	14793	35.08%
SR24	M-B B	100 ♂	F1	242	96	79	12416	36.97%
SR26	M-B C	100 ♀	F1	166	126	106	16875	37.6%
SR28	M-B C	100 ♂	F1	235	127	106	16829	38.71%
SR30	M-B D	100 ♀	F1	183	151	127	20364	39.75%
SR31	M-B D	100 ♂	F1	214	137	114	18136	39.85%
SR97	F-B A	100 ♀	F28	194	172	147	23304	42.99%
SR99	F-B A	100 ♂	F28	170	148	126	20058	40.15%
SR102	F-B B	100 ♀	F28	216	196	167	26372	45.5%
SR104	F-B B	100 ♂	F28	175	154	131	20884	40.82%
SR107	F-B C	100 ♀	F28	128	111	94	14832	34.75%
SR109	F-B C	100 ♂	F28	198	169	143	22866	41.98%
SR112	F-B D	100 ♀	F28	205	185	158	25088	43.65%
SR115	F-B D	100 ♂	F28	155	138	113	17547	39.52%
SR117	M-B A	100 ♀	F28	178	160	136	21574	41.15%
SR120	M-B A	100 ♂	F28	180	156	130	20362	40.5%
SR122	M-B B	100 ♀	F28	170	153	130	20584	39.59%
SR124	M-B B	100 ♂	F28	207	182	154	24620	42.93%
SR127	M-B C	100 ♀	F28	190	170	145	22879	42.25%
SR129	M-B C	100 ♂	F28	189	163	138	21975	41.35%
SR132	M-B D	100 ♀	F28	167	151	129	20358	40%
SR134	M-B D	100 ♂	F28	199	173	145	23613	40%
			sum	6103	4491	3784	601481	

Supplementary Table 2. Line-specific estimates of effective population sizes.

selection	line	N_e
female-biased	F-A	441.2445
	F-B	394.5069
	F-C	395.9668
	F-D	403.6390
male-biased	M-A	359.4659
	M-B	394.1269
	M-C	356.4228
	M-D	477.6465

Supplementary Table 3. Functional description and allele frequency change in SNPs selected in opposite direction between male- and female-biased lines which were significant in both treatments. Negative distances to the nearest genes are indicative of upstream location toward the gene.

SNP position	gene name	functional description	nearest gene	functional description of the nearest gene	distance to the nearest gene [bp]	Mean allele frequency change in female-biased lines	Mean allele frequency change in male-biased lines
chr2: 7,431,618	-	-	rhrob100g01380	protein-coding gene (unknown function)	-672	-0.00481	0.109
chr 2: 12,494,112	-	-	rhrob01g18520	dnaJ homolog subfamily B member 1-like heat shock protein	719	-0.244	0.232
chr2: 21,069,199	-	-	rhrob28g01000	tripartite motif-containing protein	-271	-0.266	0.225
chr2: 21,069,260	-	-	rhrob28g01000	tripartite motif-containing protein	-332	-0.270	0.237
chr8: 6,268,648	rhrob42g01420	nuclear hormone receptor HR96	-	-	0	0.195	-0.187

Supplementary Table 4. Haplotype-averaged allele frequency changes. First part of haplotype ID indicates chromosome, and second indicates their order on chromosome. Treatments in which haplotype was detected is denoted in second column. Last column shows number of SNPs with q value below 0.05 from the ACER test.

haplotype ID	treatment	Mean allele frequency change in female-biased lines	Mean allele frequency change in male-biased lines	Number of SNPs within haplotype
chr1_1	female_biased	0.15	0.04	20
chr1_2	female_biased	0.18	0.11	6847
chr1_3	female_biased	0.23	0.09	21
chr1_1	male_biased	0.09	0.17	17109
chr1_2	male_biased	0.09	0.16	1172
chr2_1	female_biased	0.18	0.03	124
chr2_2	female_biased	0.14	0.05	25
chr2_3	female_biased	0.21	0.05	29
chr2_4	female_biased	0.21	0.05	275
chr2_5	female_biased	0.16	0.03	22
chr2_6	female_biased	0.14	0.04	23
chr2_7	female_biased	0.19	0.04	66
chr2_1	male_biased	0.06	0.22	21
chr2_2	male_biased	0.04	0.22	506
chr2_6	male_biased	0.04	0.15	23
chr2_7	male_biased	0.05	0.17	58
chr2_8	male_biased	0.03	0.14	22
chr2_9	male_biased	0.03	0.14	39
chr2_10	male_biased	0.04	0.17	2483
chr2_3	male_biased	0.04	0.17	2662
chr2_11	male_biased	0.02	0.13	427
chr2_12	male_biased	0.03	0.16	41
chr2_13	male_biased	0.05	0.18	51
chr2_14	male_biased	0.03	0.12	21
chr2_15	male_biased	0.02	0.14	57
chr2_16	male_biased	0.03	0.16	73
chr2_4	male_biased	0.05	0.14	89
chr2_5	male_biased	0.05	0.17	2537
chr3_1	female_biased	0.13	0.03	26
chr3_8	female_biased	0.2	0.07	574
chr3_9	female_biased	0.2	0.02	41
chr3_10	female_biased	0.18	0.03	315
chr3_2	female_biased	0.13	0.01	65
chr3_3	female_biased	0.12	0.02	29
chr3_4	female_biased	0.13	0.02	71
chr3_5	female_biased	0.2	0.06	2436

chr3_6	female_biased	0.19	0.06	1328
chr3_7	female_biased	0.16	0.05	28
chr3_1	male_biased	0.05	0.19	22
chr3_2	male_biased	0.04	0.16	27
chr3_3	male_biased	0.04	0.15	1363
chr3_4	male_biased	0.03	0.15	2849
chr4_1	female_biased	0.2	0.03	41
chr4_2	female_biased	0.23	0.04	38
chr4_3	female_biased	0.17	0.05	215
chr4_4	female_biased	0.19	0.11	2929
chr4_5	female_biased	0.18	0.09	1213
chr4_6	female_biased	0.16	0.05	144
chr4_7	female_biased	0.16	0.03	85
chr4_1	male_biased	0.05	0.16	22
chr4_8	male_biased	0.04	0.16	853
chr4_2	male_biased	0.03	0.13	161
chr4_3	male_biased	0.11	0.17	348
chr4_4	male_biased	0.11	0.17	2815
chr4_5	male_biased	0.08	0.16	32
chr4_6	male_biased	0.1	0.16	440
chr4_7	male_biased	0.07	0.15	242
chr5_1	female_biased	0.18	0.1	40
chr5_2	female_biased	0.19	0.04	40
chr5_3	female_biased	0.2	0.07	111
chr5_4	female_biased	0.2	0.04	25
chr5_5	female_biased	0.19	0.11	20
chr5_6	female_biased	0.11	0.05	62
chr5_1	male_biased	0.08	0.21	29
chr5_2	male_biased	0.05	0.18	513
chr5_3	male_biased	0.04	0.17	609
chr5_4	male_biased	0.06	0.17	4439
chr6_1	female_biased	0.24	0.12	7092
chr6_1	male_biased	0.14	0.23	21
chr6_2	male_biased	0.06	0.17	22
chr6_3	male_biased	0.06	0.2	32
chr6_4	male_biased	0.17	0.24	20
chr6_5	male_biased	0.02	0.16	24
chr7_1	female_biased	0.17	0.03	3014
chr7_7	female_biased	0.17	0.08	59
chr7_8	female_biased	0.23	0.1	26
chr7_2	female_biased	0.2	0.04	227
chr7_3	female_biased	0.21	0.06	20
chr7_4	female_biased	0.15	0.04	20
chr7_5	female_biased	0.21	0.08	108

chr7_6	female_biased	0.21	0.09	51
chr7_1	male_biased	0.11	0.21	23
chr7_10	male_biased	0.09	0.16	20
chr7_11	male_biased	0.06	0.18	81
chr7_12	male_biased	0.07	0.19	54
chr7_13	male_biased	0.07	0.21	161
chr7_14	male_biased	0.09	0.2	149
chr7_2	male_biased	0.11	0.2	31
chr7_3	male_biased	0.03	0.15	32
chr7_4	male_biased	0.07	0.18	21
chr7_5	male_biased	0.08	0.22	29
chr7_6	male_biased	0.08	0.19	233
chr7_7	male_biased	0.06	0.19	302
chr7_8	male_biased	0.09	0.2	130
chr7_9	male_biased	0.09	0.2	211
chr8_1	female_biased	0.25	0.13	35
chr8_2	female_biased	0.17	0.05	75
chr8_3	female_biased	0.18	0.09	10550
chr8_1	male_biased	0.05	0.19	24
chr8_2	male_biased	0.06	0.19	2874
chr8_3	male_biased	0.09	0.19	6657
chr8_4	male_biased	0.09	0.2	5162

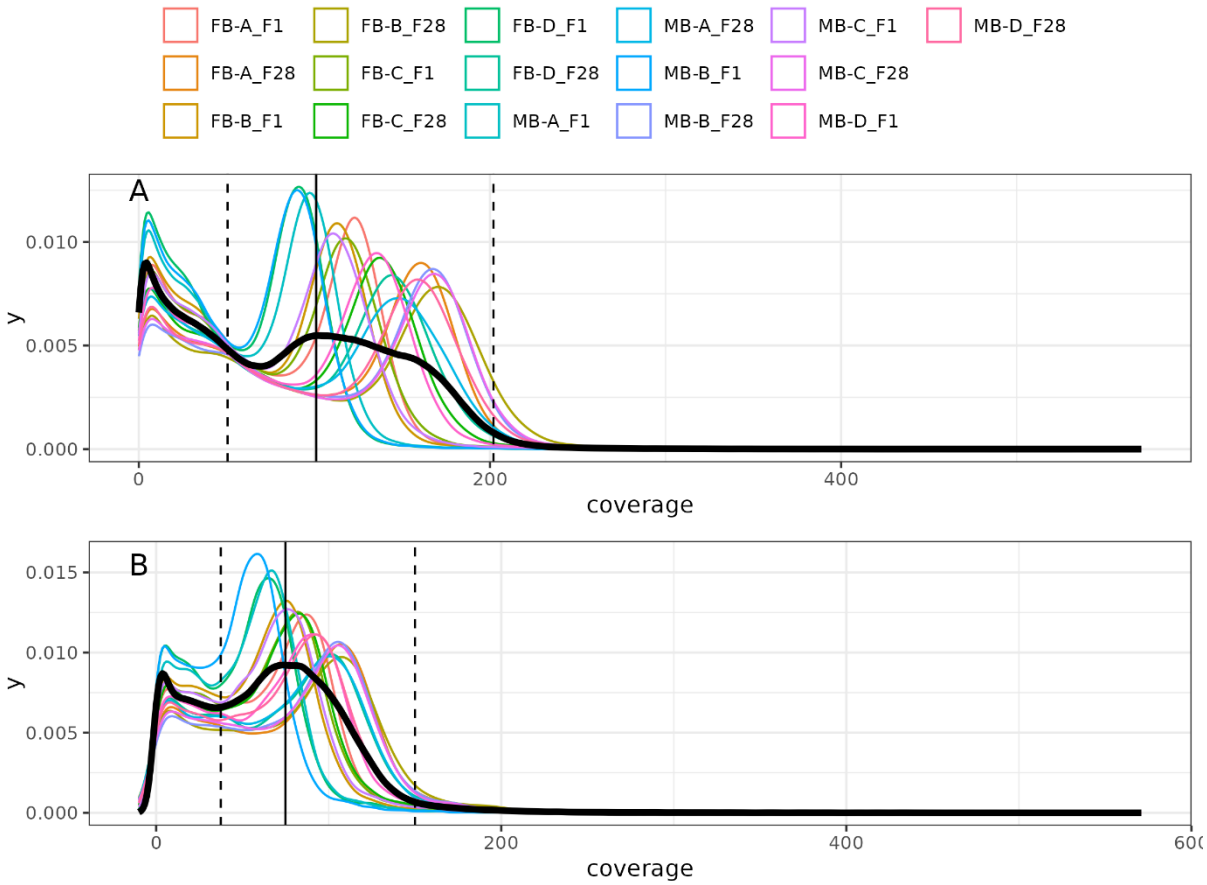

Supplementary Figure 1. Distribution of coverage for autosomal (A) and sex chromosome (B) loci. The black smoothed line indicates the average coverage across lines. The vertical solid line represents the target coverage, while the dashed lines indicate the range of informative coverage, spanning from 50% to 200% of the target coverage. In panel A, the long tail of the coverage distribution has been trimmed to the maximum coverage value of the sex chromosome (571X), removing 12 positions with high coverage values.

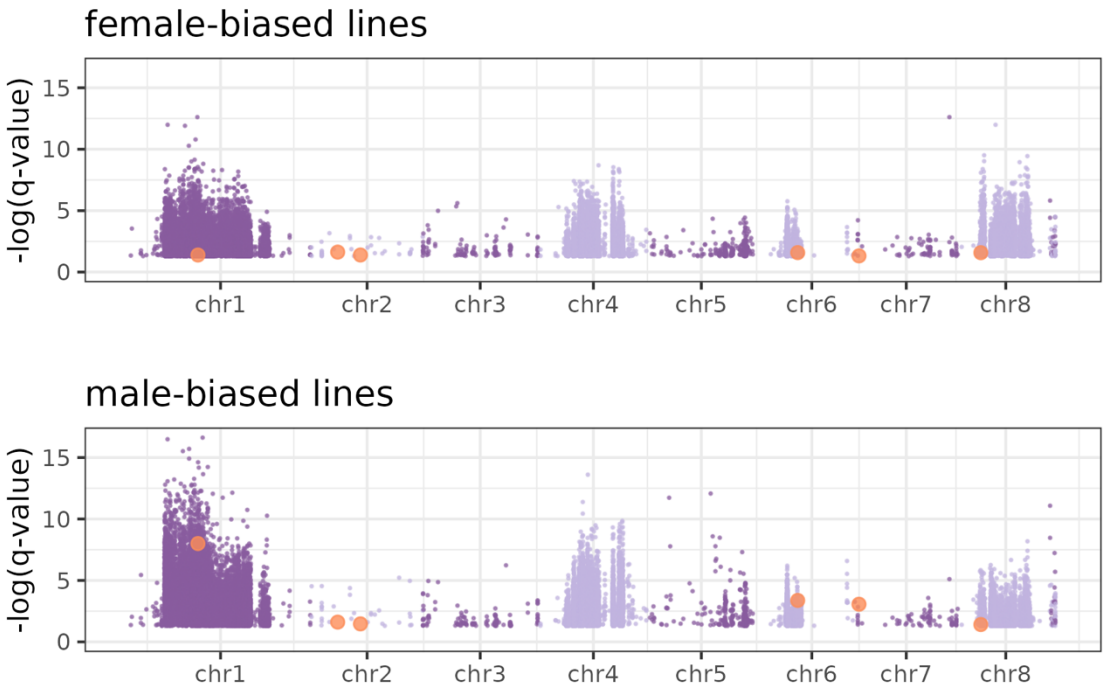

Supplementary Figure 2. Manhattan plots of SNPs that significantly diverged in both treatments between basal and evolved populations. Plots show the q value of ACER test performed on either female-biased lines (upper panel), or male-biased lines (lower panel). All SNPs, besides these highlighted in orange, changed their frequency concordantly in both treatments. SNPs highlighted in orange changed their frequency in opposite direction between female- and male-biased lines. Colours refer to the Figure 4.

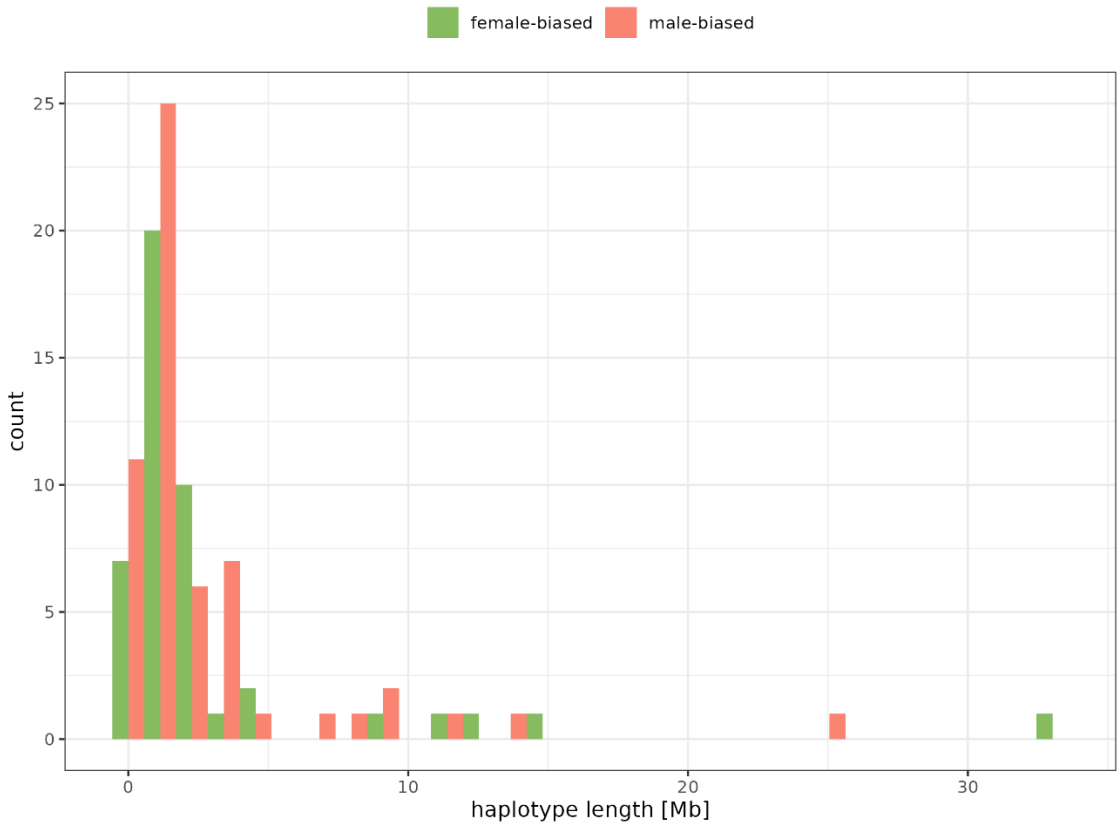

Supplementary Figure 3. Distribution of haplotype length.

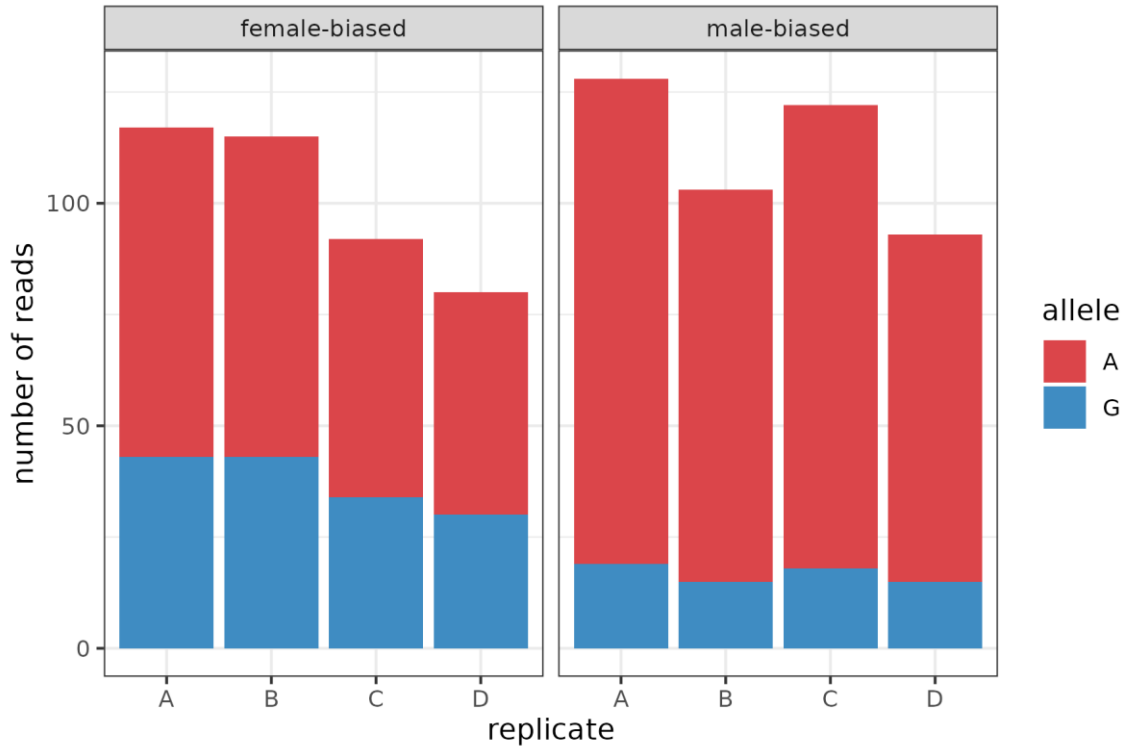

Supplementary Figure 4. Allele counts from the only SNP that was diverged between treatments in the evolved lines, as indicated by the GLM.

CHAPTER III

Supergene polymorphism and its role in male morph differentiation in the bulb mite, Rhizoglyphus robini.

SEBASTIAN CHMIELEWSKI, MATEUSZ KONCZAL, JONATHAN PARRETT, JACEK RADWAN

Evolutionary Biology Group, Adam Mickiewicz University

(unpublished)

Abstract

Sexual selection favours traits that aid reproductive competition, such as weapons or sexual ornaments. Understanding genetic underpinning of such traits is crucial for understanding the dynamics of sexual selection and its consequences for macroevolutionary processes. Here, we use whole genome re-sequencing to map genomic regions associated with expression of the sexually selected weapon in the bulb mite, *Rhizoglyphus robini*, which exhibits two distinct male morphs: armed fighters and unarmed scramblers. We identified a 3.5 Mb region on chromosome seven that plays a crucial role in the male morph expression. This region exhibits characteristics typical of non-recombining haplotypes, including significant nucleotide divergence, recombination suppression, and enrichment of transposable elements. In addition to this region, the morph is influenced by many SNPs scattered across the genome. These SNPs are enriched form low frequency, possibly deleterious variants among scramblers. Our findings highlight the interplay between major loci of large effect and genome-wide variation, the latter likely shaping expression of SSTs via their effect on condition.

Keywords: supergene, alternative reproductive tactic, genetic architecture, condition-dependence

1. Introduction

Selection arising from competition for the access to reproduction, i.e. sexual selection (Andersson, 1994; Darwin, 1872) is a powerful evolutionary force leading to evolution of spectacular adaptations, such as weaponry (horns, claws etc.) and elaborate sexual ornaments, but also shaping a range of other traits including energy allocation and metabolism, sensory systems or body size (Andersson, 1994). Production and maintenance of costly sexually selected traits (SSTs) such as weapons or ornamental feathers requires resources, and therefore

they tend to exhibit greater condition dependence than non-sexually selected traits (Bath et al., 2023; Bonduriansky, 2007; Bonduriansky & Rowe, 2005; Delcourt & Rundle, 2011; Emlen et al., 2012; Knell & Simmons, 2010). Condition-dependence optimises the trade-off between reproductive output and viability linking the expression of SSTs with a pool of metabolic resources (Bonduriansky, 2007). Given that SST development is associated with significant developmental or somatic costs (Emlen, 2001; Nijhout & Emlen, 1998), only individuals with a large pool of resources can express these traits. Therefore, SSTs can be shaped by genetic variance that affects condition, likely constituting a large mutational target (Andersson, 1986; Rowe & Houle, 1996), but at the same time enhance selection acting on this variance (Lorch et al., 2003; Parrett et al., 2022; Whitlock & Agrawal, 2009).

Condition-dependence is particularly visible in the case of discontinuous variation of male sexually-selected phenotypes, often referred as alternative reproductive phenotypes (ARPs). In many species, males in high condition develop armaments or ornaments and often aggressively fight over females, whereas poor condition males do not develop such traits and instead attempt to achieve reproductive success using other tactics, such as sneaky behaviours (Brockmann & Taborsky, 2008; Gross, 1996; Oliveira et al., 2008; Taborsky et al., 2008). However, because these are complex phenotypes linking morphology (e.g. weapons), behaviour (e.g. aggression) and other traits, such as metabolic and sensory ones, combining these traits into a single supergene may often be favoured. Indeed, large regions with little or no recombination have been reported to be involved in determination of ARPs in the ruff (Küpper et al., 2015; Lamichhaney et al., 2015), spider *Oedothorax gibbosus* (Hendrickx et al., 2021) and cichlid *Lamprologous callipterus* (Singh et al., 2023). While condition-dependence and genetic determination by single genes (or supergenes) have often been contrasted, it is possible that supergenes can co-exist with condition-dependence. This possibility has rarely been considered, despite its implications for the strength of purifying selection associated with expression of SSTs. Surprisingly, the combination of condition-dependence and genetic determination has not been reported in any species with discrete sex-limited phenotypic variation, to the best of our knowledge.

Recent studies of ARPs in the bulb mite *Rhizoglyphus robini* suggest that indeed a major locus with strong additive effects and genome-wide variation can both contribute to their genetic variance (Parrett et al., 2022). Two distinct morphs occur in this species. Fighter males use their thickened and sharply terminated third pair of legs as weapons to engage in combat with other males, while scrambler males avoid direct competition and employ sneaky strategies to obtain mating opportunities (Radwan, Czyz, et al., 2000). While expression of fighter morph can be suppressed with low quality diet resulting in poor condition (Radwan, 1995; Smallegange, 2011), male morph is also heritable and responds to artificial selection for or against fighters (Parrett et al., 2022; Plesnar Bielak et al., 2014; Radwan, 2003). A simple explanation for the co-occurrence of condition-dependence and a significant genetic determinant is genetic variance in condition, in turn affecting morph expression. Deleterious mutations segregating in natural populations are typically recessive or partially recessive, and

cause fitness decline when homozygosity is increased by inbreeding (inbreeding depression). Indeed, artificial selection lines nearly fixed for scramblers morphs showed higher inbreeding depression compared to lines nearly-fixed for fighters (Łukasiewicz et al., 2020). Further support for the role of deleterious mutations comes from genome sequencing of these lines, which showed an excess of rare, presumably deleterious variants scattered across genome in scrambler-selected lines, compared to those selected for fighter morph (Parrett et al., 2022). However, because the morph was mass-selected and allowed for reproductive competition between males within the line, the increased selection against deleterious mutations might have resulted from high prevalence of energetically costly fights in fighter lines, rather than directly from selection on prevalence of male weapon. Furthermore, a recent quantitative genetic study showed that inbreeding variance, a result of partly and completely recessive deleterious mutations segregating in populations, contributes much less than additive genetic variance to morph determination (respectively, 5% vs 63%, Parrett et al., 2023). This suggests that genetic factors other than deleterious recessives, possibly genes of large effect, contribute to morph determination in the bulb mite. Indeed, Parrett et al. (2022) observed contigs containing large density of SNPs that differentiated between fighter- and scrambler-selected lines, but the lack of chromosome-level assembly precluded further analysis of genomic regions (possibly supergenes) contributing to morph determination.

In this study, we investigated the genetic architecture of male morph determination in bulb mites. We analysed a comprehensive dataset from three different experiments, using whole-genome scans to characterize the genomic regions associated with the expression of alternative male morphs.

2. Methods

2.1 Pool-GWAS

To identify genetic loci associated with male morph determination, we firstly conducted a Pool-GWAS using two separate DNA pools, each comprising 100 fighter males and 100 scrambler males. The mites used for this study were derived from an outbred stock colony, which was established by mixing individuals from three geographically distinct populations (Mosina, Kraków, Kwiejce) approximately 42 generations before sampling (detailed description in Parrett et al., 2022).

To minimize food contamination, several thousand mites were transferred from the outbred colony into a separate dish containing a 5% agar base. After three days of starvation, we manually selected 100 scrambler and 100 fighter males and transferred them into separate vials containing ATL buffer. The samples were then homogenized using a metal micropestle and stored at -20°C.

DNA was isolated from the pools using the Qiagen DNeasy Blood & Tissue Kit (Qiagen) according to the manufacturer's protocol. DNA purity and quantity were assessed using a

Nanodrop spectrophotometer and a Qubit fluorometer, respectively. Libraries were prepared using the NebNext Ultra FS II DNA Library Prep Kit (New England Biolabs). Whole-genome resequencing was performed at the National Genomics Infrastructure (Uppsala, Sweden) on the Illumina NovaSeq 6000 platform, generating 149 million paired-end reads (2 × 150 bp) for the fighter pool and 129 million paired-end reads for the scrambler pool.

Sequencing reads were trimmed with Trimmomatic (v. 0.39, Bolger et al., 2014) and mapped to the chromosome-scale bulb mite reference genome (Chmielewski et al., 2024) using BWA-MEM (v. 0.7.17, Li, 2013) with default parameters. Duplicate reads were marked with Samtools markdup (v. 1.9, Li et al., 2009) and reads with a mapping quality below 20 were removed. An mpileup file was generated using Samtools mpileup, and indels with a minimum count of 5 were identified using the genomic-indel-regions.pl script from PoPoolation software (v. 1.2.2, Kofler, Orozco-terWengel, et al., 2011). Repeat sequence annotation (data from Chmielewski et al., 2024), indels, and the 5 base pairs flanking each indel were filtered out using the filter-pileup-by-gtf.pl script (PoPoolation). The resulting mpileup file was converted to a sync format using mpileup2sync, with a minimum base quality of 20.

To eliminate putatively duplicated and low-complexity sequences, we first calculated the average coverage for every 10,000th position of two pools and draw a distribution of these mean coverage values. The peak of this distribution, where the density was the highest, was identified as the "target coverage." This target coverage represents the most common coverage value observed across the genome, reflecting the expected coverage for regions without duplication or low complexity. Based on the target coverage, we established filtering thresholds, retaining only those positions with coverage between 50% and 250% of the target value (i.e., 27X – 135X, where the target coverage was 54X).

Differences in allelic composition between the fighter and scrambler pools were assessed using Fst values calculated in non-overlapping 10kb sliding windows, implemented in PoPoolation2 (v. 1.201, Kofler, Pandey, et al., 2011). We included only positions with a minimum allele count of 3 in both samples and windows with coverage between 27X and 135X for at least 30% of their length. Additionally, Fisher's exact test implemented in PoPoolation2 was used to analyse allele count differences for each position in the sync file. To account for multiple comparisons, q-values were calculated using the qvalue R package (v. 2.34.0, Storey JD, Bass AJ, Dabney A, 2024). All statistical analyses were performed in R (v. 4.1, R Core Team, 2024) and visualised in ggplot2 (Wickham, 2009)

2.2 Inbred lines

We sequenced 16 inbred lines, each of which had undergone full-sib mating for 14 generations, as described in Parrett et al (2023). Briefly, the inbred lines were established using either fighter males ("IW" lines) or scrambler males ("IN" lines), and for subsequent generations a male of the same morph as the founder male was selected for breeding. This selective inbreeding was intended to fix alleles specific to fighter or scrambler phenotypes within the respective lines.

Each line was sequenced using a pool of 10 females, except for line IN07, where only 9 females were available. The same procedures for DNA isolation, quality control, library preparation, sequencing, read trimming, duplicate marking, and mapping were applied as described for the Pool-GWAS. Given the high homozygosity expected from 14 generations of inbreeding (probability of fixation = 0.91, Falconer, 1996), genotypes were called jointly for all samples, treating each inbred line as a diploid sample using BCFtools mpileup and BCFtools call (v. 1.9, Li, 2011), with a minimum base and read quality threshold of 30. Repeat sequences were removed by providing repeat coordinates to Samtools view with the -*T* option. Only positions with a genotype quality of at least 30 were retained. We calculated the mean depth per site across all samples using VCFtools --*site-mean-depth* (v. 0.1.16, Danecek et al., 2011), and retained only positions with average sequencing depth between 10-42X per inbred line (target coverage = 21X). The VCF genotype file was divided into two parts: one containing invariant positions and the other containing biallelic positions, using VCFtools with options --*max-maf* 0 and --*mac* 1 --*max-mac* 2 –*maf* 0.05, respectively. The latter was used for the association test and genotype plot described below. To conservatively remove potential repeat elements, sites with heterozygous genotype calls in more than 2 out of 16 samples were excluded, and genotypes with coverage below 5 were removed using VCFtools --*minDP* 5.

2.2.1 Association test

To investigate the association between genotype and inbred line type (scrambler- or fighter-selected), we used the VCF file containing biallelic loci and performed an association test using plink software (v. 1.9, Purcell et al., 2007). The association test was based on 4,175,161 SNPs and was conducted using the *assoc* function with a permutation test to generate a null distribution by randomly shuffling phenotype labels (Steiß et al., 2012).

2.2.2 Genotype plot

Visual inspection of genotypes was performed with GenotypePlot R package (v. 0.2.1, Whiting, 2022). We used the VCF file containing biallelic loci which was subsampled to retain only SNPs separated by at least 100 bp with VCFtools function --*thin*.

2.2.3 Net nucleotide divergence

To quantify the genetic divergence between fighter- and scrambler-derived lines, we calculated Nei's net nucleotide divergence (d_a) along the genome (Hahn, 2018; Nei & Li, 1979). This measure estimates divergence between sequences since their split, according to the equation: $d_a = d_{XY} - \frac{(\pi_X + \pi_Y)}{2}$, where d_{XY} represents divergence between morphs, and π_X and π_Y denote nucleotide diversity in fighter and scrambler lines, respectively. We calculated d_{XY}, $\pi_X$and $\pi_Y$in 100-kb sliding windows using pixy (v. 1.2.11, Korunes & Samuk, 2021), based on the VCF file containing both variant and invariant sites.

2.2.4 Maximum-likelihood tree

Given the high divergence observed at the end of chromosome seven between morphs (see Results), we selected a 3.5 Mb region (24.5 Mb - 28 Mb) for phylogenetic analysis. The VCF file containing both variant and invariant genomic positions was converted to a PHYLIP alignment matrix using VCF2phylip (https://github.com/edgardomortiz/vcf2phylip), with loci genotyped in at least 10 samples. Phylogenetic trees were inferred using RAxML software (v. 8.2.12, Stamatakis, 2014) with the GTR-GAMMA model and bootstrapped 100 times. A separate tree, based on autosomes excluding chromosome 2, was created using 17,382 loci separated by at least 10,000 bp, selected using BCFtools --*thin*. Both trees included variant and invariant sites. The tree was visualised using Interactive Tree of Life (v. 6, Letunic & Bork, 2024)

2.3 Individually-Sequenced Mites

We hypothesized that the 3.5 Mb region highly diverged between scrambler- and fighter-derived haplotypes are alternative alleles of a supergene. To test this, we used DNA reads from 196 mite samples used for genetic mapping in Chmielewski et al. (2024). The sequencing reads were subsequently mapped to the reference genome, and had duplicates marked and removed reads with mapping quality below 20, in the same way as for Pool-GWAS and inbred lines samples. Genotypes were called jointly with BCFtools mpileup and BCFtools call, including only positions with mapping and base quality above 30. Only loci used as markers in genetic mapping, were retained for the following analysis. These markers were selected based on segregation distortion, genotype missingness and heterozygosity within families (for marker selection, see Chmielewski et al. 2024).

2.3.1 PCA

Firstly, we wanted to test if the clustering pattern is present in PCA performed on individually-sequenced mites. Such pattern is a typical signature of the non-recombining haploblocks. We performed principal component analysis (PCA) in SNPrelate (v. 1.36.1, Zheng et al., 2012), focusing on the 3.5 Mb segment of chromosome seven, which contained 13,759 SNP markers and gave a consistent signal of association in Pool-GWAS and inbred lines. Additionally, PCA was conducted on the remainder of the genome using a subset of 5% randomly selected loci. PCA visualization was performed twice: once plotting samples on principal components separately for each family, and once for all samples together. Because middle cluster in PCA conducted within non-recombining haploblock is expected to contain only heterozygous individuals, we calculated per-sample heterozygosity using the -*het* function in VCFtools by dividing the number of heterozygous sites by the total number of sites analysed.

2.3.2 Coverage Analysis

Coverage in 500 kb windows has been calculated using mosdepth (v. 0.3.4, Pedersen & Quinlan, 2018) and standardised by dividing by mean individual coverage of chromosome 7. Standardised coverage has been averaged across all samples from the same cluster.

2.3.3 Recombination suppression within the morph-determining supergene

Recombination between the supergene haplotypes should be effectively suppressed in heterozygotes. We tested this expectation using crossover location data from the genetic mapping study (Chmielewski et al., 2024). We plotted a Marey map of the putative supergene, with genetic distance plotted against physical position. For each crossover identified in this region, we checked the ID of individual which recombined and assigned them to one of four mapping families.

2.4 Transposable element enrichment

Non-recombining supergenes are expected to accumulate deleterious load, such as transposable elements, due to recombination suppression. We tested whether the putative supergene accumulates transposable elements by comparing their density between the region to the rest of the autosomal genome. The density of transposable elements was calculated in 100 kb non-overlapping windows by dividing the total length of transposons by the length of the window. Differences in TE density between the putative supergene and the autosomes were tested using a permutation test. A null distribution of differences was generated by randomly reassigning the labels of "autosomes" and "morph-determining supergene" across the windows 1,000 times. For each permutation, we recalculated the difference in mean TE density between the two groups. The p-value was then determined by calculating the proportion of these permuted differences that were as extreme or more extreme than the difference observed with the true labels.

2.5 GO enrichment

Finally, we assessed GO (Gene Ontology) term enrichment for genes located within the morph-determining supergene, focusing on genes expressed in adult mites (>1 FPKM, based on (Plesnar-Bielak et al., 2024). GO term enrichment was performed using the clusterProfiler R package (v. 4.10.1, Yu et al., 2012), with a background set of 8,186 genes that had significant expression and assigned GO terms.

2.6 Diverged SNPs beyond the putative supergene

We focused on SNPs beyond the putative supergene which were significantly diverged between scrambler and fighter samples in Pool-GWAS and association test. Due to high linkage disequilibrium detected at chromosome seven in inbred lines samples, we did excluded SNPs from this chromosome. Distributions of minor allele frequencies at diverged SNPs were drawn

separately for fighter and scrambler samples, and to test whether these are significantly different, we used permutation test in the same way as for the TE enrichment at the putative supergene.

3. Results

Whole-genome comparisons between scrambler and fighter pools revealed the highest genetic differentiation at the end of chromosome seven, specifically between positions 24.5-28 Mb, as indicated by Fst and Fisher's exact test results (Figure 1A, B). The signal of morph genetic differentiation was independently supported by a significant result of association test between genotypes and inbred line morphs in this region (Figure 1C), and a peak in net nucleotide divergence (Figure 1D).

Most scrambler inbred lines (i.e. IN lines) visually exhibited similar genotypes within this 3.5 Mb region and had a visibly higher proportion of missing genotypes compared to fighter inbred lines (F lines; Figure 1E, Supplementary Figure 2). In contrast, genotypes among fighter lines were more variable. However, two scrambler lines (IN2 and IN8) displayed distinct patterns: they neither had missing genotypes nor genetically resembled the other scrambler lines.

The phylogenetic tree based on the 3.5 Mb region differed from that for the rest of the genome. The former showed a strong divergence between fighter and scrambler inbred lines (Figure 2) for all, but two scrambler lines (IN2 and IN8), whereas no such divergence was observed for the rest of the genome. Furthermore, except for IN2 and IN8 lines scrambler-selected inbred lines clustered very closely to each other, while fighter lines were more diverged, with longer branches between each fighter inbred line.

High divergence of the 3.5 Mb region between fighter and scrambler inbred lines suggested it may constitute a non-recombining supergene. To test this, we carried out PCA on genotypes within the putative supergene from individually sequenced mites used for genetic mapping. PCA plots based on genotypes from the putative supergene 3.5 Mb region showed clear genetic structuring, with two extreme clusters corresponding to alternative haplotypes, and a middle cluster consisting of heterozygous individuals (Figure 3). The first two principal components explained 84.77% and 4.37% of the variance in the morph-determining supergene, respectively, so only the first PC was used for visualization. Females and scrambler males were present in all three clusters, however scramblers showed particularly low frequency in the left-side cluster (see Supplementary Table 1). Fighter males were exclusively present in the left-side cluster. In contrast, all samples from the C family clustered together and did not exhibit genetic structuring within the morph-determining supergene.
As expected for non-recombining haploblocks, samples forming the middle cluster exhibited the highest heterozygosity (mean heterozygosity = 91.5%), while heterozygosity of samples from other clusters was significantly reduced (mean heterozygosity: left cluster: 7.85%; right cluster: 3.7%). PCA of the remaining autosomal genome did not show the same three-group

separation; instead, samples were grouped according to their family of origin (Supplementary Figure 1B).

When analysing coverage within the morph-determining supergene, we observed that the samples from PCA cluster corresponding to fighter males exhibited higher coverage compared to the other two clusters. The heterozygous cluster displayed intermediate coverage levels, while the coverage in the alternative homozygous cluster fluctuated around 1 (Figure 4).

Analysis of the patterns of recombination within the morph-associated region revealed a total of seven crossover events (Figure 5), with five occurring in females and two in males. Notably, all recombining individuals belonged to the C family, which did not show structuring in the PCA within a putative supergene.

Morph-determining supergene exhibited a higher density of transposable elements (TEs) compared to the remaining part of the genome. (Figure 6A; median transposon density in morph-determining supergene = 9.3%; median transposon density in the remaining part of the genome = 3.55%). A permutation test confirmed that this difference in TE density was statistically significant (P = 0.001; Figure 6B). At the morph-determining supergene, we identified 502 genes which were significantly enriched for GO term associated with the catalysis of ester linkages within nucleic acids (GO term 0004519).

Beyond the putative supergene, we identified 569 SNPs significantly associated with morph expression in Pool-GWAS using Fisher's exact test (Figure 1B) and 1,872 SNPs in the association test using inbred lines, after excluding whole chromosome seven (Figure 1C). There was no overlap between SNPs detected by both tests. We found that these SNPs had more rare variants in scrambler lines than in fighter lines in both experiments (Figure 7, Pool-GWAS permutation test: P = 0; association test: P = 0). Genes containing SNPs diverged between fighter and scrambler lines which resided outside of the morph-determining supergene were not enriched in any GO term.

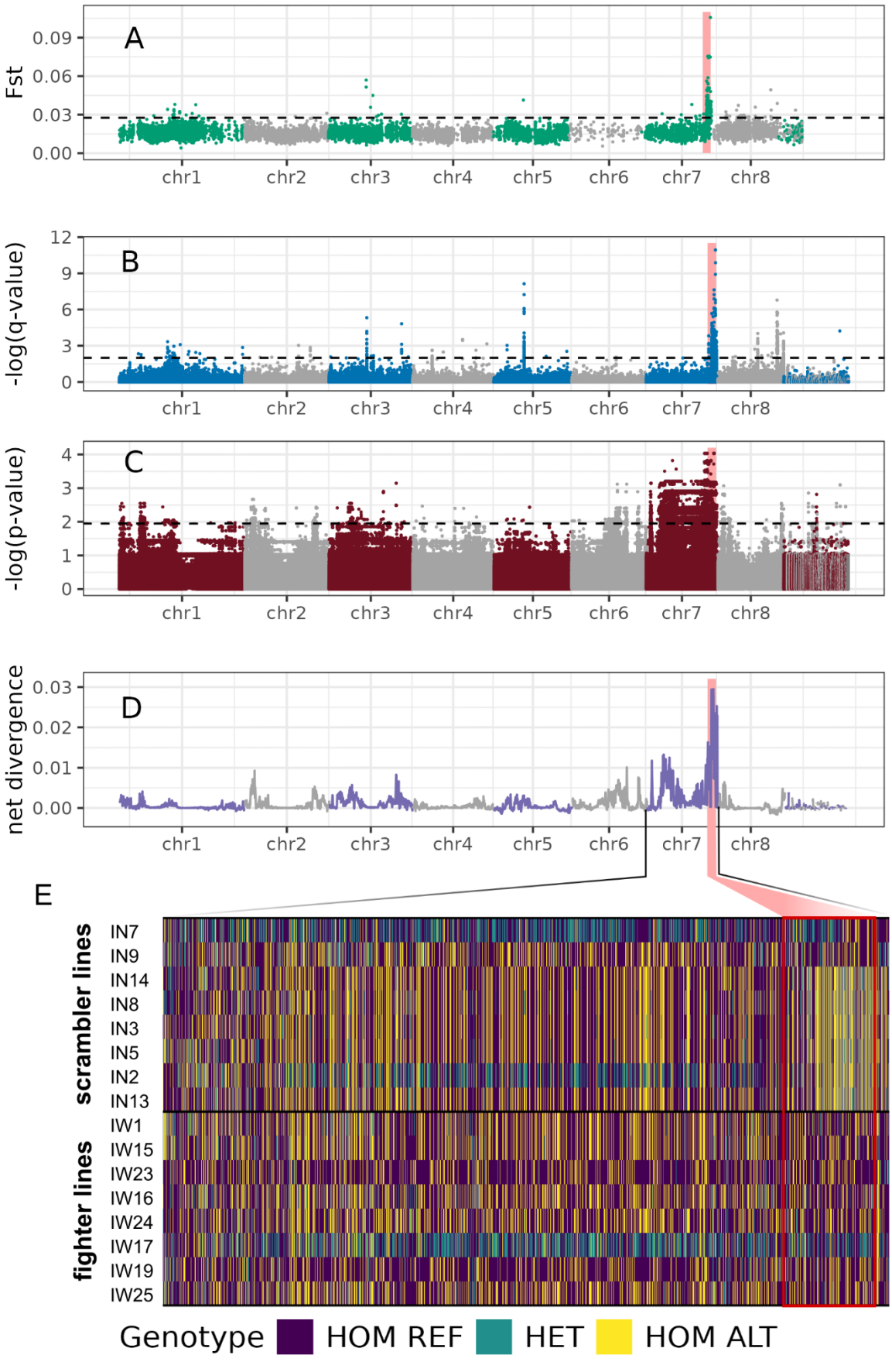
A
Fst
0.09
0.06
0.03
0.00
chr1
chr2
chr3
chr4
chr5
chr6
chr7
chr8
B
-log(q-value)
12
9
6
3
0
C
-log(p-value)
4
3
2
1
0
D
net divergence
0.03
0.02
0.01
0.00
E
scrambler lines
IN7
IN9
IN14
IN8
IN3
IN5
IN2
IN13
fighter lines
IW1
IW15
IW23
IW16
IW24
IW17
IW19
IW25
Genotype
HOM REF
HET
HOM ALT

Figure 1 (continued): Whole-genome comparison between fighter and scrambler samples. A: Pools of fighter and scrambler males show the highest genetic differentiation at the end of chromosome 7 (24.5-28 Mb, highlighted in red). Dashed line represents the 99th percentile of Fst values calculated in non-overlapping 10kb sliding windows. B: Fisher's exact test performed on each genomic locus confirms distinct allelic composition between morphs at the same region. The dashed line indicates a q-value of 0.01. C: Association test performed on scrambler- or fighter-selected inbred lines. Dots represent single loci, and the dashed line indicates the p-value of 0.05. D: net divergence between scrambler and fighter inbred lines. In all panels, chromosomes are indicated by alternating colours, and contigs not incorporated into a chromosome-level assembly are presented on the right side of chromosome 8 and ordered according to their length. E: Genotype plot of chromosome 7. Highlighted in red is a putative morph-determining region.

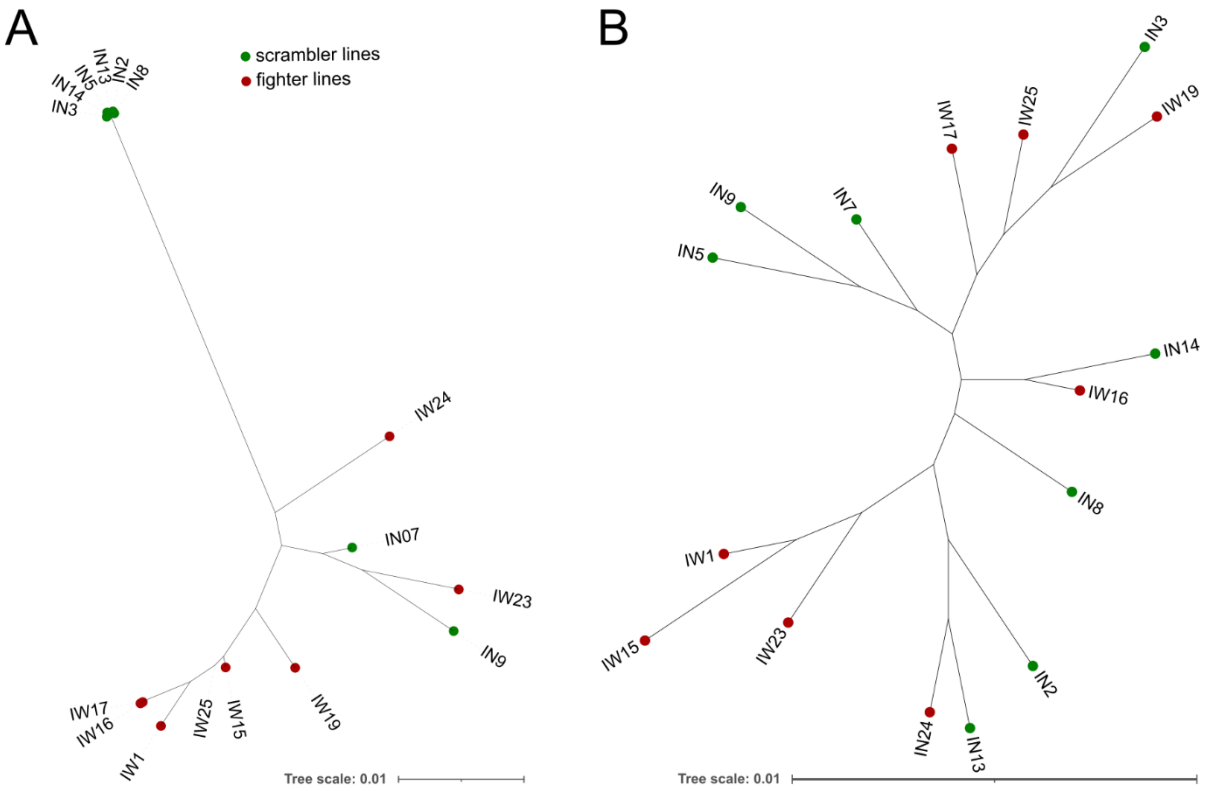

Figure 2. A: Maximum-likelihood tree for scrambler and fighter lines based on A: the associated 3.5 Mb region on chromosome 7 and B: all autosomes excluding chromosome 7.

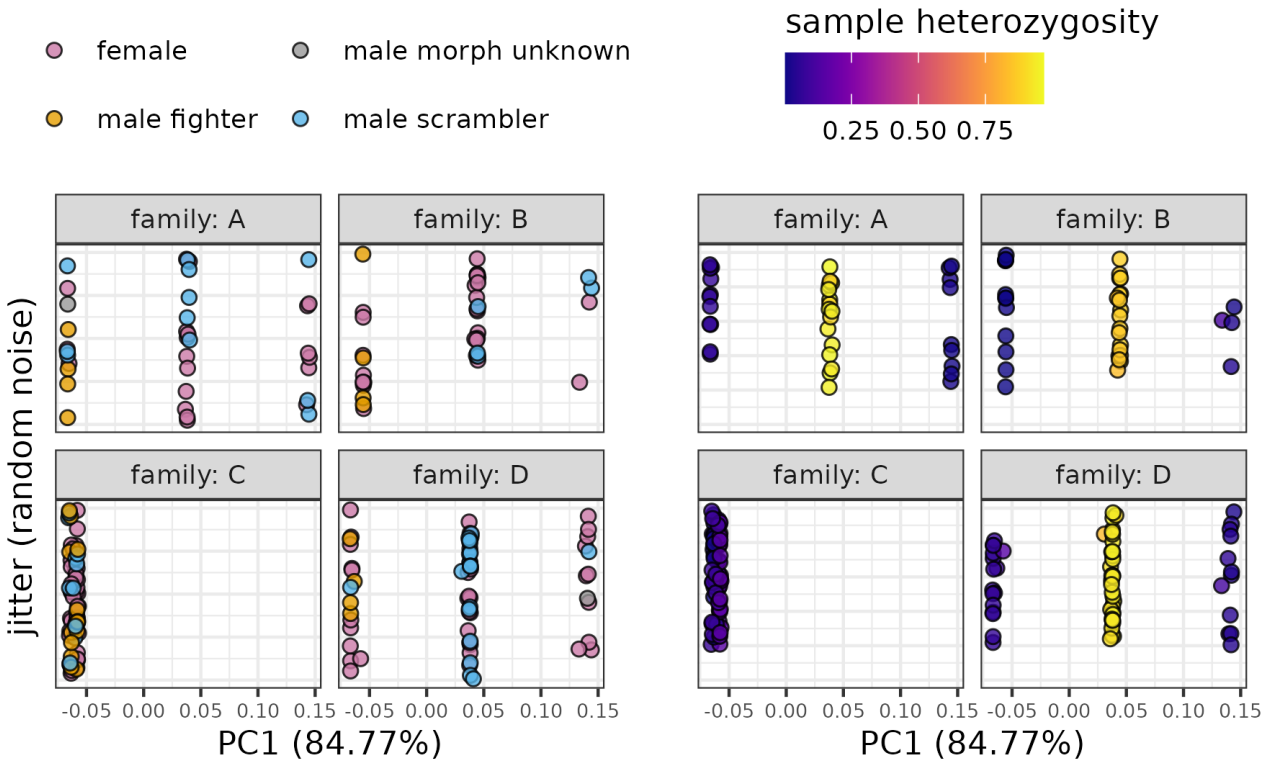

Figure 3. PCA based on genotypes from inbred lines at the morph-determining supergene shows a strong genetic clustering. A: The first principal component explains a large proportion of variance in genotypes, separating samples into three clusters. B: Proportion of heterozygous loci was significantly higher in middle cluster compared to other clusters.

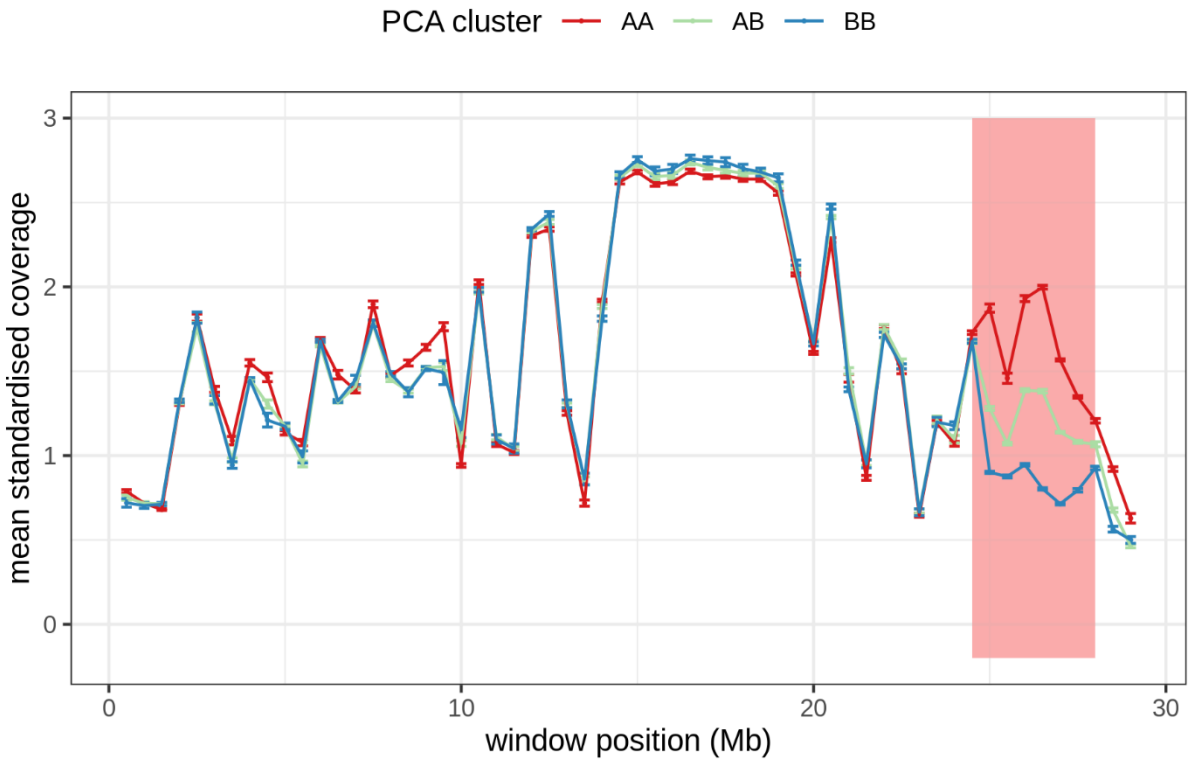

Figure 4. Coverage along chromosome 7. The samples with single mites were divided according to the corresponding clusters from PCA (cluster AA: left cluster with fighter males; cluster AB: middle heterozygous cluster; cluster BB: right cluster). Highlighted is a morph-determining supergene (34.5-38 Mb). Lines connect mean standardised coverage of a window, and error bars show ± 1 SE.

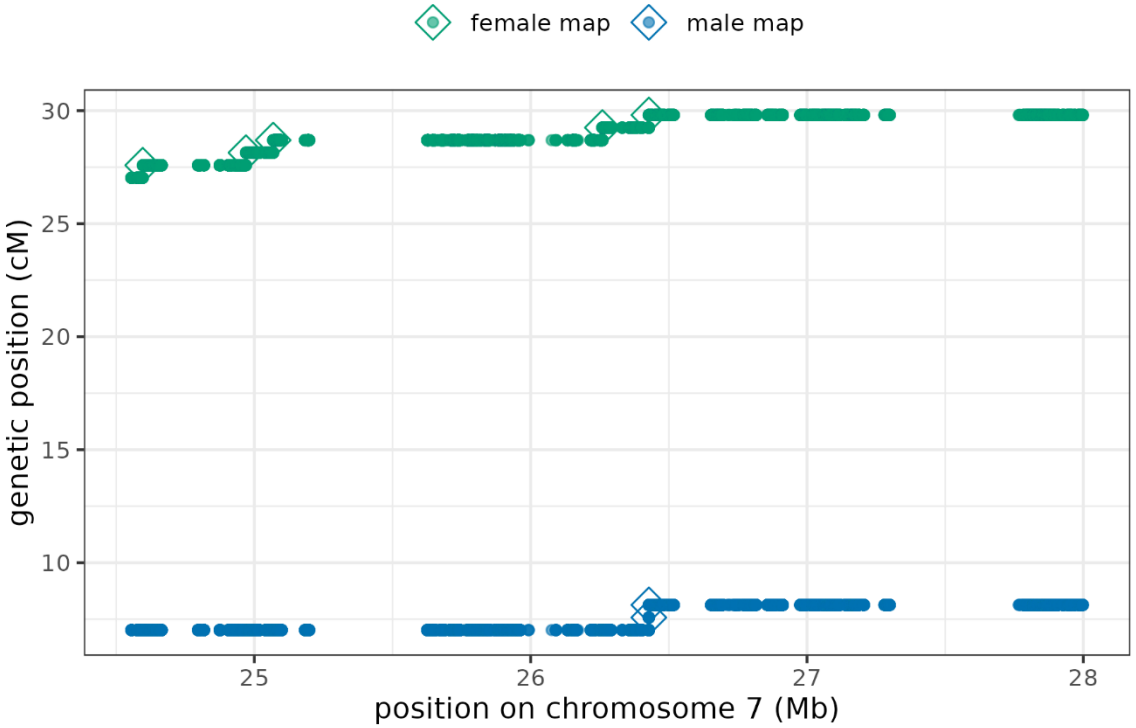

Figure 5. Marey map illustrating changes in genetic distance along the morph-determining region. Crossovers are indicated with diamonds.

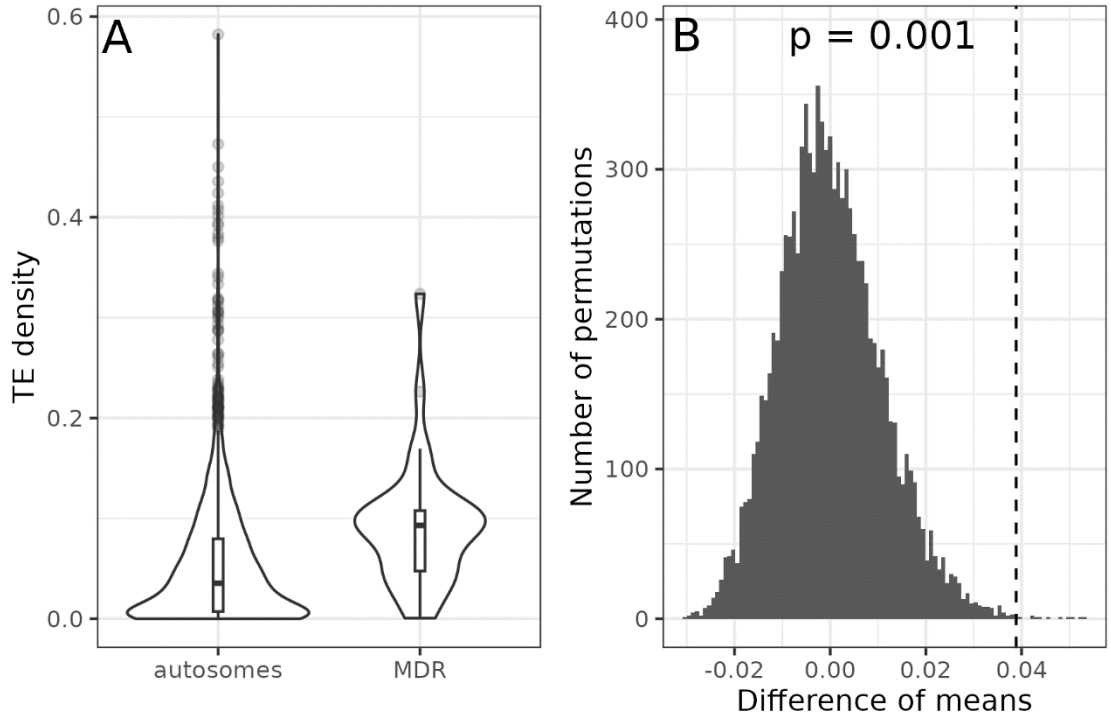

Figure 6. Comparison of transposon density in the morph-determining region and the remaining autosomal genome. A: Transposable element density is higher in the morph-determining supergene compared to the collinear part of the genome. Central lines within boxes

represent median values, with boxes indicating first and third quartiles. Whiskers extend to 1.5 times the interquartile range, and observations beyond that range are shown as points. B: Permutation test indicates that the difference in TE density is statistically significant.

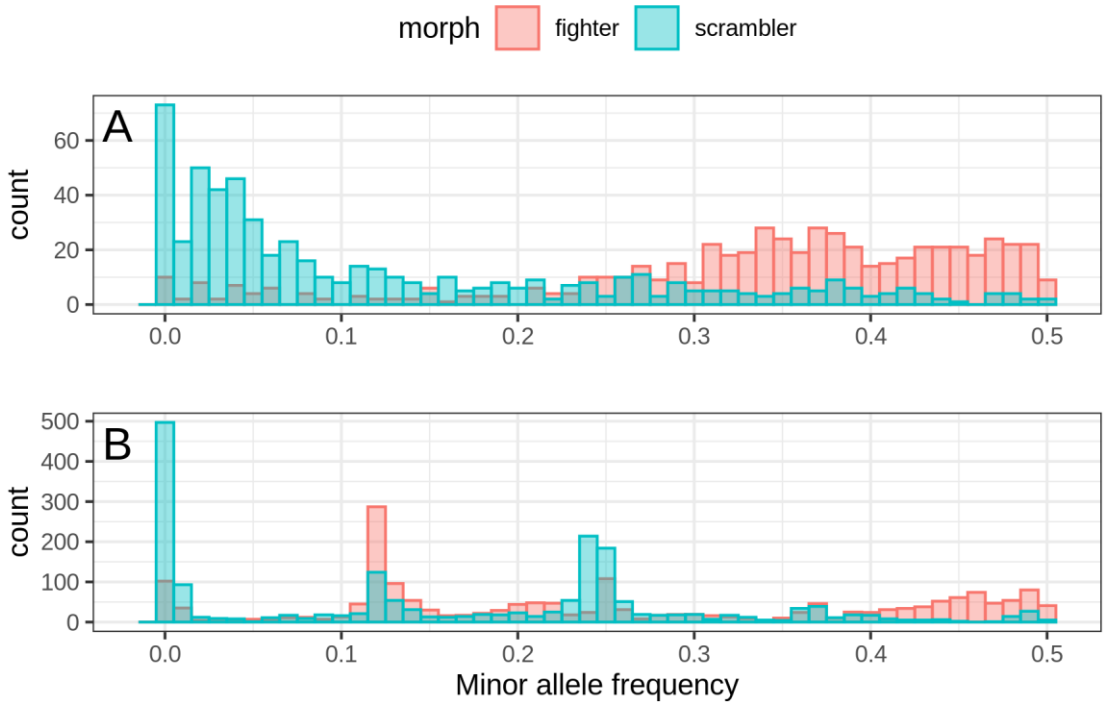

Figure 7. A histogram of minor allele frequencies of SNPs outside of the supergene region which were significantly diverged between fighter and scrambler samples in Pool-GWAS Fisher's exact test (A, 569 SNPs) or in association test performed on inbred lines after excluding all SNPs from chromosome 7 (B, 1,872 SNPs). Significant SNPs are presented on Manhattan plots on the figure 1B & 1C.

4. Discussion

In this study, we used a wide range of genomic tools to unravel the genomic architecture of male morph determination in bulb mite, *Rhizoglyphus robini*. Our findings indicate that male morph is governed by the interplay of two genetic determinants. The first is associated with polymorphisms within a single, 3.5 Mb region located on chromosome seven. The region consists of two alternative, non-recombining and highly diverged haplotypes, suggesting it can be considered a supergene. The second is a result of multiple SNPs scattered across the genome. These multiple SNPs are enriched for rare, likely deleterious variants in scramblers. Below we dissect the evidence for these two determinants in more detail and discuss their interplay.

Results of Pool-GWAS found a significant genetic differentiation between fighter and scrambler pools close to the end of chromosome seven (Figure 1A, B). This localisation was further confirmed by association study, which used inbred lines selected for fighter or scrambler morph expression (Figure 1C, D). Additional comparisons of inbred lines showed a peak in divergence

between morphs at the same genomic region (Figure 1D). We also identified over 1,800 SNPs that were significantly associated with morph expression and were scattered across the whole genome (Figure 1B, C). These SNPs were enriched in rare variants in scrambler lines (Figure 7), which indicate their deleterious character. A similar finding was reported in our previous study, where scrambler-selected lines accumulated the genetic load faster compared to fighter lines (Parrett et al., 2022). The supressing effect of mutations on SST expression is postulated by genic capture hypothesis, according to which genome-wide signal contributes to the individual's quality, affecting its ability to develop weaponry or ornaments (see introduction).

Pool-GWAS analysis indicated that alternative haplotypes of the putative morph-determining supergene have accumulated significant nucleotide divergence, with the most pronounced genetic differentiation between scrambler and fighter pools, with Fst value reaching 0.1 (Figure 1A). This indicates a moderate genetic differentiation between morph-specific haplotypes and was not as extreme as that found in other diverged non-recombining haploblocks, which usually range between 0.3 to 1 (Gutiérrez-Valencia et al., 2022; Mérot et al., 2021; Sanchez-Donoso et al., 2022; Willink et al., 2024). Our estimate might be however biased as the morph expression in bulb mite is condition dependent (Radwan, 1995; Smallegange, 2011), and it is possible that some fighters could not develop their weapon and therefore contributed to the DNA pool of scrambler males.

Signal from the association test performed using inbred lines was rather diffused along the chromosome (Figure 1C), likely resulting from a low sample size (8 fighter lines were compared against 8 scrambler lines). Additionally, the recombination rate at the whole chromosome seven is limited, being the lowest across all bulb mite chromosomes (Chmielewski et al., 2024). The selection on the male morph during inbreeding might have prevented recombination from decoupling the morph-determining supergene from its genetic background, resulting in high linkage disequilibrium along the whole chromosome (Maynard Smith & Haigh, 2008; Slatkin, 2008).

Phylogenetic analysis based on inbred line genotypes from the morph-differentiating region revealed two distinct clusters corresponding to the morphs, except for two scrambler-selected lines (IN7 and IN9) showing striking differences when compared to other scrambler inbred lines, and in contrast resembled other fighter lines (Figure 1E). These 2 inbred lines were also clustered together with other fighter lines at the phylogenetic tree (Figure 2A). These two lines could therefore represent "genetic fighters" trapped in genomes loaded with deleterious mutation, and thus prevented form expressing fighter phenotypes via condition dependence as discussed in more detail below. Except for these two lines, scrambler lines showed little divergence, in contrast to fighter lines displaying much greater genetic variability (Figure 2A). Genotype visualisation showed similar pattern, where genotypes of scrambler lines were less differentiated from each other compared to the fighter lines (Figure 1E). At the same time, maximum likelihood tree did not show morph clustering based on the whole-genome autosomal genotypes (Figure 2B).

Divergence of alternative haplotypes of a putative supergene for the male morph determination was further investigated using PCA on individually sequenced mites at the morph-determining supergene. It revealed three distinct clusters, corresponding to alternative homozygotes and heterozygotes (Figure 3), while similar analysis based on genotypes from the remaining autosomal part of the genome did not reflect clustering related to the morph (Supplementary Figure 1B). The first principal component explained exceptionally high proportion of variance in genotypes within morph-determining supergene (85%), compared to other, even old, and large supergenes (usually 10-40%), underscoring the strong genetic differentiation in this region (Harringmeyer & Hoekstra, 2022; Y. C. Huang et al., 2018; Mérot et al., 2021). The absence of fighter males in the heterozygous cluster suggests that fighter alleles are recessive, consistent with a quantitative-genetic study of (Parrett et al., 2023). In contrast, scrambler males were found in all clusters, indicating that some genetic fighters, likely due to their low condition, might fail to develop their armaments, thus developing the scrambler morph. Surprisingly, we have observed that the samples from family C, in contrast to other families, did not show distinct clustering in PCA. To establish this family, a male from IN7 inbred line was used, i.e. one of the two outliers from the inbred line analysis, which did not exhibit significant additive effect on the male morph (Parrett et al., 2023) and clustered with fighters in the present analysis (see above).

Beyond analysing nucleotide divergence between fighter and scrambler samples, we sought to evaluate the hypothesis of recombination suppression within the morph-associated region in heterozygotes. To do this, we used samples from the genetic mapping study (Chmielewski et al. 2024), where four segregating families were generated by crossing an individual from a scrambler inbred line with an individual from a fighter line. Consequently, all F1 individuals were expected to be heterozygous in a putative morph-determining region. Supergenes prevent crossovers between alternative haplotypes in heterozygotes, therefore we expected recombination suppression in these samples (Berdan et al., 2023; Faria et al., 2019; Wellenreuther & Bernatchez, 2018). While no crossovers were observed in families A, B, and D, individuals from family C, created using fighter IW15 family and scrambler IN7 family which clustered with fighter samples, exhibited seven recombination events (Figure 5, Supplementary Table 2). This evidence, combined with PCA, inbred lines, and recombination analyses, suggests that lines IN7 and IN9, as well as all samples from family C, possess a fixed fighter genotype, which likely accounts for recombination in family C despite, in contrast to suppressed recombination in other families created by crossing fighter-selected and scrambler-selected inbred lines which clustered with the expected morph at the putative supergene region.

Another hallmark of supergenes is the accumulation of deleterious load. Regions with low recombination rate are expected to acquire more genetic load due to stronger Hill-Robertson interference, and genetic hitchhiking and Muller's ratchet (B. Charlesworth & Charlesworth, 2000). In agreement with this scenario, we observed significant enrichment of transposable elements in a putative supergene, compared to the rest of the genome (Figure 6). However,

transposon enrichment may also be a direct effect of reduced selection against ectopic recombination within an inversion (Charlesworth et al. 1994; Charlesworth and Flatt 2024).

We need to acknowledge that the approach that we used may suffer from the reference bias. The reference genome was based on sequences of a single fighter-selected inbred line (namely, IW23). Due to high divergence between fighter- and scrambler-specific haplotypes, scrambler samples showed increased proportion of missing genotypes in the morph-determining region (Figure 1 E, Supplementary Figure 2). Using a divergent reference genome could affect the allele frequency estimates (Brandt et al., 2015; Chen et al., 2021), and measures which we used for identification of the morph-associated region which rely on allele frequencies (Fst, Fisher's exact test, divergence). In order to reduce the effect of the reference bias, we excluded the most diverged DNA fragments by stringently filtering out positions with high genotype missingness. On the other hand, our estimates of genetic differentiation are conservative, as we excluded positions with high genotype missingness, which are more likely to contain alternative nucleotides in scrambler haplotype. However, the reference bias does not negate other signatures of non-recombining haploblocks, such as the enrichment of transposable elements in the morph-determining supergene compared to the rest of the genome or the suppression of recombination. These lines of evidence imply that a region strongly associated with male morph expression can be considered a supergene. The supergene appears large, encompassing 3.5 Mb and over 500 genes, however exact supergene boundaries remain to be explored in the future. The genes within the supergene were enriched in function related to the hydrolysis of ester linkages within nucleic acids. This could indicate that the genes in the morph-determining supergene are associated with RNA processing and gene expression regulation, which often underlies the developmental differences between the morphs (Mank, 2017b, 2022).Lack of a scrambler-specific genome assembly prevents us from directly classifying the structural variant associated with the supergene (e.g., inversion, duplication), however we can rule out the possibility that it is hemizygous, as neither haplotype showed coverage values close to zero within this region (Figure 4). Hemizygous supergene has been reported for example in *Linum*, where it underlies floral morphology (Gutiérrez-Valencia et al., 2022).

Supergenes have been shown to underlie the determination of alternative mating tactics in several species. For example, morph of the spider *Oedothorax gibbosus* is associated with a large structural variant, most likely to be a chromosomal duplication involving a *doublesex* gene, which underlies the expression of sexually dimorphic traits across many invertebrate clades (Burtis & Baker, 1989; Hendrickx et al., 2021; Kunte et al., 2014; Rohner et al., 2021). A genomic inversion was shown to form a supergene in the ruff, *Philomachus pugnax*, which males show 3 alternative mating morphs: territorial 'independent' males, satellite males and female-mimicking feaders (Küpper et al., 2015; Lamichhaney et al., 2015). The expression of independent and faeder morph is associated with a single inversion, and satellite morph allele was created by a rare recombination event between alternative inversion arrangements. The inversion comprises 125 genes, among which the important CENP-N gene is disrupted by an inversion breakpoint, leading to homozygote lethality. Similarly, a set of tightly linked loci

clustered within a 2.4 Mb supergene has been reported to control the male morph in a shell-brooding cichlid fish *Lamprologous callipterus*. In this species, 'bourgeois' dominant males carry empty shells in which females lay eggs, and alternative dwarf males sneak behind the bourgeois males and fertilize females inside the shells. While the supergene is not well characterised, it is hypothesised that the candidate dwarfism gene *GHRHR* is a causative gene for the phenotypic differences between the morphs (Singh et al., 2023).

In addition to the putative supergene, we detected hundreds of SNPs associated with morph expression outside the putative supergene. These genes were scattered across genome, and there was no overlap between them using the two experiments (pool-GWAS and inbred lines), which analysed two different gene pools (respectively, a mix of three populations and Mosina population). This last result indicates idiosyncratic contribution of genomic position to determination of male morph expression, as would be expected if most of the SNPs consist of deleterious mutations segregating under mutation-selection balance. Indeed, inbred lines derived from scramblers were enriched for rare variants, which are likely to be enriched for deleterious mutations kept at low frequencies by selection against them. Further support from this hypothesis comes from quantitative genetic study of Parrett et al. (2023), who demonstrated that in addition to strong additive component, inbreeding decreases probability of fighter expression. This is because most deleterious mutations segregating in a population are at least partially recessive (Charlesworth & Willis, 2009), such that their negative effect on a trait is exacerbated when inbreeding increases homozygosity. Our results are also consistent with Parrett et al. (2022) who observed a similar enrichment of rare alleles in experimental evolution lines nearly fixed for scrambler lines. However, the results of Parrett et al. (2022) could be due to either/both condition-dependence of weapon expression, or/and elevated sexual selection associated with inter-male aggression. Results of this study was not confounded by the latter mechanism, as there was no opportunity for sexual selection associated with male fights during derivation of our inbred lines. Thus, our study supports the potential of condition-dependence to contribute to purifying selection via increased reproductive success of males expressing costly SSTs.

The interplay between the supergene and genome-wide variation is well exemplified by IN7 and IN9 lines, which despite being founded by scrambler males and selected for the same morph during derivation of inbred lines, clustered with fighter lines in a putative supergene region. Interestingly, both these lines were exceptional among scrambler-founded inbred lines that did not exhibit significant negative additive effects on fighter morph expression in the previous quantitative genetic study (Figure 3 in Parrett et al., 2023). Current study indicates that this is because the line in fact carried a supergene variant associated with expression of fighter morph, but the expression was suppressed by a load of deleterious mutations carried by these lines, as expected under condition-dependence.

Concluding, our analysis reveals that the morph expression is primarily driven by a 3.5 Mb region at chromosome seven bearing genomic signatures of a supergene, including a significant nucleotide divergence, lack of recombination, and an enrichment of transposable elements. The

supergene does not fully determine the male morph, expression of which also depends also on individual condition, in turn being affected by a load of deleterious mutations. Our work adds to the growing body of evidence on the role of supergenes in the evolution of alternative mating tactics across diverse taxa, while at the same time highlights the interaction between a supergene and condition-dependence.

References

The references for this chapter are located after the Conclusions section of the thesis.

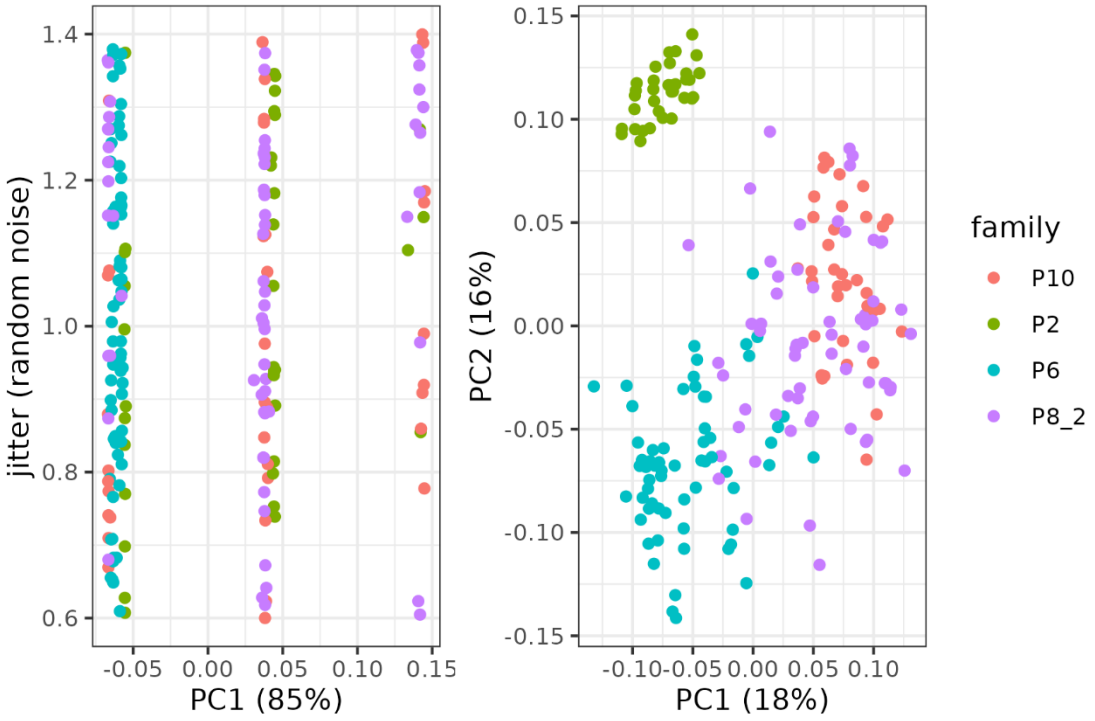

Supplementary Figure 1. PCA on genotypes from the morph-determining supergene (A) and remaining part of the genome (B).

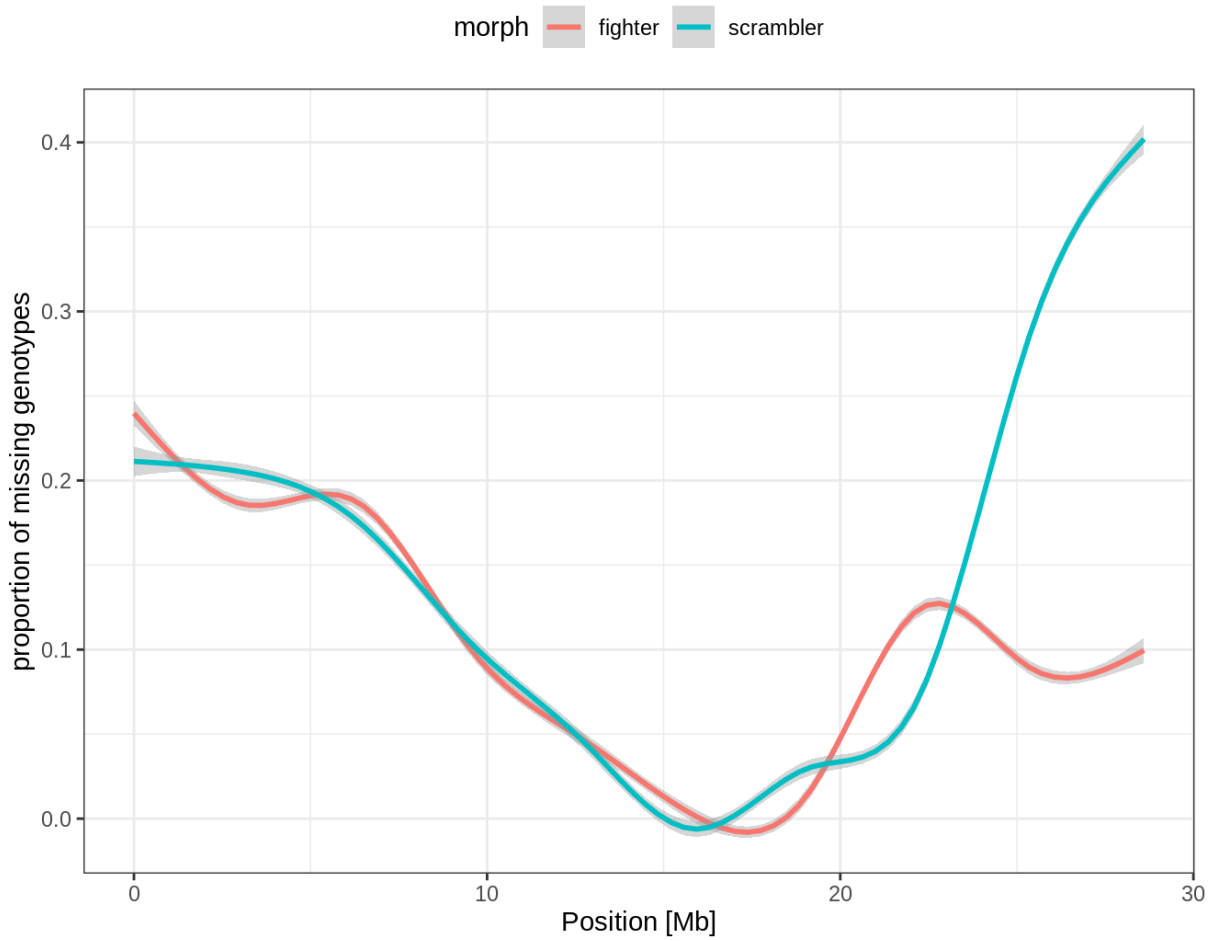

Supplementary Figure 2. Proportion of missing genotypes along chromosome 7 for fighter and scrambler inbred lines, expressed as a smoothed LOESS curve.

Supplementary Table 1. Counts of females, and males of both morphs based on clustering from principal component analysis (see Figure 3). AB is the intermediate cluster, AA and BB are left-side and right-side clusters, respectively.

family	cluster	females	fighters	scramblers	male unknown morph
A	AA	3	4	3	1
A	AB	11	0	5	0
A	BB	6	0	3	0
B	AA	8	4	0	0
B	AB	16	0	3	0
B	BB	2	0	2	0
C	AA	40	13	10	0
D	AA	11	4	1	0
D	AB	18	0	16	0
D	BB	10	0	1	1

Supplementary Table 2. Crossover positions within morph-determining supergene, with information about individuals which recombined. Map indicates the sex of F1 individual which underwent crossover.

chromosome	position	family	sex	morph	Map
2	24,595,830	P6	male	scrambler	Female
2	24,969,462	P6	male	fighter	Female
2	25,068,017	P6	female	-	Female
2	26,259,294	P6	male	scrambler	Female
2	26,427,475	P6	male	fighter	Male
2	26,427,616	P6	male	fighter	Female
2	26,427,642	P6	female	-	male

CONCLUSIONS AND FUTURE PROSPECTS

This PhD thesis explores fundamental questions in sexual selection theory, from a genomic perspective. Our results revealed that deleterious genetic load is purged from the genome through the mechanism of condition dependence acting on sexually selected traits, rather than via direct selection on individual quality through intra-sexual competition, which usually accompany strong sexual selection. We have characterised the genetic architecture of the sexually selected weapon in bulb mite, detecting the interplay between a supergene and the genome-wide accumulation of deleterious load. We have also developed valuable genomic resources for *R. robini*, including the first sex-specific genetic map of a gonochoristic organism with holocentric chromosomes, a chromosome-scale genome assembly, and a repeat annotation of the bulb mite genome. This genetic map confirmed the hypothesis that selfish meiotic drivers shape the sex-specific differences in recombination landscape.

The quality and amount of genetic variation are crucial for managing and predicting the fates of natural populations, particularly for endangered species. A better understanding of the influence of sexual selection on the genetic polymorphism may help in developing conservation plans for species expressing sexually selected traits. Additionally, mites are important pests of crops, and developing recombination map and a one of the few chromosome-scale assemblies within mites and ticks may assist in identifying genomic regions linked to resistance or sensitivity to miticides.

Future studies could expand this work by developing an alternative genome assembly of the scrambler morph. This approach could provide direct evidence on the nature of structural variation maintaining polymorphism in the morph-associated locus and allow to localise the precise boundaries of this locus. Sequencing of mites from wild populations could confirm the association between this genomic region with the male morph, offering an opportunity to investigate the natural variation segregating in this species. Additionally, future work could investigate if the phenomenon of the intralocus sexual conflict, that previous research has shown to be associated with fighter morph expression in bulb mites, is linked with alternative haplotypes of the morph-associated supergene. The proposed future studies would not only explore the proximate mechanisms underlying sexual conflict, but also contribute to our understanding of how they are resolved in natural populations.

REFERENCES

Agrawal, A. F. (2001). Sexual selection and the maintenance of sexual reproduction. *Nature*, *411*(6838), 692–695. https://doi.org/10.1038/35079590

Anderson, E. C., Skaug, H. J., & Barshis, D. J. (2014). Next-generation sequencing for molecular ecology: A caveat regarding pooled samples. *Molecular Ecology*, *23*(3), 502–512. https://doi.org/10.1111/mec.12609

Anderson, N., Jaron, K. S., Hodson, C. N., Couger, M. B., Sevcık, J., Weinstein, B., Pirro, S., Ross, L., & Roy, S. W. (2022). Gene-rich X chromosomes implicate intragenomic conflict in the evolution of bizarre genetic systems. *Proceedings of the National Academy of Sciences of the United States of America*, *119*(23), 1–7. https://doi.org/10.1073/pnas.2122580119

Andersson, M. (1986). Evolution of Condition-Dependent Sex Ornaments and Mating Preferences: Sexual Selection Based on Viability Differences. *Evolution*, *40*(4), 804. https://doi.org/10.2307/2408465

Andersson, M. (1994). *Sexual Selection*. Princeton University Press. https://doi.org/10.1515/9780691207278

Arndt, P. F., Hwa, T., & Petrov, D. A. (2005). Substantial regional variation in substitution rates in the human genome: Importance of GC content, gene density, and telomere-specific effects. *Journal of Molecular Evolution*, *60*(6), 748–763. https://doi.org/10.1007/s00239-004-0222-5

Arnqvist, G., & Rowe, L. (2005). *Sexual Conflict*. Princeton University Press. https://doi.org/10.1515/9781400850600

Aronsen, T., Berglund, A., Mobley, K. B., Ratikainen, I. I., & Rosenqvist, G. (2013). Sex Ratio And Density Affect Sexual Selection In A Sex-Role Reversed Fish. *Evolution*, *67*(11), 3243–3257. https://doi.org/10.1111/evo.12201

Barghi, N., Hermisson, J., & Schlötterer, C. (2020). Polygenic adaptation: a unifying framework to understand positive selection. *Nature Reviews Genetics*, *21*(12), 769–781. https://doi.org/10.1038/s41576-020-0250-z

Bateman, A. J. (1948). Intra-sexual selection in Drosophila. *Heredity*, *2*(3), 349–368. https://doi.org/10.1038/hdy.1948.21

Bath, E., Rostant, W., Ostridge, H. J., Smith, S., Mason, J. S., Rafaluk-Mohr, T., Mank, J. E., Chapman, T., & Perry, J. C. (2023). Sexual selection and the evolution of condition-dependence: an experimental test at two resource levels. *Evolution; International Journal of Organic Evolution*, *77*(3), 776–788. https://doi.org/10.1093/evolut/qpac066

Berdan, E. L., Barton, N. H., Butlin, R., Charlesworth, B., Faria, R., Fragata, I., Gilbert, K. J., Jay, P., Kapun, M., Lotterhos, K. E., Mérot, C., Durmaz Mitchell, E., Pascual, M., Peichel, C. L., Rafajlović, M., Westram, A. M., Schaeffer, S. W., Johannesson, K., & Flatt, T. (2023). How chromosomal inversions reorient the evolutionary process. *Journal of Evolutionary Biology*, *36*(12), 1761–1782. https://doi.org/10.1111/jeb.14242

Berdan, E. L., Blanckaert, A., Butlin, R. K., & Bank, C. (2021). Deleterious mutation accumulation and the long-term fate of chromosomal inversions. *PLOS Genetics*, *17*(3), e1009411. https://doi.org/10.1371/journal.pgen.1009411

Bergero, R., Gardner, J., Bader, B., Yong, L., & Charlesworth, D. (2019). Exaggerated heterochiasmy in a fish with sex-linked male coloration polymorphisms. *Proceedings of the National Academy of Sciences of the United States of America*, *116*(14), 6924–6931. https://doi.org/10.1073/pnas.1818486116

Bernstein, M. R., & Rockman, M. V. (2016). Fine-Scale Crossover Rate Variation on the *Caenorhabditis elegans* X Chromosome. *G3 Genes/Genomes/Genetics*, *6*(6), 1767–1776. https://doi.org/10.1534/g3.116.028001

Bolger, A. M., Lohse, M., & Usadel, B. (2014). Trimmomatic: A flexible trimmer for Illumina sequence data. *Bioinformatics*, *30*(15), 2114–2120. https://doi.org/10.1093/bioinformatics/btu170

Bolívar, P., Guéguen, L., Duret, L., Ellegren, H., & Mugal, C. F. (2019). GC-biased gene conversion conceals the prediction of the nearly neutral theory in avian genomes 06 Biological Sciences 0604 Genetics. *Genome Biology*, *20*(1), 1–13. https://doi.org/10.1186/s13059-018-1613-z

Boman, J., Mugal, C. F., & Backström, N. (2021). The Effects of GC-Biased Gene Conversion on Patterns of Genetic Diversity among and across Butterfly Genomes. *Genome Biology and Evolution*, *13*(5), 1–19. https://doi.org/10.1093/gbe/evab064

Bonduriansky, R. (2007). The evolution of condition-dependent sexual dimorphism. *American Naturalist*, *169*(1), 9–19. https://doi.org/10.1086/510214

Bonduriansky, R., & Chenoweth, S. F. (2009). Intralocus sexual conflict. *Trends in Ecology & Evolution*, *24*(5), 280–288. https://doi.org/10.1016/j.tree.2008.12.005

Bonduriansky, R., & Rowe, L. (2005). Sexual selection, genetic architecture, and the condition dependence of body shape in the sexually dimorphic fly *Prochyliza xanthostoma* (Piophilidae). *Evolution*, *59*(1), 138–151. https://doi.org/10.1111/j.0014-3820.2005.tb00901.x

Brandt, D. Y. C., Aguiar, V. R. C., Bitarello, B. D., Nunes, K., Goudet, J., & Meyer, D. (2015). Mapping bias overestimates reference allele frequencies at the HLA genes in the 1000 genomes project phase I data. *G3: Genes, Genomes, Genetics*, *5*(5), 931–941. https://doi.org/10.1534/g3.114.015784

Brandvain, Y., & Coop, G. (2012). Scrambling eggs: Meiotic drive and the evolution of female recombination rates. *Genetics*, *190*(2), 709–723. https://doi.org/10.1534/genetics.111.136721

Brazier, T., & Glémin, S. (2022). Diversity and determinants of recombination landscapes in flowering plants. *PLoS Genetics*, *18*(8), 1–29. https://doi.org/10.1371/journal.pgen.1010141

Brekke, C., Johnston, S. E., Knutsen, T. M., & Berg, P. (2023). Genetic architecture of individual meiotic crossover rate and distribution in Atlantic Salmon. *Scientific Reports*, *13*(1), 20481. https://doi.org/10.1038/s41598-023-47208-3

Brelsford, A., Rodrigues, N., & Perrin, N. (2016). High-density linkage maps fail to detect any genetic component to sex determination in a *Rana temporaria* family. *Journal of Evolutionary Biology*, *29*(1), 220–225. https://doi.org/10.1111/jeb.12747

Brockmann, H. J., & Taborsky, M. (2008). Alternative reproductive tactics and the evolution of alternative allocation phenotypes. In *Alternative Reproductive Tactics* (pp. 25–51). Cambridge University Press. https://doi.org/10.1017/CBO9780511542602.003

Burt, A., Bell, G., & Harvey, P. H. (1991). Sex differences in recombination. *Journal of Evolutionary Biology*, *4*(2), 259–277. https://doi.org/10.1046/j.1420-9101.1991.4020259.x

Burtis, K. C., & Baker, B. S. (1989). *Drosophila doublesex* gene controls somatic sexual differentiation by producing alternatively spliced mRNAs encoding related sex-specific polypeptides. *Cell*, *56*(6), 997–1010. https://doi.org/10.1016/0092-8674(89)90633-8

Cahoon, C. K., & Libuda, D. E. (2019). Leagues of their own: sexually dimorphic features of meiotic prophase I. *Chromosoma*, *128*(3), 199–214. https://doi.org/10.1007/s00412-019-00692-x

Cahoon, C. K., Richter, C. M., Dayton, A. E., & Libuda, D. E. (2023). Sexual dimorphic regulation of recombination by the synaptonemal complex in *C. elegans*. *ELife*, *12*. https://doi.org/10.7554/eLife.84538

Calsbeek, R., & Sinervo, B. (2004). Within-clutch variation in offspring sex determined by differences in sire body size: Cryptic mate choice in the wild. *Journal of Evolutionary Biology*, *17*(2), 464–470. https://doi.org/10.1046/j.1420-9101.2003.00665.x

Camperio-Ciani, A., Corna, F., & Capiluppi, C. (2004). Evidence for maternally inherited factors favouring male homosexuality and promoting female fecundity. *Proceedings of the Royal Society B: Biological Sciences*, *271*(1554), 2217–2221. https://doi.org/10.1098/rspb.2004.2872

Candolin, U., & Heuschele, J. (2008). Is sexual selection beneficial during adaptation to environmental change? *Trends in Ecology and Evolution*, *23*(8), 446–452. https://doi.org/10.1016/j.tree.2008.04.008

Charlesworth, B. (1987). The heritability of fitness. *Sexual Selection: Testing the Alternatives*, 21–40.

Charlesworth, B., & Charlesworth, D. (2000). The degeneration of Y chromosomes. *Philosophical Transactions of the Royal Society of London. Series B: Biological Sciences*, *355*(1403), 1563–1572. https://doi.org/10.1098/rstb.2000.0717

Charlesworth, D. (2017). Evolution of recombination rates between sex chromosomes. *Philosophical Transactions of the Royal Society B: Biological Sciences*, *372*(1736). https://doi.org/10.1098/rstb.2016.0456

Charlesworth, D., Bergero, R., Graham, C., Gardner, J., & Yong, L. (2020). Locating the sex determining region of linkage group 12 of guppy (Poecilia reticulata). *G3: Genes, Genomes, Genetics*, *10*(10), 3639–3649. https://doi.org/10.1534/g3.120.401573

Charlesworth, D., & Willis, J. H. (2009). The genetics of inbreeding depression. *Nature Reviews Genetics*, *10*(11), 783–796. https://doi.org/10.1038/nrg2664

Chen, N. C., Solomon, B., Mun, T., Iyer, S., & Langmead, B. (2021). Reference flow: reducing reference bias using multiple population genomes. *Genome Biology*, *22*(1), 1–17. https://doi.org/10.1186/s13059-020-02229-3

Chippindale, A. K., Gibson, J. R., & Rice, W. R. (2001). Negative genetic correlation for adult fitness between sexes reveals ontogenetic conflict in *Drosophila*. *Proceedings of the National Academy of Sciences of the United States of America*, *98*(4), 1671–1675. https://doi.org/10.1073/pnas.98.4.1671

Chmielewski, S., Konczal, M., Parrett, J. M., Rombauts, S., Radwan, J., & Babik, W. (2024). Sex-specific recombination landscape in a species with holocentric chromosomes. *BioRxiv*, 1–25. https://doi.org/10.1101/2024.04.15.589577

Cicconardi, F., Lewis, J. J., Martin, S. H., Reed, R. D., Danko, C. G., & Montgomery, S. H. (2021). Chromosome Fusion Affects Genetic Diversity and Evolutionary Turnover of Functional Loci but Consistently Depends on Chromosome Size. *Molecular Biology and Evolution*, *38*(10), 4449–4462. https://doi.org/10.1093/molbev/msab185

Clark, F. E., & Akera, T. (2021). Unravelling the mystery of female meiotic drive: where we are. *Open Biology*, *11*(9). https://doi.org/10.1098/rsob.210074

Connallon, T., & Clark, A. G. (2010). Sex linkage, sex-specific selection, and the role of recombination in the evolution of sexually dimorphic gene expression. *Evolution*, *64*(12), 3417–3442. https://doi.org/10.1111/j.1558-5646.2010.01136.x

Connallon, T., & Clark, A. G. (2012). A General Population Genetic Framework for Antagonistic Selection That Accounts for Demography and Recurrent Mutation. *Genetics*, *190*(4), 1477–1489. https://doi.org/10.1534/genetics.111.137117

Connallon, T., & Clark, A. G. (2014). Balancing Selection in Species with Separate Sexes: Insights from Fisher's Geometric Model. *Genetics*, *197*(3), 991–1006. https://doi.org/10.1534/genetics.114.165605

Cooney, C. R., Mank, J. E., & Wright, A. E. (2021). Constraint and divergence in the evolution of male and female recombination rates in fishes. *Evolution*, *75*(11), 2857–2866. https://doi.org/10.1111/evo.14357

Coop, G., & Przeworski, M. (2007). An evolutionary view of human recombination. *Nature Reviews Genetics*, *8*(1), 23–34. https://doi.org/10.1038/nrg1947

Cotton, S., Fowler, K., & Pomiankowski, A. (2004). Do sexual ornaments demonstrate heightened condition-dependent expression as predicted by the handicap hypothesis? *Proceedings of the Royal Society B: Biological Sciences*, *271*(1541), 771–783. https://doi.org/10.1098/rspb.2004.2688

Cox, R. M., & Calsbeek, R. (2009). Sexually antagonistic selection, sexual dimorphism, and the resolution of intralocus sexual conflict. *American Naturalist*, *173*(2), 176–187. https://doi.org/10.1086/595841

Danecek, P., Auton, A., Abecasis, G., Albers, C. A., Banks, E., DePristo, M. A., Handsaker, R. E., Lunter, G., Marth, G. T., Sherry, S. T., McVean, G., & Durbin, R. (2011). The variant call format and VCFtools. *Bioinformatics*, *27*(15), 2156–2158. https://doi.org/10.1093/bioinformatics/btr330

Darwin, C. (1872). *The Descent of Man, and Selection in Relation to Sex* (Issue t. 1). D. Appleton.

Davies, N., Janicke, T., & Morrow, E. H. (2023). Evidence for stronger sexual selection in males than in females using an adapted method of Bateman's classic study of *Drosophila melanogaster*. *Evolution*, *77*(11), 2420–2430. https://doi.org/10.1093/evolut/qpad151

de Bigliardo, G. R., Virla, E. G., Caro, S., & Dasso, S. M. (2011). Karyotype and male pre-reductional meiosis of the sharpshooter Tapajosa rubromarginata (Hemiptera: Cicadellidae). *Revista de Biologia Tropical*, *59*(1), 309–314. https://doi.org/10.15517/rbt.v59i1.3200

Delcourt, M., & Rundle, H. D. (2011). Condition dependence of a multicomponent sexual display trait in *Drosophila serrata*. *American Naturalist*, *177*(6), 812–823. https://doi.org/10.1086/659949

Delph, L. F., Gehring, J. L., Frey, F. M., Arntz, A. M., & Levri, M. (2004). Genetic constraints on floral evolution in a sexually dimorphic plant revealed by artificial selection. *Evolution*, *58*(9), 1936–1946. https://doi.org/10.1111/j.0014-3820.2004.tb00481.x

DePristo, M. A., Banks, E., Poplin, R., Garimella, K. V, Maguire, J. R., Hartl, C., Philippakis, A. A., del Angel, G., Rivas, M. A., Hanna, M., McKenna, A., Fennell, T. J., Kernytsky, A. M., Sivachenko, A. Y., Cibulskis, K., Gabriel, S. B., Altshuler, D., & Daly, M. J. (2011). A framework for variation discovery and genotyping using next-

generation DNA sequencing data. *Nature Genetics*, *43*(5), 491–498. https://doi.org/10.1038/ng.806

Díaz, A., Okabe, K., Eckenrode, C. (2002). Biology, ecology, and management of the bulb mites of the genus *Rhizoglyphus* (Acari: Acaridae). *Entomologia Experimentalis et Applicata*, *103*(3), 239–248. https://doi.org/https://doi.org/10.1023/A:1006304300657

Dugand, R. J., Tomkins, J. L., & Kennington, W. J. (2019). Molecular evidence supports a genic capture resolution of the lek paradox. *Nature Communications*, *10*(1), 1–8. https://doi.org/10.1038/s41467-019-09371-y

Duret, L., & Galtier, N. (2009). Biased gene conversion and the evolution of mammalian genomic landscapes. *Annual Review of Genomics and Human Genetics*, *10*, 285–311. https://doi.org/10.1146/annurev-genom-082908-150001

Duret, L., Marais, G., & Biemont, C. (2000). Transposons but not retrotransposons are located preferentially in regions of high recombination rate in *Caenorhabditis elegans*. *Genetics*, *156*(4), 1661–1669. https://doi.org/10.1093/genetics/156.4.1661

Ellegren, H., & Galtier, N. (2016). Determinants of genetic diversity. *Nature Reviews Genetics*, *17*(7), 422–433. https://doi.org/10.1038/nrg.2016.58

Emlen, D. J. (2001). Costs and the diversification of exaggerated animal structures. *Science*, *291*(5508), 1534–1536. https://doi.org/10.1126/science.1056607

Emlen, D. J., Warren, I. A., Johns, A., Dworkin, I., & Lavine, L. C. (2012). A Mechanism of Extreme Growth and Reliable Signaling in Sexually Selected Ornaments and Weapons. *Science*, *337*(6096), 860–864. https://doi.org/10.1126/science.1224286

Ewels, P., Magnusson, M., Lundin, S., & Käller, M. (2016). MultiQC: Summarize analysis results for multiple tools and samples in a single report. *Bioinformatics*, *32*(19), 3047–3048. https://doi.org/10.1093/bioinformatics/btw354

Falconer, D. S. (1996). *Introduction to Quantitative Genetics*. Pearson Education.

Falque, M., Mercier, R., Mézard, C., De Vienne, D., & Martin, O. C. (2007). Patterns of recombination and MLH1 foci density along mouse chromosomes: Modeling effects of interference and obligate chiasma. *Genetics*, *176*(3), 1453–1467. https://doi.org/10.1534/genetics.106.070235

Faria, R., Johannesson, K., Butlin, R. K., & Westram, A. M. (2019). Evolving Inversions. *Trends in Ecology and Evolution*, *34*(3), 239–248. https://doi.org/10.1016/j.tree.2018.12.005

Fedorka, K. M., & Mousseau, T. A. (2004). Female mating bias results in conflicting sex-specific offspring fitness. *Nature*, *429*(6987), 65–67. https://doi.org/10.1038/nature02492

Felsenstein, J. (1988). Sex and the evolution of recombination. In Richard E. Michod; Bruce R. Levin (Ed.), *The Evolution of sex : an examination of current ideas* (pp. 74–86). Sinauer Associates Inc.

Fierst, J. L. (2015). Using linkage maps to correct and scaffold de novo genome assemblies: methods, challenges, and computational tools. *Frontiers in Genetics*, *6*, 1–8. https://doi.org/10.3389/fgene.2015.00220

Fisher, R. A. (1930). *The genetical theory of natural selection*. Clarendon Press. https://doi.org/10.5962/bhl.title.27468

Fisher, R. A., & Bennett, J. H. (1999). *The Genetical Theory of Natural Selection: A Complete Variorum Edition*. OUP Oxford.

Fisk, G. J., & Thummel, C. S. (1995). Isolation, regulation, and DNA-binding properties of three *Drosophila* nuclear hormone receptor superfamily members. *Proceedings of the National Academy of Sciences of the United States of America*, *92*(23), 10604–10608. https://doi.org/10.1073/pnas.92.23.10604

Flynn, J. M., Hubley, R., Goubert, C., Rosen, J., Clark, A. G., Feschotte, C., & Smit, A. F. (2020). RepeatModeler2 for automated genomic discovery of transposable element families. *Proceedings of the National Academy of Sciences of the United States of America*, *117*(17), 9451–9457. https://doi.org/10.1073/pnas.1921046117

Foerster, K., Coulson, T., Sheldon, B. C., Pemberton, J. M., Clutton-Brock, T. H., & Kruuk, L. E. B. (2007). Sexually antagonistic genetic variation for fitness in red deer. *Nature*, *447*(7148), 1107–1110. https://doi.org/10.1038/nature05912

Franssen, S. U., Nolte, V., Tobler, R., & Schlotterer, C. (2015). Patterns of linkage disequilibrium and long range hitchhiking in evolving experimental *Drosophila melanogaster* populations. *Molecular Biology and Evolution*, *32*(2), 495–509. https://doi.org/10.1093/molbev/msu320

Futschik, A., & Schlötterer, C. (2010). The next generation of molecular markers from massively parallel sequencing of pooled DNA samples. *Genetics*, *186*(1), 207–218. https://doi.org/10.1534/genetics.110.114397

García-Alcalde, F., Okonechnikov, K., Carbonell, J., Cruz, L. M., Götz, S., Tarazona, S., Dopazo, J., Meyer, T. F., & Conesa, A. (2012). Qualimap: Evaluating next-generation sequencing alignment data. *Bioinformatics*, *28*(20), 2678–2679. https://doi.org/10.1093/bioinformatics/bts503

Gerson, U., Cohen, E., & Capua, S. (1991). Bulb mite*, Rhizoglyphus robini* (Astigmata: Acaridae) as an experimental animal. *Experimental & Applied Acarology*, *12*(1–2), 103–110. https://doi.org/10.1007/BF01204403

Gowaty, P. A., Kim, Y. K., & Anderson, W. W. (2012). No evidence of sexual selection in a repetition of Bateman's classic study of *Drosophila melanogaster*. *Proceedings of*

the National Academy of Sciences of the United States of America, *109*(29), 11740–11745. https://doi.org/10.1073/pnas.1207851109

Gregory, T. R., & Young, M. R. (2020). Small genomes in most mites (but not ticks). *International Journal of Acarology*, *46*(1), 1–8. https://doi.org/10.1080/01647954.2019.1684561

Gross, M. R. (1996). Alternative reproductive strategies and tactics: diversity within sexes. *Trends in Ecology & Evolution*, *11*(2), 92–98. https://doi.org/10.1016/0169-5347(96)81050-0

Gutiérrez-Valencia, J., Fracassetti, M., Berdan, E. L., Bunikis, I., Soler, L., Dainat, J., Kutschera, V. E., Losvik, A., Désamoré, A., Hughes, P. W., Foroozani, A., Laenen, B., Pesquet, E., Abdelaziz, M., Pettersson, O. V., Nystedt, B., Brennan, A. C., Arroyo, J., & Slotte, T. (2022). Genomic analyses of the Linum distyly supergene reveal convergent evolution at the molecular level. *Current Biology*, *32*(20), 4360-4371.e6. https://doi.org/10.1016/j.cub.2022.08.042

Haenel, Q., Laurentino, T. G., Roesti, M., & Berner, D. (2018). Meta-analysis of chromosome-scale crossover rate variation in eukaryotes and its significance to evolutionary genomics. *Molecular Ecology*, *27*(11), 2477–2497. https://doi.org/10.1111/mec.14699

Hahn, M. W. (2018). *Molecular Population Genetics*. Sinauer Associates.

Haig, D. (2010). Games in tetrads: Segregation, recombination, and meiotic drive. *American Naturalist*, *176*(4), 404–413. https://doi.org/10.1086/656265

Harringmeyer, O. S., & Hoekstra, H. E. (2022). Chromosomal inversion polymorphisms shape the genomic landscape of deer mice. *Nature Ecology and Evolution*, *6*(12), 1965–1979. https://doi.org/10.1038/s41559-022-01890-0

Hassold, T., & Hunt, P. (2001). To err (meiotically) is human: The genesis of human aneuploidy. *Nature Reviews Genetics*, *2*(4), 280–291. https://doi.org/10.1038/35066065

Hassold, T., Maylor-Hagen, H., Wood, A., Gruhn, J., Hoffmann, E., Broman, K. W., & Hunt, P. (2021). Failure to recombine is a common feature of human oogenesis. *American Journal of Human Genetics*, *108*(1), 16–24. https://doi.org/10.1016/j.ajhg.2020.11.010

Heckmann, S., Jankowska, M., Schubert, V., Kumke, K., Ma, W., & Houben, A. (2014). Alternative meiotic chromatid segregation in the holocentric plant *Luzula elegans*. *Nature Communications*, *5*, 1–10. https://doi.org/10.1038/ncomms5979

Hendrickx, F., De Corte, Z., Sonet, G., Van Belleghem, S. M., Köstlbacher, S., Vangestel, C., Corte, Z. De, Sonet, G., Belleghem, S. M. Van, Köstlbacher, S., & Vangestel, C. (2021). A masculinizing supergene underlies an exaggerated male

reproductive morph in a spider. *Nature Ecology & Evolution*, 2021.02.09.430505. https://doi.org/10.1038/s41559-021-01626-6

Huang, S., Kang, M., & Xu, A. (2017). HaploMerger2: Rebuilding both haploid sub-assemblies from high-heterozygosity diploid genome assembly. *Bioinformatics*, *33*(16), 2577–2579. https://doi.org/10.1093/bioinformatics/btx220

Huang, Y. C., Dang, V. D., Chang, N. C., & Wang, J. (2018). Multiple large inversions and breakpoint rewiring of gene expression in the evolution of the fire ant social supergene. *Proceedings of the Royal Society B: Biological Sciences*, *285*(1878). https://doi.org/10.1098/rspb.2018.0221

Hughes, S. E., & Hawley, R. S. (2020). Meiosis: Location, Location, Location, How Crossovers Ensure Segregation. *Current Biology*, *30*(7), R311–R313. https://doi.org/10.1016/j.cub.2020.02.020

Hunt, P. A., & Hassold, T. J. (2002). Sex matters in meiosis. *Science*, *296*(5576), 2181–2183. https://doi.org/10.1126/science.1071907

Iglesias-Carrasco, M., Taboada, B., Lozano, M., Carazo, P., Garcia-Roa, R., Rodriguez-Exposito, E., & Garcia-Gonzalez, F. (2024). Sexual selection buffers the negative consequences of population fragmentation on adaptive plastic responses to increasing temperatures. *Evolution*, *78*(1), 86–97. https://doi.org/10.1093/evolut/qpad193

Iwasa, Y., Pomiankowski, A., & Nee, S. (1991). The Evolution of Costly Mate Preferences II. The "Handicap" Principle. *Evolution*, *45*(6), 1431. https://doi.org/10.2307/2409890

Jain, K., & Stephan, W. (2017). Modes of Rapid Polygenic Adaptation. *Molecular Biology and Evolution*, *34*(12), 3169–3175. https://doi.org/10.1093/molbev/msx240

Jarzebowska, M., & Radwan, J. (2009). Sexual selection counteracts extinction of small populations of the bulb mites. *Evolution*. https://doi.org/10.1111/j.1558-5646.2009.00905.x

Jeffries, D. L., Lavanchy, G., Sermier, R., Sredl, M. J., Miura, I., Borzée, A., Barrow, L. N., Canestrelli, D., Crochet, P. A., Dufresnes, C., Fu, J., Ma, W. J., Garcia, C. M., Ghali, K., Nicieza, A. G., O'Donnell, R. P., Rodrigues, N., Romano, A., Martínez-Solano, Í., ... Perrin, N. (2018). A rapid rate of sex-chromosome turnover and non-random transitions in true frogs. *Nature Communications*, *9*(1). https://doi.org/10.1038/s41467-018-06517-2

Ji, M., Vandenhole, M., De Beer, B., De Rouck, S., Villacis-Perez, E., Feyereisen, R., Clark, R. M., & Van Leeuwen, T. (2023). A nuclear receptor HR96-related gene underlies large trans-driven differences in detoxification gene expression in a generalist herbivore. *Nature Communications*, *14*(1). https://doi.org/10.1038/s41467-023-40778-w

Joag, R., Stuglik, M., Konczal, M., Plesnar-Bielak, A., Skrzynecka, A., Babik, W., & Radwan, J. (2016). Transcriptomics of intralocus sexual conflict: Gene expression patterns in females change in response to selection onamale secondary sexual trait in the bulb mite. *Genome Biology and Evolution*, *8*(8), 2351–2357. https://doi.org/10.1093/gbe/evw169

John, B. (1990). *Meiosis*. Cambridge University Press.

Johnston, S. E., Gratten, J., Berenos, C., Pilkington, J. G., Clutton-Brock, T. H., Pemberton, J. M., & Slate, J. (2013). Life history trade-offs at a single locus maintain sexually selected genetic variation. *Nature*, *502*(7469), 93–95. https://doi.org/10.1038/nature12489

Jurka, J., Kapitonov, V. V., Pavlicek, A., Klonowski, P., Kohany, O., & Walichiewicz, J. (2005). Repbase Update, a database of eukaryotic repetitive elements. *Cytogenetic and Genome Research*, *110*(1–4), 462–467. https://doi.org/10.1159/000084979

Kai, W., Kikuchi, K., Tohari, S., Chew, A. K., Tay, A., Fujiwara, A., Hosoya, S., Suetake, H., Naruse, K., Brenner, S., Suzuki, Y., & Venkatesh, B. (2011). Integration of the genetic map and genome assembly of fugu facilitates insights into distinct features of genome evolution in teleosts and mammals. *Genome Biology and Evolution*, *3*(1), 424–442. https://doi.org/10.1093/gbe/evr041

Kasimatis, K. R., Sánchez-Ramírez, S., & Stevenson, Z. C. (2021). Sexual Dimorphism through the Lens of Genome Manipulation, Forward Genetics, and Spatiotemporal Sequencing. *Genome Biology and Evolution*, *13*(2), 1–13. https://doi.org/10.1093/gbe/evaa243

Kaur, T., & Rockman, M. V. (2014). Crossover heterogeneity in the absence of hotspots in *Caenorhabditis elegans*. *Genetics*, *196*(1), 137–148. https://doi.org/10.1534/genetics.113.158857

Kawakami, T., Smeds, L., Backström, N., Husby, A., Qvarnström, A., Mugal, C. F., Olason, P., & Ellegren, H. (2014). A high-density linkage map enables a second-generation collared flycatcher genome assembly and reveals the patterns of avian recombination rate variation and chromosomal evolution. *Molecular Ecology*, *23*(16), 4035–4058. https://doi.org/10.1111/mec.12810

Kawecki, T. J., Lenski, R. E., Ebert, D., Hollis, B., Olivieri, I., & Whitlock, M. C. (2012). Experimental evolution. *Trends in Ecology and Evolution*, *27*(10), 547–560. https://doi.org/10.1016/j.tree.2012.06.001

Kejnovsky, E., Kubat, Z., Macas, J., Hobza, R., Mracek, J., & Vyskot, B. (2006). Retand: a novel family of gypsy-like retrotransposons harboring an amplified tandem repeat. *Molecular Genetics and Genomics*, *276*(3), 254–263. https://doi.org/10.1007/s00438-006-0140-x

Kent, T. V., Uzunović, J., & Wright, S. I. (2017). Coevolution between transposable elements and recombination. *Philosophical Transactions of the Royal Society B: Biological Sciences*, *372*(1736). https://doi.org/10.1098/rstb.2016.0458

Kim, I., Choi, B., Park, W., Kim, Y., Kim, B., Mun, S., Choi, H., & Kim, D. (2022). Nuclear receptor HR96 up-regulates cytochrome P450 for insecticide detoxification in *Tribolium castaneum*. *Pest Management Science*, *78*(1), 230–239. https://doi.org/10.1002/ps.6626

Kirkpatrick, M., & Ryan, M. J. (1991). The evolution of mating preferences and the paradox of the lek. *Nature*, *350*(6313), 33–38. https://doi.org/10.1038/350033a0

Knell, R. J., & Simmons, L. W. (2010). Mating tactics determine patterns of condition dependence in a dimorphic horned beetle. *Proceedings of the Royal Society B: Biological Sciences*, *277*(1692), 2347–2353. https://doi.org/10.1098/rspb.2010.0257

Koehler, K. E., Hawley, R. S., Sherman, S., & Hassold, T. (1996). Recombination and nondisjunction in humans and flies. *Human Molecular Genetics*, *5*(REVIEW), 1495–1504. https://doi.org/10.1093/hmg/5.supplement_1.1495

Kofler, R., Orozco-terWengel, P., de Maio, N., Pandey, R. V., Nolte, V., Futschik, A., Kosiol, C., & Schlötterer, C. (2011). Popoolation: A toolbox for population genetic analysis of next generation sequencing data from pooled individuals. *PLoS ONE*, *6*(1). https://doi.org/10.1371/journal.pone.0015925

Kofler, R., Pandey, R. V., & Schlötterer, C. (2011). PoPoolation2: Identifying differentiation between populations using sequencing of pooled DNA samples (Pool-Seq). *Bioinformatics*, *27*(24), 3435–3436. https://doi.org/10.1093/bioinformatics/btr589

Kofler, R., & Schlötterer, C. (2014). A guide for the design of evolve and resequencing studies. *Molecular Biology and Evolution*, *31*(2), 474–483. https://doi.org/10.1093/molbev/mst221

Kokko, H., & Brooks, R. (2003). Sexy to die for? Sexual selection and the risk of extinction. *Annales Zoologici Fennici*, *40*(2), 207–219.

Kołodziejczyk, M., & Radwan, J. (2003). The effect of mating frequency on female lifetime fecundity in the bulb mite*, Rhizoglyphus robini* (Acari: Acaridae). *Behavioral Ecology and Sociobiology*, *53*(2), 110–115. https://doi.org/10.1007/s00265-002-0557-0

Konior, M., Radwan, J., Kołodziejczyk, M., & Keller, L. (2006). Strong association between a single gene and fertilization efficiency of males and fecundity of their mates in the bulb mite. *Proceedings of the Royal Society B: Biological Sciences*, *273*(1584), 309–314. https://doi.org/10.1098/rspb.2005.3302

Korneliussen, T. S., Albrechtsen, A., & Nielsen, R. (2014). Angsd. *BMC Bioinformatics*, *15*(1), 1–13.

Korunes, K. L., & Samuk, K. (2021). pixy: Unbiased estimation of nucleotide diversity and divergence in the presence of missing data. *Molecular Ecology Resources*, *21*(4), 1359–1368. https://doi.org/10.1111/1755-0998.13326

Král, J., Forman, M., Kořínková, T., Lerma, A. C. R., Haddad, C. R., Musilová, J., Řezáč, M., Herrera, I. M. Á., Thakur, S., Dippenaar-Schoeman, A. S., Marec, F., Horová, L., & Bureš, P. (2019). Insights into the karyotype and genome evolution of haplogyne spiders indicate a polyploid origin of lineage with holokinetic chromosomes. *Scientific Reports*, *9*(1), 1–14. https://doi.org/10.1038/s41598-019-39034-3

Kunte, K., Zhang, W., Tenger-Trolander, A., Palmer, D. H., Martin, A., Reed, R. D., Mullen, S. P., & Kronforst, M. R. (2014). Doublesex is a mimicry supergene. *Nature*, *507*(7491), 229–232. https://doi.org/10.1038/nature13112

Küpper, C., Stocks, M., Risse, J. E., Dos Remedios, N., Farrell, L. L., McRae, S. B., Morgan, T. C., Karlionova, N., Pinchuk, P., Verkuil, Y. I., Kitaysky, A. S., Wingfield, J. C., Piersma, T., Zeng, K., Slate, J., Blaxter, M., Lank, D. B., & Burke, T. (2015). A supergene determines highly divergent male reproductive morphs in the ruff. *Nature Genetics*, *48*(1), 79–83. https://doi.org/10.1038/ng.3443

Kyriacou, R. G., Mulhair, P. O., & Holland, P. W. H. (2023). GC content across insect genomes: phylogenetic patterns, causes and consequences. *BioRxiv*, 2023.09.11 [accessed 2024 April 5th]. https://www.biorxiv.org/content/10.1101/2023.09.11.557135v1

Lamichhaney, S., Fan, G., Widemo, F., Gunnarsson, U., Thalmann, D. S., Hoeppner, M. P., Kerje, S., Gustafson, U., Shi, C., Zhang, H., Chen, W., Liang, X., Huang, L., Wang, J., Liang, E., Wu, Q., Lee, S. M. Y., Xu, X., Höglund, J., ... Andersson, L. (2015). Structural genomic changes underlie alternative reproductive strategies in the ruff (Philomachus pugnax). *Nature Genetics*, *48*(1), 84–88. https://doi.org/10.1038/ng.3430

Lenormand, T. (2003). The evolution of sex dimorphism in recombination. *Genetics*, *163*(2), 811–822. https://doi.org/10.1093/genetics/163.2.811

Lenormand, T., & Dutheil, J. (2005). *Recombination Difference between Sexes : A Role for Haploid Selection*. *3*(3). https://doi.org/10.1371/journal.pbio.0030063

Letunic, I., & Bork, P. (2024). Interactive Tree of Life (iTOL) v6: Recent updates to the phylogenetic tree display and annotation tool. *Nucleic Acids Research*, *52*(W1), W78–W82. https://doi.org/10.1093/nar/gkae268

Li, H. (2011). A statistical framework for SNP calling, mutation discovery, association mapping and population genetical parameter estimation from sequencing data. *Bioinformatics*, *27*(21), 2987–2993. https://doi.org/10.1093/bioinformatics/btr509

Li, H. (2013). *Aligning sequence reads, clone sequences and assembly contigs with BWA-MEM*. *00*(00), 1–3. http://arxiv.org/abs/1303.3997

Li, H. (2018). Minimap2: Pairwise alignment for nucleotide sequences. *Bioinformatics*, *34*(18), 3094–3100. https://doi.org/10.1093/bioinformatics/bty191

Li, H., Handsaker, B., Wysoker, A., Fennell, T., Ruan, J., Homer, N., Marth, G., Abecasis, G., & Durbin, R. (2009). The Sequence Alignment/Map format and SAMtools. *Bioinformatics*, *25*(16), 2078–2079. https://doi.org/10.1093/bioinformatics/btp352

Li, H., & Homer, N. (2010). A survey of sequence alignment algorithms for next-generation sequencing. *Briefings in Bioinformatics*, *11*(5), 473–483. https://doi.org/10.1093/bib/bbq015

Li, Y., Park, H., Smith, T. E., Moran, N. A., & Singh, N. (2019). Gene Family Evolution in the Pea Aphid Based on Chromosome-Level Genome Assembly. *Molecular Biology and Evolution*, *36*(10), 2143–2156. https://doi.org/10.1093/molbev/msz138

Liu, H., Jiang, F., Wang, S., Wang, H., Wang, A., Zhao, H., Xu, D., Yang, B., & Fan, W. (2022). Chromosome-level genome of the globe skimmer dragonfly (Pantala flavescens). *GigaScience*, *11*, 1–8. https://doi.org/10.1093/gigascience/giac009

Long, A., Liti, G., Luptak, A., & Tenaillon, O. (2015). Elucidating the molecular architecture of adaptation via evolve and resequence experiments. *Nature Reviews Genetics*, *16*(10), 567–582. https://doi.org/10.1038/nrg3937

Long, T. A. F., Agrawal, A. F., & Rowe, L. (2012). The effect of sexual selection on offspring fitness depends on the nature of genetic variation. *Current Biology*, *22*(3), 204–208. https://doi.org/10.1016/j.cub.2011.12.020

Lorch, P. D., Proulx, S., Rowe, L., & Day, T. (2003). Condition-dependent sexual selection can accelerate adaptation. *Evolutionary Ecology Research*, *5*(6), 867–881.

Łukasiewicz, A. (2020). Juvenile diet quality and intensity of sexual conflict in the mite Sancassania berlesei. *BMC Evolutionary Biology*, *20*(1), 1–11. https://doi.org/10.1186/s12862-020-1599-5

Łukasiewicz, A., Niśkiewicz, M., & Radwan, J. (2020b). Sexually selected male weapon is associated with lower inbreeding load but higher sex load in the bulb mite. *Evolution*, *74*(8), 1851–1855. https://doi.org/10.1111/evo.14033

Lukhtanov, V. A., Dinca, V., Friberg, M., Síchová, J., Olofsson, M., Vila, R., Marec, F., & Wiklund, C. (2018). Versatility of multivalent orientation, inverted meiosis, and rescued fitness in holocentric chromosomal hybrids. *Proceedings of the National Academy of Sciences of the United States of America*, *115*(41), E9610–E9619. https://doi.org/10.1073/pnas.1802610115

Lumley, A. J., Michalczyk, Ł., Kitson, J. J. N., Spurgin, L. G., Morrison, C. A., Godwin, J. L., Dickinson, M. E., Martin, O. Y., Emerson, B. C., Chapman, T., & Gage,

M. J. G. (2015). Sexual selection protects against extinction. *Nature*, *522*(7557), 470–473. https://doi.org/10.1038/nature14419

Mank, J. E. (2009). The evolution of heterochiasmy: the role of sexual selection and sperm competition in determining sex-specific recombination rates in eutherian mammals. *Genetics Research*, *91*(5), 355–363. https://doi.org/10.1017/S0016672309990255

Mank, J. E. (2017a). Population genetics of sexual conflict in the genomic era. *Nature Reviews Genetics*, *18*(12), 721–730. https://doi.org/10.1038/nrg.2017.83

Mank, J. E. (2017b). The transcriptional architecture of phenotypic dimorphism. *Nature Ecology and Evolution*, *1*(1), 1–7. https://doi.org/10.1038/s41559-016-0006

Mank, J. E. (2022). Sex-specific morphs: the genetics and evolution of intra-sexual variation. *Nature Reviews Genetics*, *0123456789*. https://doi.org/10.1038/s41576-022-00524-2

Maynard Smith, J., & Haigh, J. (2008). The hitch-hiking effect of a favourable gene. *Genetics Research*, *89*(5–6), 391–403. https://doi.org/10.1017/S0016672308009579

Meneely, P. M., Farago, A. F., & Kauffman, T. M. (2002). Crossover distribution and high interference for both the X chromosome and an autosome during oogenesis and spermatogenesis in *Caenorhabditis elegans*. *Genetics*, *162*(3), 1169–1177. https://doi.org/10.1093/genetics/162.3.1169

Mérot, C., Berdan, E. L., Cayuela, H., Djambazian, H., Ferchaud, A. L., Laporte, M., Normandeau, E., Ragoussis, J., Wellenreuther, M., & Bernatchez, L. (2021). Locally Adaptive Inversions Modulate Genetic Variation at Different Geographic Scales in a Seaweed Fly. *Molecular Biology and Evolution*, *38*(9), 3953–3971. https://doi.org/10.1093/molbev/msab143

Mérot, C., Llaurens, V., Normandeau, E., Bernatchez, L., & Wellenreuther, M. (2020). Balancing selection via life-history trade-offs maintains an inversion polymorphism in a seaweed fly. *Nature Communications*, *11*(1). https://doi.org/10.1038/s41467-020-14479-7

Mugal, C. F., Weber, C. C., & Ellegren, H. (2015). GC-biased gene conversion links the recombination landscape and demography to genomic base composition: GC-biased gene conversion drives genomic base composition across a wide range of species. *BioEssays*, *37*(12), 1317–1326. https://doi.org/10.1002/bies.201500058

Nagaoka, S. I., Hassold, T. J., & Hunt, P. A. (2012). Human aneuploidy: mechanisms and new insights into an age-old problem. *Nature Reviews Genetics*, *13*(7), 493–504. https://doi.org/10.1038/nrg3245

Nambiar, M., Chuang, Y.-C., & Smith, G. R. (2019). Distributing meiotic crossovers for optimal fertility and evolution. *DNA Repair*, *81*, 102648. https://doi.org/10.1016/j.dnarep.2019.102648

Nambiar, M., & Smith, G. R. (2016). Repression of harmful meiotic recombination in centromeric regions. *Seminars in Cell and Developmental Biology*, *54*, 188–197. https://doi.org/10.1016/j.semcdb.2016.01.042

Näsvall, K., Boman, J., Höök, L., Vila, R., Wiklund, C., & Backström, N. (2023). Nascent evolution of recombination rate differences as a consequence of chromosomal rearrangements. *PLoS Genetics*, *19*(8), 1–21. https://doi.org/10.1371/journal.pgen.1010717

Nei, M., & Li, W. H. (1979). Mathematical model for studying genetic variation in terms of restriction endonucleases. *Proceedings of the National Academy of Sciences of the United States of America*, *76*(10), 5269–5273. https://doi.org/10.1073/pnas.76.10.5269

Nijhout, H. F., & Emlen, D. J. (1998). Developmental biology, evolution competition among body parts in the development and evolution of insect morphology. *Proceedings of the National Academy of Sciences of the United States of America*, *95*(7), 3685–3689. https://doi.org/10.1073/pnas.95.7.3685

Nokkala, S., Kuznetsova, V. G., Maryanska-Nadachowska, A., & Nokkala, C. (2004). Holocentric chromosomes in meiosis. I. Restriction of the number of chiasmata in bivalents. *Chromosome Research*, *12*(7), 733–739. https://doi.org/10.1023/B:CHRO.0000045797.74375.70

Nuzhdin, S. V., & Turner, T. L. (2013). Promises and limitations of hitchhiking mapping. *Current Opinion in Genetics and Development*, *23*(6), 694–699. https://doi.org/10.1016/j.gde.2013.10.002

Oliveira, R. F., Taborsky, M., & Brockmann, H. J. (2008). *Alternative Reproductive Tactics: An Integrative Approach*. Cambridge University Press.

Onozawa, M., Zhang, Z., Kim, Y. J., Goldberg, L., Varga, T., Bergsagel, P. L., Kuehl, W. M., & Aplan, P. D. (2014). Repair of DNA double-strand breaks by templated nucleotide sequence insertions derived from distant regions of the genome. *Proceedings of the National Academy of Sciences of the United States of America*, *111*(21), 7729–7734. https://doi.org/10.1073/pnas.1321889111

Otte, K. A., Nolte, V., Mallard, F., & Schlötterer, C. (2021). The genetic architecture of temperature adaptation is shaped by population ancestry and not by selection regime. *Genome Biology*, *22*(1), 1–25. https://doi.org/10.1186/s13059-021-02425-9

Otte, K. A., & Schlötterer, C. (2021). Detecting selected haplotype blocks in evolve and resequence experiments. *Molecular Ecology Resources*, *21*(1), 93–109. https://doi.org/10.1111/1755-0998.13244

Otto, S. P., & Payseur, B. A. (2019). Crossover Interference: Shedding Light on the Evolution of Recombination. *Annual Review of Genetics*, *53*, 19–44. https://doi.org/10.1146/annurev-genet-040119-093957

Ottolini, C. S., Newnham, L. J., Capalbo, A., Natesan, S. A., Joshi, H. A., Cimadomo, D., Griffin, D. K., Sage, K., Summers, M. C., Thornhill, A. R., Housworth, E., Herbert, A. D., Rienzi, L., Ubaldi, F. M., Handyside, A. H., & Hoffmann, E. R. (2015). Genome-wide maps of recombination and chromosome segregation in human oocytes and embryos show selection for maternal recombination rates. *Nature Genetics*, *47*(7), 727–735. https://doi.org/10.1038/ng.3306

Pardue, M. Lou, & DeBaryshe, P. G. (2011). Retrotransposons that maintain chromosome ends. *Proceedings of the National Academy of Sciences of the United States of America*, *108*(51), 20317–20324. https://doi.org/10.1073/pnas.1100278108

Parrett, J. M., Chmielewski, S., Aydogdu, E., Łukasiewicz, A., Rombauts, S., Szubert-Kruszyńska, A., Babik, W., Konczal, M., & Radwan, J. (2022). Genomic evidence that a sexually selected trait captures genome-wide variation and facilitates the purging of genetic load. *Nature Ecology & Evolution*, *6*(9), 1330–1342. https://doi.org/10.1038/s41559-022-01816-w

Parrett, J. M., Ghobert, V., Cullen, F. S., & Knell, R. J. (2021). Strong sexual selection fails to protect against inbreeding-driven extinction in a moth. *Behavioral Ecology*, *32*(5), 875–882. https://doi.org/10.1093/beheco/arab056

Parrett, J. M., Łukasiewicz, A., Chmielewski, S., Szubert-Kruszyńska, A., Maurizio, P. L., Grieshop, K., & Radwan, J. (2023). A sexually selected male weapon characterized by strong additive genetic variance and no evidence for sexually antagonistic polyphenic maintenance. *Evolution*, *77*(6), 1289–1302. https://doi.org/10.1093/evolut/qpad039

Pedersen, B. S., & Quinlan, A. R. (2018). Mosdepth: Quick coverage calculation for genomes and exomes. *Bioinformatics*, *34*(5), 867–868. https://doi.org/10.1093/bioinformatics/btx699

Peñalba, J. V., & Wolf, J. B. W. (2020). From molecules to populations: appreciating and estimating recombination rate variation. *Nature Reviews Genetics*, *21*(8), 476–492. https://doi.org/10.1038/s41576-020-0240-1

Peterson, A. L., & Payseur, B. A. (2021). Sex-specific variation in the genome-wide recombination rate. *Genetics*, *217*(1), 1–11. https://doi.org/10.1093/GENETICS/IYAA019

Pischedda, A., & Chippindale, A. K. (2006). Intralocus sexual conflict diminishes the benefits of sexual selection. *PLoS Biology*, *4*(11), 2099–2103. https://doi.org/10.1371/journal.pbio.0040356

Plesnar Bielak, A., Skrzynecka, A. M., Miler, K., & Radwan, J. (2014). Selection for alternative male reproductive tactics alters intralocus sexual conflict. *Evolution*, *68*(7), 2137–2144. https://doi.org/10.1111/evo.12409

Plesnar-Bielak, A., Jawor, A., & Kramarz, P. E. (2013). Complex response in size-related traits of bulb mites (*Rhizoglyphus robini*) under elevated thermal conditions-An experimental evolution approach. *Journal of Experimental Biology*, *216*(24), 4542–4548. https://doi.org/10.1242/jeb.090951

Plesnar-Bielak, A., Parrett, J. M., Chmielewski, S., Dudek, K., Łukasiewicz, A., Marszałek, M., Babik, W., & Konczal, M. (2022). Transcriptomics of differences in thermal plasticity associated with selection for an exaggerated male sexual trait. *ResearchSquare*, preprint [accessed 2024 April 5th]. https://doi.org/https://doi.org/10.21203/rs.3.rs-1862013/v1

Plesnar-Bielak, A., Parrett, J. M., Chmielewski, S., Dudek, K., Łukasiewicz, A., Marszałek, M., Babik, W., & Konczal, M. (2024). Transcriptomics of differences in thermal plasticity associated with selection for an exaggerated male sexual trait. *Heredity*, *May*, 1–11. https://doi.org/10.1038/s41437-024-00691-4

Plesnar-Bielak, A., Skwierzyńska, A. M., & Radwan, J. (2020). Sexual and ecological selection on a sexual conflict gene. *Journal of Evolutionary Biology*, *33*(10), 1433–1439. https://doi.org/10.1111/jeb.13680

Prokuda, A. Y., & Roff, D. A. (2014). The quantitative genetics of sexually selected traits, preferred traits and preference: A review and analysis of the data. *Journal of Evolutionary Biology*, *27*(11), 2283–2296. https://doi.org/10.1111/jeb.12483

Purcell, S., Neale, B., Todd-Brown, K., Thomas, L., Ferreira, M. A. R., Bender, D., Maller, J., Sklar, P., De Bakker, P. I. W., Daly, M. J., & Sham, P. C. (2007). PLINK: A tool set for whole-genome association and population-based linkage analyses. *American Journal of Human Genetics*, *81*(3), 559–575. https://doi.org/10.1086/519795

Quinlan, A. R., & Hall, I. M. (2010). BEDTools: A flexible suite of utilities for comparing genomic features. *Bioinformatics*, *26*(6), 841–842. https://doi.org/10.1093/bioinformatics/btq033

R Core Team. (2024). *R: A Language and Environment for Statistical Computing*. https://www.r-project.org/

Radwan, J. (1995). Male morph determination in two species of acarid mites. *Heredity*, *74*(6), 669–673. https://doi.org/10.1038/hdy.1995.91

Radwan, J. (1997). Sperm precedence in the bulb mite, *Rhizoglyphus robini*: Context-dependent variation. *Ethology Ecology and Evolution*, *9*(4), 373–383. https://doi.org/10.1080/08927014.1997.9522879

Radwan, J. (2003). Heritability of male morph in the bulb mite, *Rhizoglyphus robini* (Astigmata, Acaridae). *Experimental and Applied Acarology*, *29*(1–2), 109–114. https://doi.org/10.1023/A:1024260719013

Radwan, J. (2007). Sexual selection and conflict in the bulb mite, *Rhizoglyphus robini* (Astigmata: Acaridae). *Experimental and Applied Acarology*, *42*(3), 151–158. https://doi.org/10.1007/s10493-007-9086-x

Radwan, J. (2009). Alternative Mating Tactics in Acarid Mites. In *Advances in the Study of Behavior* (1st ed., Vol. 39, Issue 09, pp. 185–208). Elsevier Inc. https://doi.org/10.1016/S0065-3454(09)39006-3

Radwan, J., Czyż, M., Konior, M., & Kolodziejczyk, M. (2000). Aggressiveness in Two Male Morphs of the Bulb Mite *Rhizoglyphus robini*. *Ethology*, *106*(1), 53–62. https://doi.org/10.1046/j.1439-0310.2000.00498.x

Radwan, J., Engqvist, L., & Reinhold, K. (2016). A Paradox of Genetic Variance in Epigamic Traits: Beyond "Good Genes" View of Sexual Selection. *Evolutionary Biology*, *43*(2), 267–275. https://doi.org/10.1007/s11692-015-9359-y

Radwan, J., & Klimas, M. (2001). Male dimorphism in the bulb mite, *Rhizoglyphus robini*: Fighters survive better. *Ethology Ecology and Evolution*, *13*(1), 69–79. https://doi.org/10.1080/08927014.2001.9522788

Radwan, J., & Siva-Jothy, M. T. (1996). The function of post-insemination mate association in the bulb mite, *Rhizoglyphus robini*. *Animal Behaviour*, *52*(4), 651–657. https://doi.org/10.1006/anbe.1996.0209

Rastas, P. (2017). Lep-MAP3: Robust linkage mapping even for low-coverage whole genome sequencing data. *Bioinformatics*, *33*(23), 3726–3732. https://doi.org/10.1093/bioinformatics/btx494

Rastas, P. (2020). Lep-Anchor: Automated construction of linkage map anchored haploid genomes. *Bioinformatics*, *36*(8), 2359–2364. https://doi.org/10.1093/bioinformatics/btz978

Rice, W. R., & Chippindale, A. K. (2001). Intersexual ontogenetic conflict. *Journal of Evolutionary Biology*, *14*(5), 685–693. https://doi.org/10.1046/j.1420-9101.2001.00319.x

Ritz, K. R., Noor, M. A. F., & Singh, N. D. (2017). Variation in Recombination Rate: Adaptive or Not? *Trends in Genetics*, *33*(5), 364–374. https://doi.org/10.1016/j.tig.2017.03.003

Rohner, P. T., Linz, D. M., & Moczek, A. P. (2021). Doublesex mediates species-, sex-, environment- and trait-specific exaggeration of size and shape. *Proceedings of the Royal Society B: Biological Sciences*, *288*(1953). https://doi.org/10.1098/rspb.2021.0241

Rowe, L., & Houle, D. (1996). The lek paradox and the capture of genetic variance by condition dependent traits. *Proceedings of the Royal Society B: Biological Sciences*, *263*(1375), 1415–1421. https://doi.org/10.1098/rspb.1996.0207

Rusuwa, B. B., Chung, H., Allen, S. L., Frentiu, F. D., & Chenoweth, S. F. (2022). Natural variation at a single gene generates sexual antagonism across fitness components in *Drosophila*. *Current Biology*, *32*(14), 3161-3169.e7. https://doi.org/10.1016/j.cub.2022.05.038

Ruzicka, F., Hill, M. S., Pennell, T. M., Flis, I., Ingleby, F. C., Mott, R., Fowler, K., Morrow, E. H., & Reuter, M. (2019). Genome-wide sexually antagonistic variants reveal long-standing constraints on sexual dimorphism in fruit flies. *PLOS Biology*, *17*(4), e3000244. https://doi.org/10.1371/journal.pbio.3000244

Safari, I., & Goymann, W. (2021). The evolution of reversed sex roles and classical polyandry: Insights from coucals and other animals. *Ethology*, *127*(1), 1–13. https://doi.org/10.1111/eth.13095

Sanchez-Donoso, I., Ravagni, S., Rodríguez-Teijeiro, J. D., Christmas, M. J., Huang, Y., Maldonado-Linares, A., Puigcerver, M., Jiménez-Blasco, I., Andrade, P., Gonçalves, D., Friis, G., Roig, I., Webster, M. T., Leonard, J. A., & Vilà, C. (2022). Massive genome inversion drives coexistence of divergent morphs in common quails. *Current Biology*, *32*(2), 462-469.e6. https://doi.org/10.1016/j.cub.2021.11.019

Sardell, J. M., Cheng, C., Dagilis, A. J., Ishikawa, A., Kitano, J., Peichel, C. L., & Kirkpatrick, M. (2018). Sex differences in recombination in sticklebacks. *G3: Genes, Genomes, Genetics*, *8*(6), 1971–1983. https://doi.org/10.1534/g3.118.200166

Sardell, J. M., & Kirkpatrick, M. (2020). Sex differences in the recombination landscape. *American Naturalist*, *195*(2), 361–379. https://doi.org/10.1086/704943

Sayadi, A., Martinez Barrio, A., Immonen, E., Dainat, J., Berger, D., Tellgren-Roth, C., Nystedt, B., & Arnqvist, G. (2019). The genomic footprint of sexual conflict. *Nature Ecology and Evolution*, *3*(12), 1725–1730. https://doi.org/10.1038/s41559-019-1041-9

Sella, G., & Barton, N. H. (2019). Thinking About the Evolution of Complex Traits in the Era of Genome-Wide Association Studies. *Annual Review of Genomics and Human Genetics*, *20*(1), 461–493. https://doi.org/10.1146/annurev-genom-083115-022316

Sharda, S., Hollis, B., & Kawecki, T. J. (2024). Sex ratio affects sexual selection against mutant alleles in a locus-specific way. *Behavioral Ecology*, *35*(1). https://doi.org/10.1093/beheco/arad110

Siller, S. (2001). Sexual selection and the maintenance of sex. *Nature*, *411*(6838), 689–692. https://doi.org/10.1038/35079578

Singh, P., Taborsky, M., Peichel, C. L., & Sturmbauer, C. (2023). Genomic basis of Y-linked dwarfism in cichlids pursuing alternative reproductive tactics. *Molecular Ecology*, *32*(7), 1592–1607. https://doi.org/10.1111/mec.16839

Singhal, S., Leffler, E. M., Sannareddy, K., Turner, I., Venn, O., Hooper, D. M., Strand, A. I., Li, Q., Raney, B., Balakrishnan, C. N., Griffith, S. C., McVean, G., & Przeworski, M. (2015). Stable recombination hotspots in birds. *Science*, *350*(6263), 928–932. https://doi.org/10.1126/science.aad0843

Skwierzyńska, A. M., & Plesnar-Bielak, A. (2018). Proximate mechanisms of the differences in reproductive success of males bearing different alleles of Pgdh – a gene involved in a sexual conflict in bulb mite. *Journal of Evolutionary Biology*, *31*(5), 657–664. https://doi.org/10.1111/jeb.13250

Slatkin, M. (2008). Linkage disequilibrium - Understanding the evolutionary past and mapping the medical future. *Nature Reviews Genetics*, *9*(6), 477–485. https://doi.org/10.1038/nrg2361

Smallegange, I. M. (2011). Complex environmental effects on the expression of alternative reproductive phenotypes in the bulb mite. *Evolutionary Ecology*, *25*(4), 857–873. https://doi.org/10.1007/s10682-010-9446-6

Smallegange, I. M., Caswell, H., Toorians, M. E. M., & de Roos, A. M. (2017). Mechanistic description of population dynamics using dynamic energy budget theory incorporated into integral projection models. *Methods in Ecology and Evolution*, *8*(2), 146–154. https://doi.org/10.1111/2041-210X.12675

Smith, J. M. (1985). The evolution of recombination. *Journal of Genetics*, *64*(2–3), 159–171. https://doi.org/10.1007/BF02931144

Snook, R. R., Brüstle, L., & Slate, J. (2009). A Test And Review Of The Role Of Effective Population Size On Experimental Sexual Selection Patterns. *Evolution*, *63*(7), 1923–1933. https://doi.org/10.1111/j.1558-5646.2009.00682.x

Spitzer, K., Pelizzola, M., & Futschik, A. (2020). Modifying the chi-square and the cmh test for population genetic inference: Adapting to overdispersion. *Annals of Applied Statistics*, *14*(1), 202–220. https://doi.org/10.1214/19-AOAS1301

Stamatakis, A. (2014). RAxML version 8: A tool for phylogenetic analysis and post-analysis of large phylogenies. *Bioinformatics*, *30*(9), 1312–1313. https://doi.org/10.1093/bioinformatics/btu033

Stapley, J., Feulner, P. G. D., Johnston, S. E., Santure, A. W., & Smadja, C. M. (2017). Variation in recombination frequency and distribution across eukaryotes: Patterns and processes. *Philosophical Transactions of the Royal Society B: Biological Sciences*, *372*(1736). https://doi.org/10.1098/rstb.2016.0455

Steiß, V., Letschert, T., Schäfer, H., & Pahl, R. (2012). PERMORY-MPI: A program for high-speed parallel permutation testing in genome-wide association studies. *Bioinformatics*, *28*(8), 1168–1169. https://doi.org/10.1093/bioinformatics/bts086

Sterck, L., Billiau, K., Abeel, T., Rouzé, P., & Van De Peer, Y. (2012). ORCAE: Online resource for community annotation of eukaryotes. *Nature Methods*, *9*(11), 1041. https://doi.org/10.1038/nmeth.2242

Sterner, D. E., & Berger, S. L. (2000). Acetylation of Histones and Transcription-Related Factors. *Microbiology and Molecular Biology Reviews*, *64*(2), 435–459. https://doi.org/10.1128/mmbr.64.2.435-459.2000

Storey JD, Bass AJ, Dabney A, R. D. (2024). *qvalue: Q-value estimation for false discovery rate control.* (R package version 2.36.0).

Sugimoto, N., Takahashi, A., Ihara, R., Itoh, Y., Jouraku, A., Van Leeuwen, T., & Osakabe, M. (2020). QTL mapping using microsatellite linkage reveals target-site mutations associated with high levels of resistance against three mitochondrial complex II inhibitors in Tetranychus urticae. *Insect Biochemistry and Molecular Biology*, *123*(February), 103410. https://doi.org/10.1016/j.ibmb.2020.103410

Sullivan, G. T., & Ozman-Sullivan, S. K. (2021). Alarming evidence of widespread mite extinctions in the shadows of plant, insect and vertebrate extinctions. *Austral Ecology*, *46*(1), 163–176. https://doi.org/10.1111/aec.12932

Taborsky, M., Oliveira, R. F., & Brockmann, H. J. (2008). The evolution of alternative reproductive tactics: concepts and questions. In *Alternative Reproductive Tactics* (pp. 1–22). Cambridge University Press. https://doi.org/10.1017/CBO9780511542602.002

Talbert, P. B., Bayes, J. J., & Henikoff, S. (2009). Evolution of Centromeres and Kinetochores: A Two-Part Fugue. In *The Kinetochore:* (pp. 1–37). Springer New York. https://doi.org/10.1007/978-0-387-69076-6_7

Talla, V., Soler, L., Kawakami, T., DincCrossed D Signf, V., Vila, R., Friberg, M., Wiklund, C., Backström, N., & Gonzalez, J. (2019). Dissecting the Effects of Selection and Mutation on Genetic Diversity in Three Wood White (Leptidea) Butterfly Species. *Genome Biology and Evolution*, *11*(10), 2875–2886. https://doi.org/10.1093/gbe/evz212

Tarailo-Graovac, M., & Chen, N. (2009). Using RepeatMasker to identify repetitive elements in genomic sequences. *Current Protocols in Bioinformatics*, *SUPPL. 25*, 1–14. https://doi.org/10.1002/0471250953.bi0410s25

Taus, T., Futschik, A., & Schlötterer, C. (2017). Quantifying Selection with Pool-Seq Time Series Data. *Molecular Biology and Evolution*, *34*(11), 3023–3034. https://doi.org/10.1093/molbev/msx225

The *C. elegans* Sequencing Consortium. (1998). Genome Sequence of the Nematode *C. elegans*: A Platform for Investigating Biology. *Science*, *282*(5396), 2012–2018. https://doi.org/10.1126/science.282.5396.2012

Thuriaux, P. (1977). Is recombination confined to structural genes on the eukaryotic genome? *Nature*, *268*(5619), 460–462. https://doi.org/10.1038/268460a0

Tobler, R., Franssen, S. U., Kofler, R., Orozco-Terwengel, P., Nolte, V., Hermisson, J., & Schlötterer, C. (2014). Massive habitat-specific genomic response in D. melanogaster populations during experimental evolution in hot and cold environments. *Molecular Biology and Evolution*, *31*(2), 364–375. https://doi.org/10.1093/molbev/mst205

Tomkins, J. L., Radwan, J., Kotiaho, J. S., & Tregenza, T. (2004). Genic capture and resolving the lek paradox. *Trends in Ecology and Evolution*, *19*(6), 323–328. https://doi.org/10.1016/j.tree.2004.03.029

Torres, A. P., Höök, L., Näsvall, K., Shipilina, D., Wiklund, C., Vila, R., Pruisscher, P., & Backström, N. (2023). The fine-scale recombination rate variation and associations with genomic features in a butterfly. *Genome Research*, *33*(5), 810–823. https://doi.org/10.1101/gr.277414.122

Trivers, R. (1988). The Evolution of Sex: An Examination of Current Ideas. In Richard E. Michod (Ed.), *The evolution of sex* (pp. 270–286). Sinauer Associates Inc.

Turner, B. M. (1991). Histone acetylation and control of gene expression. *Journal of Cell Science*, *99*(1), 13–20. https://doi.org/10.1242/jcs.99.1.13

Ullmann, A. J., Piesman, J., Dolan, M. C., & Black IV, W. C. (2003). A preliminary linkage map of the hard tick, Ixodes scapularis. *Insect Molecular Biology*, *12*(2), 201–210. https://doi.org/10.1046/j.1365-2583.2003.00402.x

Unnikrishnan, P., Grzesik, S., Trojańska, M., Klimek, B., & Plesnar-Bielak, A. (2024). 6Pgdh polymorphism in wild bulb mite populations: prevalence, environmental correlates and life history trade-offs. *Experimental and Applied Acarology*, *93*(1), 115–132. https://doi.org/10.1007/s10493-024-00909-4

Veller, C., Kleckner, N., & Nowak, M. A. (2019). A rigorous measure of genome-wide genetic shuffling that takes into account crossover positions and Mendel's second law. *Proceedings of the National Academy of Sciences of the United States of America*, *116*(5), 1659–1668. https://doi.org/10.1073/pnas.1817482116

Walter, D. E., & Proctor, H. C. (2013). Mites: Ecology, Evolution & Behaviour. In *Mites: Ecology, Evolution & Behaviour*. Springer Netherlands. https://doi.org/10.1007/978-94-007-7164-2

Watterson, G. A. (1975). On the number of segregating sites in genetical models without recombination. *Theoretical Population Biology*, *7*(2), 256–276. https://doi.org/10.1016/0040-5809(75)90020-9

Webster, M. T., & Hurst, L. D. (2012). Direct and indirect consequences of meiotic recombination: Implications for genome evolution. *Trends in Genetics*, *28*(3), 101–109. https://doi.org/10.1016/j.tig.2011.11.002

Wellenreuther, M., & Bernatchez, L. (2018). Eco-Evolutionary Genomics of Chromosomal Inversions. *Trends in Ecology and Evolution*, *33*(6), 427–440. https://doi.org/10.1016/j.tree.2018.04.002

White, M. J. D. (1973). *Animal cytology and evolution* (3rd ed.). Cambridge University Press.

Whiting, J. R. (2022). *Genotype Plot*. https://doi.org/10.5281/zenodo.5913504

Whitlock, M. C., & Agrawal, A. F. (2009). Purging the genome with sexual selection: reducing mutation load through selection on males. *Evolution*, *63*(3), 569–582. https://doi.org/10.1111/j.1558-5646.2008.00558.x

Wiberg, R. A. W., Gaggiotti, O. E., Morrissey, M. B., & Ritchie, M. G. (2017). Identifying consistent allele frequency differences in studies of stratified populations. *Methods in Ecology and Evolution*, *8*(12), 1899–1909. https://doi.org/10.1111/2041-210X.12810

Wickham, H. (2009). *ggplot2: Elegant Graphics for Data Analysis*. Springer New York. https://doi.org/10.1007/978-0-387-98141-3

Wickham, H. (2016). *Elegant Graphics for Data Analysis*. Springer International Publishing. https://doi.org/10.1007/978-3-319-24277-4

Wilfert, L., Gadau, J., & Schmid-Hempel, P. (2007). Variation in genomic recombination rates among animal taxa and the case of social insects. *Heredity*, *98*(4), 189–197. https://doi.org/10.1038/sj.hdy.6800950

Willink, B., Tunström, K., Nilén, S., Chikhi, R., Lemane, T., Takahashi, M., Takahashi, Y., Svensson, E. I., & Wheat, C. W. (2024). The genomics and evolution of inter-sexual mimicry and female-limited polymorphisms in damselflies. *Nature Ecology and Evolution*, *8*(1), 83–97. https://doi.org/10.1038/s41559-023-02243-1

Wrensch, D. L., Kethley, J. B., & Norton, R. A. (1994). Cytogenetics of Holokinetic Chromosomes and Inverted Meiosis: Keys to the Evolutionary Success of Mites, with Generalizations on Eukaryotes. *Mites*, 282–343. https://doi.org/10.1007/978-1-4615-2389-5_11

Xiong, Q., Wan, A. T. Y., & Tsui, S. K.-W. (2020). A Mini-review of the Genomes and Allergens of Mites and Ticks. *Current Protein & Peptide Science*, *21*(2), 114–123. https://doi.org/10.2174/1389203720666190719150432

Yu, G., Wang, L. G., Han, Y., & He, Q. Y. (2012). ClusterProfiler: An R package for comparing biological themes among gene clusters. *OMICS A Journal of Integrative Biology*, *16*(5), 284–287. https://doi.org/10.1089/omi.2011.0118

Zahavi, A. (1975). Mate selection-A selection for a handicap. *Journal of Theoretical Biology*, *53*(1), 205–214. https://doi.org/10.1016/0022-5193(75)90111-3

Zajitschek, F., & Connallon, T. (2018). Antagonistic pleiotropy in species with separate sexes, and the maintenance of genetic variation in life-history traits and fitness. *Evolution*, *72*(6), 1306–1316. https://doi.org/10.1111/evo.13493

Zhang, L., Liang, Z., Hutchinson, J., & Kleckner, N. (2014). Crossover Patterning by the Beam-Film Model: Analysis and Implications. *PLoS Genetics*, *10*(1), e1004042. https://doi.org/10.1371/journal.pgen.1004042

Zheng, X., Levine, D., Shen, J., Gogarten, S. M., Laurie, C., & Weir, B. S. (2012). A high-performance computing toolset for relatedness and principal component analysis of SNP data. *Bioinformatics*, *28*(24), 3326–3328. https://doi.org/10.1093/bioinformatics/bts606

Zhou, Y., Klimov, P. B., Gu, X., Yu, Z., Cui, X., Li, Q., Pan, R., Yuan, C., Cai, F., & Cui, Y. (2023). Chromosome-level genomic assembly and allergome inference reveal novel allergens in Tyrophagus putrescentiae. *Allergy: European Journal of Allergy and Clinical Immunology*, *78*(6), 1691–1695. https://doi.org/10.1111/all.15656

Zickler, D., & Kleckner, N. (2016). A few of our favorite things: Pairing, the bouquet, crossover interference and evolution of meiosis. *Seminars in Cell and Developmental Biology*, *54*, 135–148. https://doi.org/10.1016/j.semcdb.2016.02.024

Zou, S., Kim, J. M., & Voytas, D. F. (1996). The Saccharomyces retrotransposon Ty5 influences the organization of chromosome ends. *Nucleic Acids Research*, *24*(23), 4825–4831. https://doi.org/10.1093/nar/24.23.4825

AUTHORSHIP STATEMENTS

Poznań, 19.09.2024

Authorship statements of the PhD candidate

1. Chmielewski, S., Konczal, M., Parrett, J. M., Rombauts, S., Dudek, K., Radwan, J., & Babik, W. 2024. "Sex-specific recombination landscape in a species with holocentric chromosomes" under review in *Genetics*
   I declare that I contributed to all major tasks in this chapter, including conceiving the study, performing experimental crosses, data analysis, interpretation of results, writing the first draft and revising the manuscript. My contribution to this study was 80%.

2. Chmielewski, S., Parrett, J. M., Konczal, M., & Radwan, J. „The impact of sex ratio manipulation on genome-wide genetic diversity during experimental evolution." (unpublished).
   I declare that I contributed to all major tasks in this chapter, including conceiving the study, performing the experiment, data analysis, interpretation of results, writing the first draft and revising the manuscript. My contribution to this study was 70%.

3. Chmielewski, S., Konczal, M., Parrett, J.M, & Radwan, J. 2024. „Supergene polymorphism and its role in male morph differentiation in the bulb mite, *Rhizoglyphus robini*." (unpublished). I declare that I contributed to all major tasks in this chapter, including conceiving the study, performing the experiment, data analysis, interpretation of results, writing the first draft and revising the manuscript. My contribution to this study was 80%.

Sebastian Chmielewski

Supervisor confirmation

prof. dr hab. Jacek Radwan

Poznań, 19.09.2024

I confirm that I am co-author of the paper: Chmielewski, S., Konczal, M., Parrett, J. M., Rombauts, S., Dudek, K., Radwan, J., & Babik, W. "Sex-specific recombination landscape in a species with holocentric chromosomes" under review in *Genetics* (2024). I declare that I contributed to conceiving the study, interpreting the results, and to revising the manuscript.

prof. dr hab. Jacek Radwan
Evolutionary Biology Group
Adam Mickiewicz University

I confirm that I am co-author of the paper: "The impact of sex ratio manipulation on genome- wide genetic diversity during experimental evolution" (unpublished). I declare that I contributed to conceiving the study, interpreting the results, writing the first version and to revising the manuscript.

prof. dr hab. Jacek Radwan
Evolutionary Biology Group
Adam Mickiewicz University

I confirm that I am co-author of the paper: "Supergene polymorphism and its role in male morph differentiation in the bulb mite, *Rhizoglyphus robini*" (unpublished). I declare that I contributed to conceiving the study, interpreting the results, writing the first version and to revising the manuscript.

prof. dr hab. Jacek Radwan
Evolutionary Biology Group
Adam Mickiewicz University

Poznań, 13.09.2024

I confirm that I am co-author of the paper: Chmielewski, S., Konczal, M., Parrett, J. M., Rombauts, S., Dudek, K., Radwan, J., & Babik, W. "Sex-specific recombination landscape in a species with holocentric chromosomes" under review in *Genetics* (2024). I declare that I contributed to the interpretation of the results and revising the manuscript and I assisted in statistical analysis.

dr Mateusz Konczal
Evolutionary Biology Group
Adam Mickiewicz University

I confirm that I am co-author of the paper: "The impact of sex ratio manipulation on genome-wide genetic diversity during experimental evolution" (unpublished). I declare that I contributed to the data interpretation and revising the manuscript.

dr Mateusz Konczal
Evolutionary Biology Group
Adam Mickiewicz University

I confirm that I am co-author of the paper: "Supergene polymorphism and its role in male morph differentiation in the bulb mite, *Rhizoglyphus robini*" (unpublished). I declare that I contributed to the data interpretation and revising the manuscript.

dr Mateusz Konczal
Evolutionary Biology Group
Adam Mickiewicz University

Poznań, 12.09.2024

I confirm that I am co-author of the paper: Chmielewski, S., Konczal, M., Parrett, J. M., Rombauts, S., Dudek, K., Radwan, J., & Babik, W. "Sex-specific recombination landscape in a species with holocentric chromosomes" under review in *Genetics* (2024). I declare that I contributed to the interpretation of the results, assistance in statistical analysis and revising the manuscript.

dr Jonathan Parrett
Evolutionary Biology Group
Adam Mickiewicz University

I confirm that I am co-author of the paper: Chmielewski, S., Parrett, J. M., Konczal, M. & Radwan, J. "The impact of sex ratio manipulation on genome-wide genetic diversity during experimental evolution." (unpublished). I declare that I contributed to the performing experiment, data interpretation, revising the manuscript and I assisted in statistical analysis.

dr Jonathan Parrett
Evolutionary Biology Group
Adam Mickiewicz University

I confirm that I am co-author of the paper: Chmielewski, S., Parrett, J. M., Konczal, M. & Radwan, J. "Supergene polymorphism and its role in male morph differentiation in the bulb mite, *Rhizoglyphus robini*." (unpublished). I declare that I contributed to the data interpretation revising the manuscript and I assisted in statistical analysis.

dr Jonathan Parrett
Evolutionary Biology Group
Adam Mickiewicz University

Kraków, 12.09.2024

I confirm that I am co-author of the paper: Chmielewski, S., Konczal, M., Parrett, J. M., Rombauts, S., Dudek, K., Radwan, J., & Babik, W. "Sex-specific recombination landscape in a species with holocentric chromosomes" under review in *Genetics* (2024). I declare that I contributed to conceiving the study, data analysis, interpretation of the results and revising the manuscript.

prof. dr hab. Wiesław Babik

Institute of Environmental Sciences

Jagiellonian University

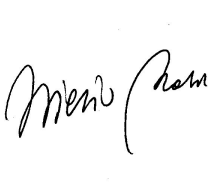

Elektronicznie podpisany przez Wiesław Babik
Data: 2024.09.16 08:51:44 +02'00'